THE "DOUBLE THRESHOLD" RADAR RECEIVER FOR REDUCTION OF FALSE TARGETS CAUSED BY INTERFERING PULSES

Isham W. Linder

THE "DOUBLE THRESHOLD" RADAR RECEIVER FOR REDUCTION OF FALSE TARGETS CAUSED BY INTERFERING PULSES

by

Isham W. Linder
Lieutenant, United States Navy

Submitted in partial fulfillment
of the requirements
for the degree of
MASTER OF SCIENCE
IN
ENGINEERING ELECTRONICS

United States Naval Postgraduate School
Monterey, California

1956

THE "DOUBLE THRESHOLD" RADAR RECEIVER FOR REDUCTION OF FALSE TARGETS CAUSED BY INTERFERING PULSES

* * * *

Isham W. Linder

This work is accepted as fulfilling

the thesis requirements for the degree of

MASTER OF SCIENCE

IN

ENGINEERING ELECTRONICS

from the

United States Naval Postgraduate School

PREFACE

The development of automatic radar detection systems has focused attention on the effects on the performance of a radar receiver of the interfering pulses from other radars. It is essential to the successful performance of an automatic system that the false indications caused by interference be almost completely suppressed. This paper is a mathematical investigation of one type of radar receiver which discriminates against false target indications. A double threshold radar receiver is found to be capable of controlling the false target interference. The double threshold receiver is shown to have a slightly lower radar range capability than a normal receiver.

Sincere thanks are due Mr. John Mallett and Dr. Peter Swerling of the RAND Corporation, Santa Monica, California, for their guidance and assistance in the pursuit of this investigation.

TABLE OF CONTENTS

TABLE OF SYMBOLS

X	Signal-to-Noise Power Ratio.
N	Integration Number (for a scanning radar, the number of target echoes each time the antenna scans past the target).
T_{fa}	False Alarm Time
n	False Alarm Number; number of range gates occurring in the false alarm time.
M	Second Threshold Number.
Y_b	First Threshold; power level.
σ	Number of range gates per second.
$\eta = \frac{1}{\sigma}$	Range gate width in seconds.
f_r	Radar repetition frequency, cps.
S	Average number of random interfering pulses per second.
$\delta = (S)(\eta)$	Average number of interfering pulses per gate width.
p_M	Probability of a false alarm in one range gate.
$p_{fa}(T)$	Probability of one or more false alarms in time equal to T.
p_X	Probability of detection of a signal of signal-to-noise ratio X in one range gate.
P_d	Probability of detection of a signal in N repetition periods.

CHAPTER I

INTRODUCTION

The continuing development of radar systems in recent years has led to an increasing usefullness of these systems for search and for control functions. The operational utilization of radar by the armed forces, even though high at the end of World War II, has continued to grow ever since. Operational planners have called for greater and greater numbers of radars to meet the service requirements. But with this growth in numbers of radars the effect that they would have upon each other has been rather generally ignored. A basic analysis of the numbers of radars involved in current plans indicates that a very high signal density is developing in all operating areas. A radar receiver in this operating situation will intercept the pulses transmitted by many other radars in the area and will have to contend with the large numbers of false indications which these interfering pulses will cause.

The presence of randomly occurring interfering pulses intercepted by a manned search radar are presently not a primary limitation on the performance of the radar system. These interfering pulses, the transmitted signals of other radars, appear on the PPI scope of a search radar as false targets; however, in nearly all cases proper training of the radar operator permits him to evaluate them correctly, and the overall system (radar-plus-operator) performs properly. In some dense signal environments the training necessary to permit the operator to identify false targets caused by interfering signals may become lengthy. However, he eventually is able to carry out his role as the essential evaluation

element in the radar system. In some locations in England today, where the density of radars is relatively high, the numbers of interfering pulses are so great that a new operator in a GCI radar installation requires approximately one week of training to become familiar with the many false targets presented by the transmissions of other radars.

With the advent of more nearly automatic systems, the presence of false targets becomes a primary limitation on system performance. With new air search radar systems and with guided missile systems the trend is to remove the operator from the system and to substitute automatic computers of various degrees of complexity. In these systems the randomness in space and in time of the false targets makes it extremely difficult if not impossible to handle them properly in the computers. Interfering pulses can cause the performance of these automatic and semi-automatic systems to break down completely. The computers cannot evaluate large numbers of false targets correctly, and the system approaches such a state of saturation that an actual target would very probably be missed. The large numbers of radars now coming into use in our armed services are causing an ever-increasing density of signals which the automatic systems must contend with. Consideration of present radars indicates that a search radar in the X-band would now be confronted with an interference density level of several thousand pulses per second. Acquisition of new radar systems will steadily increase this figure.

The development of a radar receiver that can eliminate large numbers of interfering pulses without a significant loss in its actual target detection capability becomes a matter of paramount concern. If this can be accomplished, then the data actually fed to the computers can be handled correctly resulting in an overall efficient and accurate system

performance. This report is an investigation, by use of a mathematical model, of a method for handling interfering pulses in the radar receiver.

One characteristic of the interfering pulses which can be useful in distinguishing them from target echoes is their randomness of occurrence in space and time. As the rotating antenna of a search radar scans past a target all of the target echoes occur at very nearly the same range. With most present air search radars the antenna rotation rate, the beam width, and the pulse repetition frequency are such that from ten to fifty echo pulses can be expected to be returned from a target in one scan of the antenna. During this short interval of time (approximately 0.05 to 0.1 seconds) the target range cannot change appreciably (in 0.1 second a 1200 knot aircraft travels approximately 70 yards). The interfering pulses which may be intercepted by the radar in this same time interval occur at random, and the probability that more than a very few occur at times corresponding to one range in the search radar becomes very small. It is proposed that this difference between interfering pulses and actual target echoes be utilized in a radar receiver system designed to suppress the false targets.

A receiver with this capability would conceivably be designed with its effective search range divided into discrete range intervals. If each of these range intervals corresponded to the pulse duration, then the returned target echoes would occur in one interval or in two adjacent intervals. A target would be announced only when the number of signals occurring in one range interval in the time equivalent to the antenna scanning past a target exceeded some preassigned number. This number would be established high enough to minimize the probability of a false target indication from randomly occurring interfering pulses while still permitting an actual target to be recognized.

CHAPTER II

SIGNAL DETECTION THEORIES

Before proceeding with a detailed analysis of the performance of a radar receiver of this type it would be well to review the work on radar signal detection theory that has been accomplished in recent years. Workers at the Bell Laboratories and at the RAND Corporation have identified the statistical nature of the noise in a radar receiver and have employed the laws of statistics to develop a theory for the probability of detection of a target.

The basis of all of the theories on the statistical nature of signal detection is the work of S. O. Rice[5]. He has defined the probability distribution function for noise and has developed the distribution functions that describe the effect of filtering.

Both the thermal noise voltage across a resistor and the noise voltage due to the shot effect in a vacuum tube approach a normal distribution when the number of electrons involved per second in the processes tends toward infinity. In practice, it may usually be assumed that the total noise voltage between any two points due to any combination of thermal, shot, and cosmic noise sources can be represented by the distribution function

$$p = \frac{1}{\sqrt{2\pi\psi_o}} \, e^{-v^2/2\psi_o} \qquad (1)$$

where ψ_o is the mean square value of the noise voltage. This distribution is valid provided all elements involved in the composition of the total noise voltage have been linear.

If this noise is now passed through a linear filter of center fre-

quency f_m , having a pass band which is narrow compared to f_m , the output will have an envelope which has a probability density function

$$p = \frac{R}{\psi_o} e^{-R^2/2\psi_o} \tag{2}$$

where R is the amplitude of the envelope. ψ_o is the mean square noise voltage, given by

$$\psi_o = \int_o^\infty w(f) \quad df \tag{3}$$

$w(f)$ is the power spectrum of the filter.

If the input to a filter consists of a sine wave of frequency f_m, as well as noise, then the probability density function of the output envelope is

$$p = \frac{R}{\psi_o} e^{-\frac{(R^2+P^2)}{2\psi_o}} I_o\left(\frac{RP}{\psi_o}\right) \qquad R > 0 \tag{4}$$

$$p = 0 \qquad R < 0$$

where P is the amplitude that the sine wave would have at the output of the filter in the absence of noise and I_o is the modified Bessel function of the first kind.

The envelope of the output has a correlation time which is approximately equal to the reciprocal of the bandwidth of the filter. Thus, it is improbable that the envelope will change by an appreciable percentage in times much less than the correlation time, but it is quite probable that it will change by a goodly percentage in times large compared with the correlation time. It is therefore assumed that values of the envelope $1/\Delta f$ seconds apart are independent, where Δf is the bandwidth of the filter.

Starting with these basic expressions, J. I. Marcum of the RAND Corporation [2] and E. L. Kaplan of Bell Laboratories [1] have

independently developed theories of signal detection by pulsed radar. These two have used slightly different mathematical definitions for the process of detection. For this reason, the mathematical steps leading to the final result are different. The final results in the two developments can be shown to be equivalent.

Marcum assumes that the radar receiver is a linear integrator. In this concept the receiver linearly adds the voltage output of N samples from the rectifier. Because of the time elapsing between sampling, these samples are considered to be independent. The samples are considered to be either of signal-plus-noise or of noise alone. If the sum of the N samples exceeds the bias level calculated from the probability density function for N variates of noise alone, then a signal is said to be present.

The integrator may take the sum of the squares of the N variates, or, in general, the sum of N variates where each variate has been processed by some general function. As long as the same weight is applied to each variate, the integrator is called linear.

The best possible function to produce integrable equations in the development of the detection theory is that given by a square law rectifier. Both Marcum and Kaplan show that linear rectification does not give very different results (about 0.2 db).

In discussing Marcum's results the following terms will be used:

P_{d_N} - probability of detection; the probability that the sum of N samples of signal-plus-noise will exceed the bias level.

Y - integrator output for the sum of N variates.

Y_b - bias level.

X - signal-to-noise power ratio of the input signal.

Γ_N - probability of a false target; the probability that the sum of N samples of noise alone will exceed the bias level.

Since the receiver noise is normally distributed, there is a finite probability that the sum of N noise variates alone will exceed the bias level, Y_b, no matter how high this may be set. This will result in a false target indication, or a false alarm. In Marcum's mathematical model of a radar receiver this bias level is established at a level which will give a desired probability of false alarm from noise alone.

This false alarm probability can be related to the time interval between false alarms. As explained above, values of the receiver output envelope $1/\Delta f$ seconds apart are independent. Since the receiver noise is present at all times, in a time interval T there are $T \cdot \Delta f$ independent chances for a false alarm to occur from noise alone. Thus the probability of the occurrence of at least one false alarm is a function of time. Marcum has chosen to define the false alarm time as the time in which the probability is one-half that noise alone will not exceed the bias level. He has defined the false alarm number as the $T \cdot \Delta f$ independent chances for a false alarm in this false alarm time, T.

With this description of the mathematical model, Marcum's results can be summarized:

$$\Gamma_N = \frac{N}{n} \ln 2 = \frac{N}{n} (0.693) \qquad (5)$$

where n is the false alarm number defined above ($n = T \cdot \Delta f$).

$$\Gamma_N = 1 - I\left(\frac{Y_b}{N}, N - 1\right) \qquad (6)$$

where $I\left(\frac{Y_b}{N}, N-1\right)$ is the incomplete gamma function. Tables of I (u, p) have been compiled by Pearson [4].

In practice n and N are given and the desired result is the bias level Y_b. Since the equation cannot be solved directly for Y_b, computations are facilitated if curves are first plotted showing the general relationship of equations (5) and (6).

Knowing the required bias level for a given false alarm interval, the cumulative probability of detection for N variates of signal-plus-noise is

$$P_{d_N} = \int_{Y_b}^{\infty} \left(\frac{Y}{NX}\right)^{\frac{N-1}{2}} e^{-(Y+NX)} I_{N-1}(2\sqrt{NXY})\, dY \qquad (7)$$

where $I_{N-1}(2\sqrt{NXY})$ is the modified Bessel function.

This integral is not solvable directly in terms of well-known functions. For N = 1 (the probability that one signal-plus-noise pulse, with signal-to-noise ratio X, exceeds the bias level Y_b) the equation has been solved by machine computation at the RAND Corporation. Since this function will be used in later developments, the solution is presented graphically in Figure 54 for various values of Y_b.

For N>1 the solution to the detection integral has been shown to be

$$P_{d_N} = 1 - T_{\sqrt{Y_b}}(2N-1, N-1, \sqrt{NX}) \qquad (8)$$

where $T_B(m,n,r) = 2\, r^{n-m+1}\, e^{-r^2} \int_0^B t^{m-n}\, e^{-t^2}\, I_n(2rt)\, dt$

is the incomplete Toronto function. Curves of this function are available in reference (2).

Peter Swerling, also of the RAND Corporation, has extended Marcum's basic theory in two reports. In the first [6] he has considered the effects of fluctuation in the amplitude of target echo signals on the probability of target detection. In general, two situations were investigated: (1) the target echo signals would have constant amplitude during the time for the radar antenna to scan past a target but would fluctuate independently from scan to scan; and (2) the amplitude of the target echo signals would fluctuate independently from pulse to pulse.

For scan to scan fluctuations Swerling found

$$N = 1, \qquad P_{d_1} = \epsilon^{-\frac{Y_b}{1+\bar{x}}} \tag{9}$$

$$N \quad 1, \qquad P_{d_N} = 1 - I\left[\frac{Y_b}{\sqrt{N-1}}, N-2\right] + \left(1+\frac{1}{N\bar{x}}\right)^{N-1} I\left[\frac{Y_b}{\left(1+\frac{1}{N\bar{x}}\right)\sqrt{N-1}}, N-2\right]\epsilon^{-\frac{Y_b}{1+N\bar{x}}} \tag{10}$$

where I (u, p) is the incomplete gamma function and $\bar{x}$ is the mean over all values. The target range at which there was a 90% probability of detection with scan to scan target echo fluctuations was found to be about 3/5 of that found for constant target echoes. The range for 50% probability of detection with scan to scan fluctuations was about 9/10 of the range for constant echoes.

For pulse to pulse fluctuations Swerling's results were

$$P_{d_N} = 1 - I\left[\frac{Y_b}{(1+\bar{x})\sqrt{N}}, N-1\right] \tag{11}$$

The range for 90% probability of detection with pulse to pulse target echo fluctuations was about 19/20 of that for constant target echoes, and the range for 50% probability of detection was approximately equal to the range for constant echoes.

In Swerling's second report [7] a mathematical analysis was made of a so-called "double threshold" receiver, considering only interference from receiver noise. This is the type of receiver described earlier as having possible advantages in the suppression of false alarms from interfering pulses. The first threshold is the bias level Y_b. The receiver counts the number of pulses which exceed this bias level. A target is declared to be present if this number is at least equal to some fixed number M. If there are N target echoes per scan, then $M \leq N$. The number M is called the second threshold.

If p_X represents the probability that a single signal-plus-noise pulse exceeds the bias level Y_b (as defined in equation (7) and illustrated graphically in figure 54) then Swerling's results can be stated

$$P_{d_N} = \sum_{i}^{N} {}_{M} C_i^N \quad (1 - p_X)^{N-i} \quad p_X^i \qquad (12)$$

where C_i^N stands for the binomial coefficients.

Swerling found that this method has a 0.5 to 1.0 db loss in sensitivity as compared to a normal integrating receiver. He also found that for any N there is an optimum value for M/N which, in the range of interest to present search radar systems, varied from $M/N = 0.6$ for $N = 10$ to $M/N = 0.4$ for $N = 40$.

E. L. Kaplan has assumed the following detection procedure. The

rectified output is sampled at N different instants of time which are far enough apart so that the values of the noise are independent. If the average output at these instants exceeds the average noise level Y by an amount kY or more, a signal is announced. The noise envelope at the output of a narrow band filter has a Rayleigh distribution (equation (2)). The average of N such values (assuming independence) has a chi-square (χ^2) distribution with $2N$ degrees of freedom. This distribution is manipulated to obtain the desired expressions for the results.

In a discussion of these results, u is the standard normal deviate. And, using the previous notation,

$$\Gamma_N = \Pr(u>u_\Gamma) = \int_{u_\Gamma}^{\infty} \frac{e^{-u^2/2}}{\sqrt{2\pi}} \, du$$

$$P_d = \Pr(u>u_p) = \int_{u_p}^{\infty} \frac{e^{-u^2/2}}{\sqrt{2\pi}} \, du$$

For the steady target echo case, Kaplan's results give the signal-to-noise ratio required to achieve the desired probability of detection with the desired false alarm probability.

$$X = \frac{u_\Gamma - u_p}{\sqrt{N}} + \frac{u_p(u_p-u_\Gamma) + (u_\Gamma^2 - 1)/3}{N} \qquad (13)$$

Approximations in the derivations introduce some inaccuracy at $N = 1$. Curves of X as a function of N are plotted in reference (1) for the steady target echo case and for the fluctuating target echo cases. Kaplan discusses the double threshold receiver and concludes that it

requires a signal-to-noise ratio about 1.4 db above that which sufficed for equal performance using averages.

All of this work on signal detection theory has been an application of the statistical theory of receiver noise to the pulsed radar situation. The probability of a false target indication and the false alarm number have been based on noise considerations alone. The effects of interfering pulses from other radars have not been included, although they will obviously increase the numbers of false alarms appreciably.

A very general look at the semi-automatic radar systems coming into operation today indicates a desired false alarm time (false alarms from noise and from interfering pulses combined) in the order of a few minutes. False alarms occurring at intervals of one minute or greater can be handled satisfactorily in the automatic computers. The double threshold receiver will be analyzed for false alarm times of one minute and of ten minutes.

Preliminary analyses of the numbers of interfering pulses occurring in dense signal enviornments indicate that a radar in any one of the present operating bands must be equipped to handle interference amounting to thousands of pulses per second. The double threshold receiver will be analyzed for interference levels of 10,000, 30,000, and 50,000 pulses per second.

CHAPTER III

THE DOUBLE THRESHOLD RECEIVER - NON-FLUCTUATING TARGET ECHOES

A double threshold receiver counts the number of pulses whose amplitude exceeds a preassigned bias level Y_b (first threshold). Beyond this first threshold the pulse amplitude is not considered. If the number of pulses counted in one range gate in N successive radar repetition periods exceeds a preassigned number M (second threshold), a target is declared to be present.

A false alarm occurs when either a burst of noise or an interfering pulse occurs in one range gate on M of N successive repetition periods. To calculate the probability of a false alarm it is necessary first to determine the probability of the single occurrence of a noise pulse or an interfering pulse. This single occurrence probability is then used in a partial sum of the binomial expansion from M to N to arrive at false alarm probability.

In this analysis the envelope of the output is assumed to have a correlation time which is approximately equal to the range gate width. Thus a noise burst occurring in a range gate can be considered as occupying the entire range gate, and values of the envelope in adjacent range gates can be considered to be independent as far as random noise is concerned.

All pulses, both target signals and interfering pulses, are assumed to be of duration equal to the range gate. An interfering pulse occurring at random in the repetition period will not coincide exactly with an established range gate but will overlap so that a portion of the pulse is in each of two successive range gates. Therefore, each pulse is considered to "ring" two adjacent range gates.

As a preliminary step in investigating false alarms from interfering pulses and receiver noise, it is convenient to calculate the effect that this double threshold receiver will have on interfering pulses alone. The following additional terms will be used:

$p_{(1)}$ - the probability that one or more pulses will occur in one range gate.

p_M - the probability that pulses will occur in one range gate on M or more of N successive repetition periods (a false alarm).

σ - number of discrete range gates per second.

η - range gate width, $= 1/\sigma$.

S - average number of random interfering pulses per second.

Assuming a random arrival of interfering pulses (a Poisson Model), the probability that one or more pulses will occur in a chosen range gate is

$$p_{(1)} = 1 - e^{-2S/\sigma} = 1 - e^{-2\eta S} \tag{14}$$

Since in cases considered here $2\eta S \ll 1$, the exponential can be represented by the first two terms of its series expansion, and the desired probability becomes

$$p_{(1)} = 2\eta S \tag{15}$$

Twice the range gate width is used in this expression since a pulse is assumed to ring two adjacent range gates.

The probability of a false alarm in the chosen range gate becomes

$$p_M = \sum_{i=M}^{N} C_i^N \; p_{(1)}^{\,i} \left(1 - p_{(1)}\right)^{N-i} \tag{16}$$

$$P_M = \sum_{i=M}^{N} C_i^N (2\eta S)^i (1 - 2\eta S)^{N-i} \qquad (17)$$

Figures 33 through 41 are working curves that show the partial sum of the binomial expansion [3] from M to N for N = 10, N = 20, and N = 30. After $p_{(1)}$ has been found from the radar characteristics and from the density of interference, the probability of false alarm in a chosen range gate, P_M, can be calculated (equation 16 or 17) by use of these figures.

The receiver is assumed to have σ discrete range gates per second, or σ/f_r discrete range gates in each repetition period. A double threshold radar receiver has σ/f_r possibilities for a false alarm in a time interval equivalent to N repetition periods. The probability of false alarm in this interval is

$$P_{fa} = 1 - e^{-(\sigma/f_r)P_M} \qquad (18)$$

Figure I shows the effect of the second threshold on the probability of false alarm from interfering pulses for N = 10, N = 20, and N = 30. In this figure the number of interfering pulses per second (S) multiplied by the gate width (η) is equal to 0.05 ($S\eta = \delta = .05$). This corresponds to 50,000 interfering pulses per second for a radar with a one microsecond gate width.

Although this figure demonstrates the false alarm situation over a very short period of time, it is useful here to show the effect of varying the second threshold, M, for each value of N. For each N there is a very definite lower value for M below which the double threshold technique offers no advantages in eliminating false alarms. For values of M above this lower limit the probability of false alarm decreases very rapidly with increasing M.

It is now necessary to relate the probability of false alarm to a longer interval of time. In this connection, use will be made of the false alarm time, T_{fa}, previously defined by Marcum (i.e., the time in which the probability is one-half that a false alarm will not occur).

The probability of at least one false alarm in time T is

$$P_{fa}(T) = 1 - \left[(1-p_{M1}) \cdot (1-p_{M2}) \cdot (1-p_{M3}) \cdots (1-p_{Mr})\right] \qquad (19)$$

where p_{M1} is the probability that a false alarm will occur in the first range gate, etc.; and r, the last range gate in the time interval, equals $\frac{T}{N\eta}$.

An interfering pulse is considered to ring two adjacent range gates. Therefore, the probability of false alarm in one range gate is not stochastically independent of the time of occurrence of interfering pulses in either adjacent gate. If a false alarm occurs in one range gate, the probability of a false alarm in an adjacent gate is increased. The effect of this dependence is examined in Appendix I. It is shown that an assumption of independence gives results which are very close, in the cases of interest here, to those that would be obtained by very lengthy calculations which would result from the exact consideration of dependence. Any error acts to make the curves presented here conservative representations of the exact results.

Therefore,

$$P_{fa}(T) = 1 - e^{-rp_M} = 1 - e^{-(\frac{T}{\eta N})p_M} \qquad (20)$$

For false alarm time, T_{fa}, $1 - P_{fa} = \frac{1}{2}$ (21)

$$\frac{1}{2} = e^{-(\frac{p_M}{\eta N})T_{fa}}$$

$$\ln 2 = \left(\frac{P_M}{\eta N}\right) T_{fa} \tag{22}$$

$$T_{fa} = (\ln 2)\left(\frac{Nn}{P_M}\right) \tag{23}$$

now, $n = \frac{T_{fa}}{\eta}$ where n is the false alarm number.

so, $p_M = \frac{N}{n} \ln 2$ (24)

Equation (23) relates p_M to a false alarm time, while equation (24) relates p_M to a false alarm number.

The equations for p_M that have been developed so far have considered only the effects of random interfering pulses. To complete the picture, the effect of receiver noise must be considered. From equation (2), the probability that one noise pulse exceeds the established bias level is

$$p_o = e^{-Y_b} \tag{25}$$

Then the probability that an interfering pulse or, in the absence of such a pulse, a noise pulse will occur in a chosen range gate is

$$p_{(1)} = e^{-Y_b}(1 - 2\eta S) + 2\eta S \tag{26}$$

$$= e^{-Y_b}(1 - 2\delta) + 2\delta$$

And the probability of a false alarm in the chosen range gate is

$$p_M = \sum_{i=M}^{N} C_i^N \; p_{(1)}^{\;i} \; (1 - p_{(1)})^{N-i} \tag{27}$$

Figures 42 through 53 are further working curves based on equations (26) and (24). With a given density of interfering pulses and a given false alarm number, the resulting bias level is shown for various values of M and N.

As shown in the equations above, the bias level, Y_b, is determined

by the level of interference and the desired false alarm time. Once this bias level has been established, it is possible to proceed to the calculation of the probability of detection of a target by the radar. From equation (7), the probability that one signal-plus-noise pulse, with signal-to-noise ratio X, exceeds the bias level Y_b is

$$p_X = \int_{Y_b}^{\infty} e^{-(X+Y)} \, I_o \left(2\sqrt{XY}\right) dY \qquad (28)$$

Figure 54 shows this relationship for various values of Y_b.

Using this single signal probability p_X, the desired probability of detection is the partial sum of the binomial expansion from M to N.

$$P_d = \sum_{i=M}^{N} C_i^N \; p_X^{\,i} \; (1-p_X)^{N-i} \qquad (29)$$

In analyzing the double threshold receiver the false alarm number, n, was chosen as 6×10^7 or 6×10^6, corresponding to false alarm times of one minute or ten minutes, respectively, for a radar receiver having a one microsecond gate width. With the bias level thus established, it is possible to display the relationship between the signal-to-noise ratio, X, required to give a stated probability of detection and the value of the second threshold M. Figures 2 through 10 show this relationship for various values of P_d and N.

In each figure there is evident an optimum value for M. This optimum M is a function of the number of interfering pulses present; it increases, as would be expected, as the interference density increases. When interference is present the curves also show a minimum value for M below which the desired false alarm time cannot be realized.

In each calculation all of the interfering pulses were assumed

to be large enough to pass the first threshold, Y_b. The increase in signal-to-noise ratio required for a constant probability of detection as the numbers of interfering pulses increase is caused by the necessity for raising the first threshold to reduce the effect of the receiver noise. The probability of false alarms from noise must be reduced in this case in order to maintain the specified over-all false alarm time.

On each curve the signal-to-noise ratio required for a single threshold integrating receiver in the absence of interfering pulses is shown. It should be remembered that the specified false alarm time applies to this case only in the absence of interfering pulses. It is not possible to achieve the desired T_{fa} with this type of receiver when interfering pulses are present without such a large increase in bias level that practically all desired echo pulses would be eliminated.

In all these figures, the curves relating to the integrating receiver have been derived from conclusions in reference (2).

In plotting these curves, the bias level, Y_b, and the second threshold, M, were chosen so as to achieve the given false alarm time in the presence of interference. The signal-to-noise ratio required for the stated detection probability was calculated in the absence of interference. No attempt was made to consider the increased probability of detection resulting from the simultaneous reception of an interfering pulse and a target echo pulse. Therefore, the curves represent upper limits for X in the presence of interference and give a conservative representation of the results.

The expected range performance of a radar receiver using the

double threshold technique may be seen by plotting the probability of detection in one scan, P_d, against normalized range, R/R_o. R_o in this expression is the solution to the familiar radar range equation for a signal-to-noise ratio of one. And

$$\frac{R}{R_o} = \frac{1}{(x)^{\frac{1}{4}}} \tag{30}$$

Figures 11, 12, and 13 show these range curves for radar receivers having N = 10, N = 20, and N = 30. In each figure range performance curves are given for three cases: (1) integrating receiver with no interference, (2) double threshold receiver with no interference, and (3) double threshold receiver with a maximum level of interference. The double threshold receiver in conditions of no interference exhibits a range capability approximately 5% below that for an integrating receiver operating under the same conditions. When interference is present the integrating receiver is no longer able to meet the false alarm specifications. The double threshold receiver which is able to achieve the desired false alarm time has a range capability between 5% and 10% below that for the integrating receiver operating with no interference.

The range capability of the double threshold receiver is relatively insensitive to changes in the desired false alarm time. Figures 14 and 15 compare the range performances for several values of false alarm number, n. For a probability of detection of one-half an increase in false alarm number from 10^4 to 10^{10} (corresponding to an increase in false alarm time from 0.01 seconds to nearly 3 hours for a one microsecond range gate radar receiver) results in a loss of maximum range capability of about 20%.

CHAPTER IV

THE DOUBLE THRESHOLD RECEIVER - FLUCTUATING TARGET ECHOES

The expected performance of the double threshold radar receiver with target echo signals which are fluctuating in amplitude can be calculated with the results of the previous section as a basis. Rather detailed pulse studies of the target echo signals from aircraft indicate that the most reasonable probability density for the signal-to-noise power ratio is

$$p_{(X,\,\overline{X})} = \frac{1}{\overline{X}}\, e^{-X/\overline{X}} \qquad X \geq 0 \qquad (31)$$

where X = signal-to-noise power ratio

$\overline{X}$ = average of X over all fluctuations.

This density must be applied to the case where the target echo amplitude fluctuates independently from pulse to pulse, and must be applied to the case where the target amplitude is assumed to be constant for a single scan (N periods) but to fluctuate independently from scan to scan. Most actual targets would probably present fluctuations which were somewhere between these two extreme situations.

From equations (9) and (11), the probability that one signal-plus-noise pulse with average signal-to-noise power ratio $\overline{X}$ exceeds the bias level Y_b is

$$p_X = e^{-Y_b/(1+\overline{X})} \qquad (32)$$

For pulse to pulse fluctuations, the probability of detection in a single scan with a double threshold receiver is

$$P_d = \sum_{i=M}^{N} C_i^N \, p_X^{\,i} \, (1-p_X)^{N-i} \qquad (33)$$

As with the case of the non-fluctuating target echoes, the bias level, Y_b, is determined by the desired false alarm time. This time is not affected by any fluctuations of the target echo signal.

Figures 16 through 21 show the signal-to-noise ratio as a function of the second threshold when pulse to pulse fluctuations are assumed. For comparison purposes the same gate width, false alarm time, and numbers of interfering pulses have been chosen as for the curves in the corresponding non-fluctuating cases. The curves have the same general shape as for the curves in the non-fluctuating situation. Again there is a definite optimum value for M and, when interference is present, there is a definite minimum value for M. This minimum value of the second threshold is the same as for the corresponding non-fluctuating cases. The pulse to pulse target fluctuations cause an increase in the signal-to-noise ratio that is required to achieve a stated probability of detection for values of M approaching N, as compared to the non-fluctuating target echoes. Note that this increase made it necessary to use a two cycle logarithmic scale for X, while a one cycle logarithmic scale has been adequate for all previous figures.

Figures 22 through 24 show the probability of detection as a function of the normalized range when pulse to pulse target fluctuations are considered. These curves correspond to figures 11 through 13 for the non-fluctuating case. A comparison of the three figures indicates that the optimum range performance relative to an integrating radar receiver requires use of high values of N when pulse to pulse fluctuations are present. For N = 30 the double threshold receiver with no pulse interference has a maximum range loss of about 10% relative to an

integrating receiver. For high interference levels this double threshold receiver has a range loss of about 20% relative to an integrating receiver operating without interference.

When scan to scan target fluctuations are considered, the expression for the probability of detection becomes

$$P_d = \int_0^\infty \frac{1}{\bar{X}} e^{-X/\bar{X}} P_d' \, dX \qquad (34)$$

where P_d' is the detection probability for the corresponding non-fluctuating case. This expression cannot be solved in closed form and graphical integration methods have been used to obtain P_d. Figures 25 through 27 show the probability of detection as a function of the normalized range for scan to scan fluctuations. The range performance of the double threshold radar receiver relative to the integrating receiver is seen to correspond approximately to the non-fluctuating case. A range loss of 5% to 10% occurs in the double threshold receiver as compared to the interference-free integrating receiver. This range performance is seen to be apparently independent of N.

A comparison of the fluctuating and non-fluctuating target echo cases is shown in Figure 28. For reasonably high probabilities of detection, target fluctuation is seen to have a very great effect on range performance. These curves correspond in shape and in relative position to those computed by Swerling for the integrating radar receiver [6].

CHAPTER V

ANTENNA BEAM SHAPE EFFECTS

The effect of the beam shape as a radar antenna scans past the target can be considered as a pulse to pulse fluctuation with a probability density function determined by the squared power pattern (the two-way pattern). A reasonable assumption for the beam shape is

$$f(\Theta) = X = X_m e^{-\alpha\Theta^2} \qquad \text{for } X \geq \tfrac{1}{4}X_m \qquad (35)$$

where X_m is the signal-to-noise power ratio at the center of the beam. The details of the derivation of the beam density function are given in Appendix II. The resulting beam density function is

$$p_b = \frac{0.423}{X\sqrt{\ln X_m/X}} \qquad \tfrac{1}{4}X_m \geq X \geq X_m \qquad (36)$$

Graphical integration methods were used to determine the probability of detection. Figures 29 through 32 show the X vs. M curves for N = 10 and N= 20, comparing the curves obtained in the non-fluctuating case with those obtained by considering beam shape losses.

Consideration of beam shape does not alter the general shape of the curves. It introduces a constant loss in all curves. The effect of beam shape can be included in range calculations by applying a 1.5 db correction to the signal-to-noise power ratio.

CHAPTER VI

CONCLUSIONS

Analysis of the figures of performance of the double threshold type of radar receiver lead to the following general conclusions:

1. The double threshold technique permits the retention of any reasonable false alarm time in the presence of large numbers of interfering pulses.

2. Reasonable false alarm times are not possible with an integrating radar receiver in the presence of large numbers of interfering pulses. The double threshold receiver which does give the desired false alarm time results in a loss of maximum radar range of from 5% to 10% as compared to the integrating receiver operating in the absence of interference.

3. For any value of N, the number of target echoes which are received when an antenna scans past the target, there is an optimum value of M, the second threshold number. This optimum M increases with increase in the number of interfering pulses which must be handled.

4. For any number of interfering pulses there is a minimum value of M below which the desired false alarm time cannot be realized.

5. Fluctuation in the amplitude of target echoes results in minor modifications in the value of M which is optimum, but fluctuation does not alter the minimum value of M which permits desired operation.

BIBLIOGRAPHY

1. Kaplan, E. L., "Signal-Detection Studies, with Applications", The Bell System Technical Journal, Vol. 34 (March 1955), p. 403.

2. Marcum, J. I., A Statistical Theory of Target Detection by Pulsed Radar, The RAND Corporation, Research Memorandum RM-754, Dec. 1, 1947; and A Statistical Theory of Target Detection by Pulsed Radar: Mathematical Appendix, The RAND Corporation, Research Memorandum RM-753, July 1, 1948.

3. National Bureau of Standards, Tables of the Binomial Probability Distribution, Washington: U.S. Government Printing Office, 1949

4. Pearson, K., Tables of the Incomplete Gamma Function, Cambridge University Press, 1946.

5. Rice, S. O., "Mathematical Analysis of Random Noise", The Bell System Technical Journal, Vol. 23 (October 1944) and Vol. 24 (January 1945).

6. Swerling, P., Probability of Detection for Fluctuating Targets, The RAND Corporation, Research Memorandum RM-1217, March 17, 1954.

7. Swerling, P., The "Double Threshold" Method of Detection, The RAND Corporation, Research Memorandum RM-1008, Dec. 17, 1952.

APPENDIX I

STOCHASTIC DEPENDENCE OF FALSE ALARMS IN ADJACENT RANGE GATES

The probability of at least one false alarm in time T is:

$$P_{fa}(T) = 1 - \left[\left(1 - p_{M1}\right)\left(1 - p_{M2}\right)\left(1 - p_{M3}\right) - - - - - -\left(1 - p_{M_r}\right)\right]$$

where p_{M_n} is the probability that pulses will occur in the n-th range gate on M or more of N successive repetition periods (a false alarm in the n-th range gate); and r, the last range gate in the time interval T, equals $\frac{T}{N\eta}$.

The probability of false alarm in one range gate is not independent of the time of occurrence of interfering pulses in either adjacent range gate. If a false alarm occurs in one range gate, the probability of a false alarm in an adjacent gate is increased. However, as only alternate gates are considered, the probabilities of false alarms are stochastically independent.

for even numbered gates - - $P_{fa_{even}} = 1 - \left[\left(1-p_{M_2}\right)\left(1-p_{M_4}\right) - - -\right]$

$$= 1 - e^{-\frac{r}{2} p_M}$$

for odd numbered gates - - $P_{fa_{odd}} = 1 - \left[\left(1-p_{M_1}\right)\left(1-p_{M_3}\right) - - -\right]$

$$= 1 - e^{-\frac{r}{2} p_M}$$

$$P_{fa}(T) = P_{(fa_{even} \text{ or } fa_{odd})}$$

$$= P_{fa_{even}} + P_{fa_{odd}} - P_{(fa_{even} \text{ and } fa_{odd})}.$$

but, $P_{(fa_{even} \text{ and } fa_{odd})} = P_{fa_{even}} \times P(fa_{odd} \mid fa_{even})$

so, $P_{fa}(T) = 2\,(1-e^{-\frac{r}{2}p_M}) - (1-e^{-\frac{r}{2}p_M})(1-e^{-\frac{r}{2}p_M+\alpha})$

where α is the factor showing the increased probability of false alarm in one range gate when there has been a false alarm in an adjacent gate.

$$P_{fa}(T) = 1 - e^{-rp_M} - \alpha\,(1 - e^{-\frac{r}{2}p_M})$$

Now, since $P(fa_{odd} \mid fa_{even}) = (1 - e^{-\frac{r}{2}p_M+\alpha})$

then $0 < \alpha < e^{-\frac{r}{2}p_M}$.

For the values of M, N, and p_M are encountered in this discussion of the double threshold receiver, α was found to be very close to zero. Typical values, obtained by enumerating the ways of obtaining a false alarm in one range gate when a false alarm has occurred in the adjacent gate, are :

N	M	α
10	5	0.35
10	7	0.077
20	10	0.115
20	14	0.0043

By assuming $\alpha = 0$, the curves of false alarm number and of the performance of the double threshold receiver are conservative representations of the exact values. In most cases the difference between the curves obtained by assuming $\alpha = 0$ and by calculating the correct value of α is too small to be shown graphically.

Therefore,

$$P_{fa}(T) = 1 - e^{-rp_M} = 1 - e^{-\left(\frac{T}{\eta N}\right)p_M}.$$

When T equals the false alarm time, T_{fa}, then

$$1 - P_{fa} = \tfrac{1}{2}$$

and

$$\tfrac{1}{2} = e^{-\left(\frac{p_M}{\eta N}\right)T_{fa}}$$

$$T_{fa} = (\ln 2)\left(\frac{N\eta}{p_M}\right).$$

APPENDIX II

DERIVATION OF ANTENNA BEAM SHAPE DENSITY FUNCTION

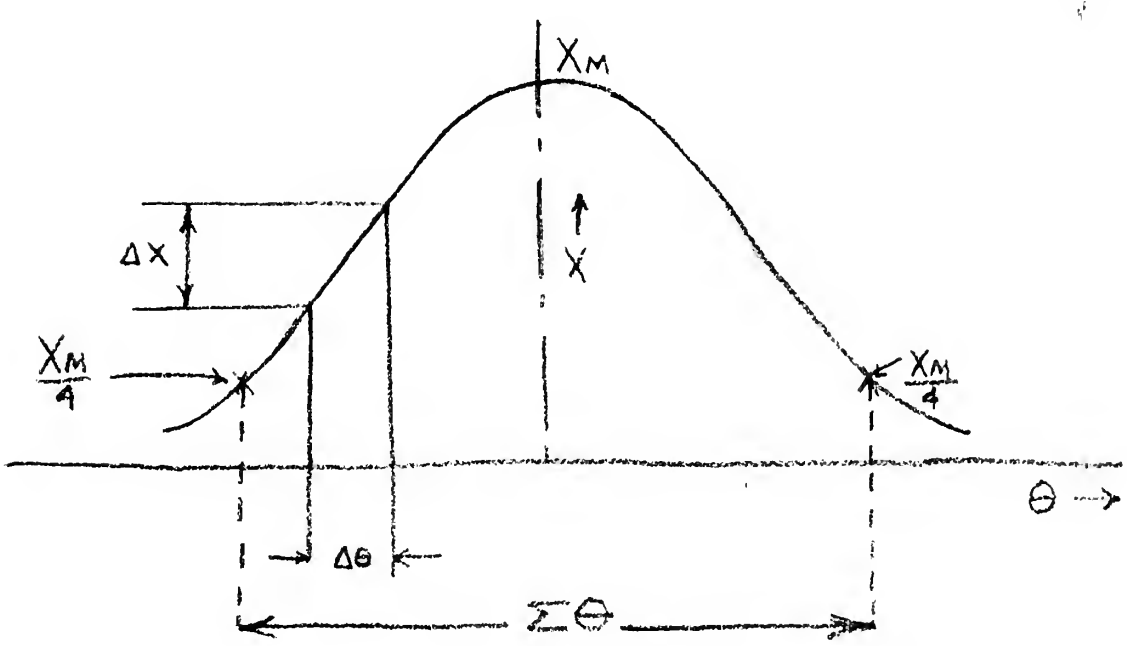

$$X = f(\Theta)$$

$$dx = f'(\Theta)\, d\Theta \qquad \Delta\Theta = \frac{\Delta X}{f'(\Theta)}$$

$$p(X, X+\Delta X) = \frac{\Delta\Theta}{\Sigma\Theta/2} \qquad \text{for} \quad X \geq \frac{X_M}{4}$$

$$= \frac{\Delta X}{f'(\Theta)\,\frac{\Sigma\Theta}{2}}$$

It is reasonable to assume $f(\Theta) = X = X_m e^{-\alpha\Theta^2}$ for $X \geq \frac{1}{4} X_m$.

since the same antenna is assumed for transmitted and received signals, the beamwidth is calculated between the $\frac{1}{4}X_m$ points of this two-way power beam pattern.

$$f'(\theta) = -2\alpha\theta X_M e^{-\alpha\theta^2} = -2\alpha\theta X$$

$$\theta^2 = \frac{1}{\alpha} \ln \frac{X_M}{X}$$

$$f'(\theta) = -2\alpha X \sqrt{\frac{1}{\alpha} \ln \frac{X_M}{X}}$$

$$p(X, X+dx)\,dx = \frac{dx}{2\alpha X \frac{\Sigma\theta}{2} \sqrt{\frac{1}{\alpha} \ln \frac{X_M}{X}}}$$

$$\frac{\Sigma\theta}{2} = \left(f(\theta) \text{ at } X = \frac{X_M}{4} \right)$$

$$\alpha\theta^2 = 1.39$$

$$\theta = \frac{1.18}{\sqrt{\alpha}}$$

$$p(X, X+dx)\,dx = \frac{0.423\,dx}{X \sqrt{\ln \frac{X_M}{X}}}$$

The probability that a single signal-plus-noise pulse will exceed the bias level Y_b is

$$P_X' = \int_{X_M/4}^{X_M} \left(\frac{0.423}{X \sqrt{\ln X_M/X}} \right) p_X \, dx$$

In this equation, p_X is the probability of detection in one range gate if beam shape is not considered. The solution of this beam shape equation for p_X' has been carried out by graphical integration.

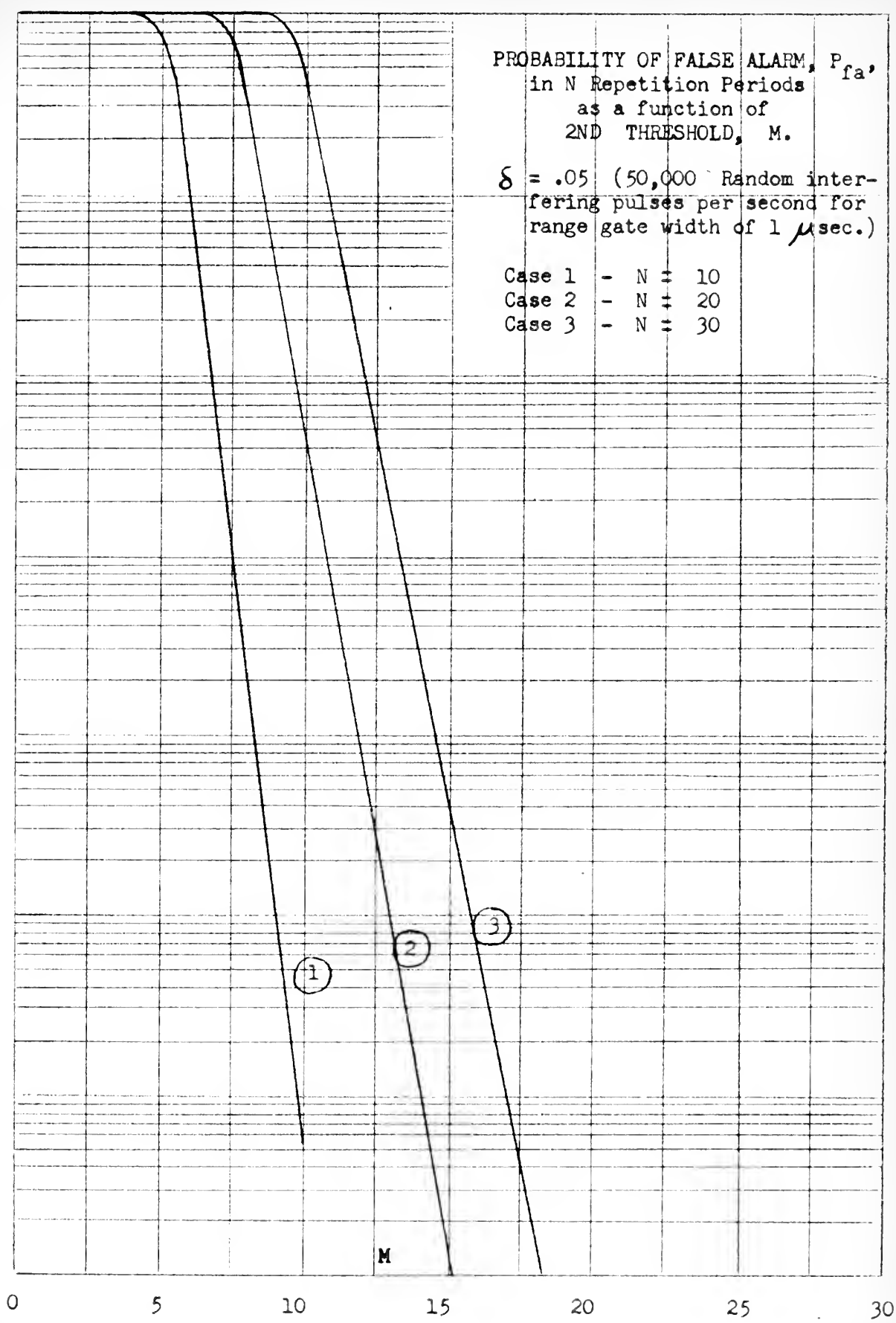
PROBABILITY OF FALSE ALARM, P_{fa}, in N Repetition Periods as a function of 2ND THRESHOLD, M.
δ = .05 (50,000 Random interfering pulses per second for range gate width of 1 μsec.)
Case 1 - N = 10
Case 2 - N = 20
Case 3 - N = 30
1
10^{-1}
10^{-2}
10^{-3}
P_{fa}
10^{-4}
10^{-5}
10^{-6}
10^{-7}
1
2
3
M
0
5
10
15
20
25
30

FIGURE 1

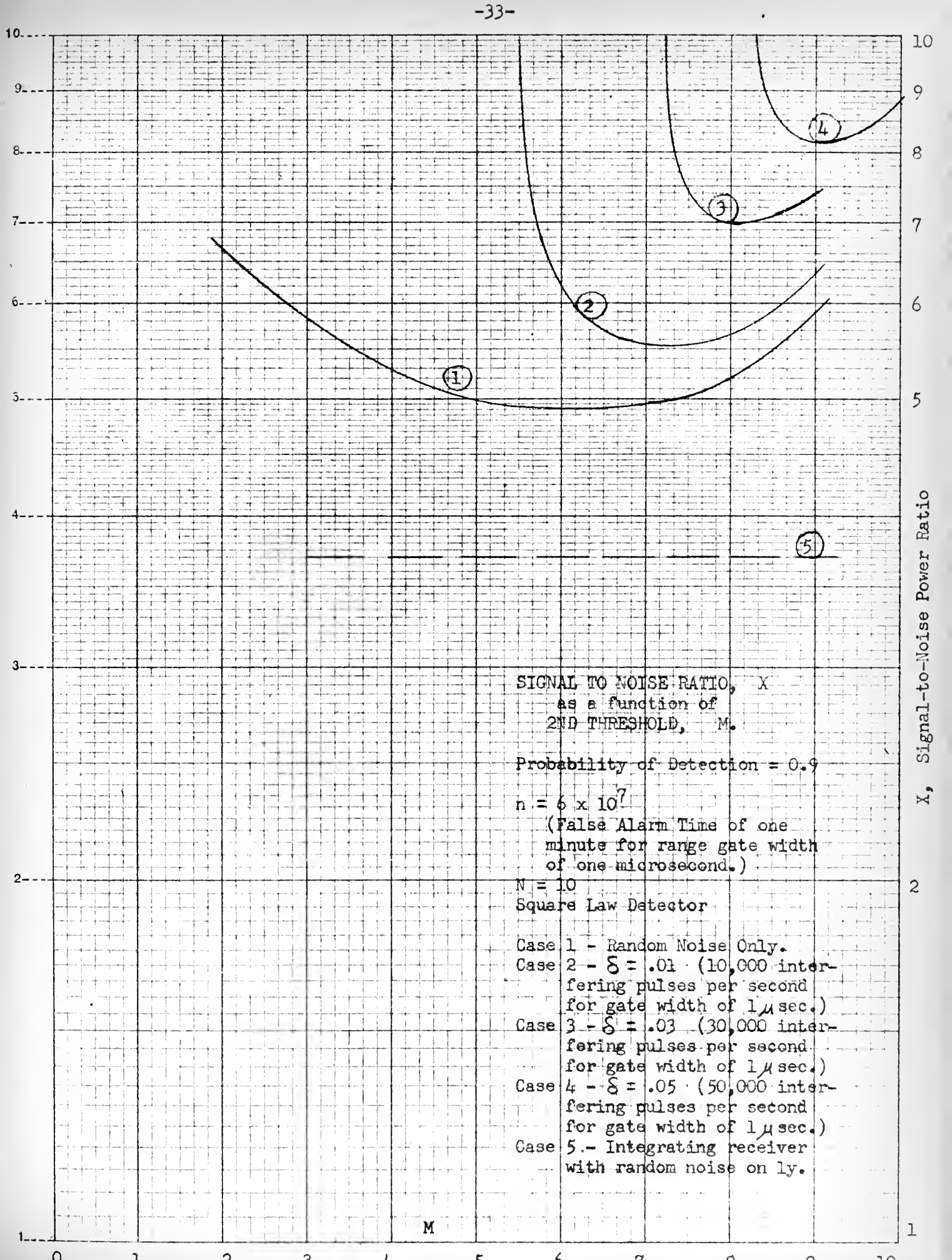
SIGNAL TO NOISE RATIO, X
as a function of
2ND THRESHOLD, M.
Probability of Detection = 0.9
n = 6 x 10^7
(False Alarm Time of one minute for range gate width of one microsecond.)
N = 10
Square Law Detector
Case 1 - Random Noise Only.
Case 2 - δ = .01 (10,000 interfering pulses per second for gate width of 1 μsec.)
Case 3 - δ = .03 (30,000 interfering pulses per second for gate width of 1 μsec.)
Case 4 - δ = .05 (50,000 interfering pulses per second for gate width of 1 μsec.)
Case 5.- Integrating receiver with random noise only.
M
X, Signal-to-Noise Power Ratio
1
2
3
4
5
6
7
8
9
10
0

FIGURE 2

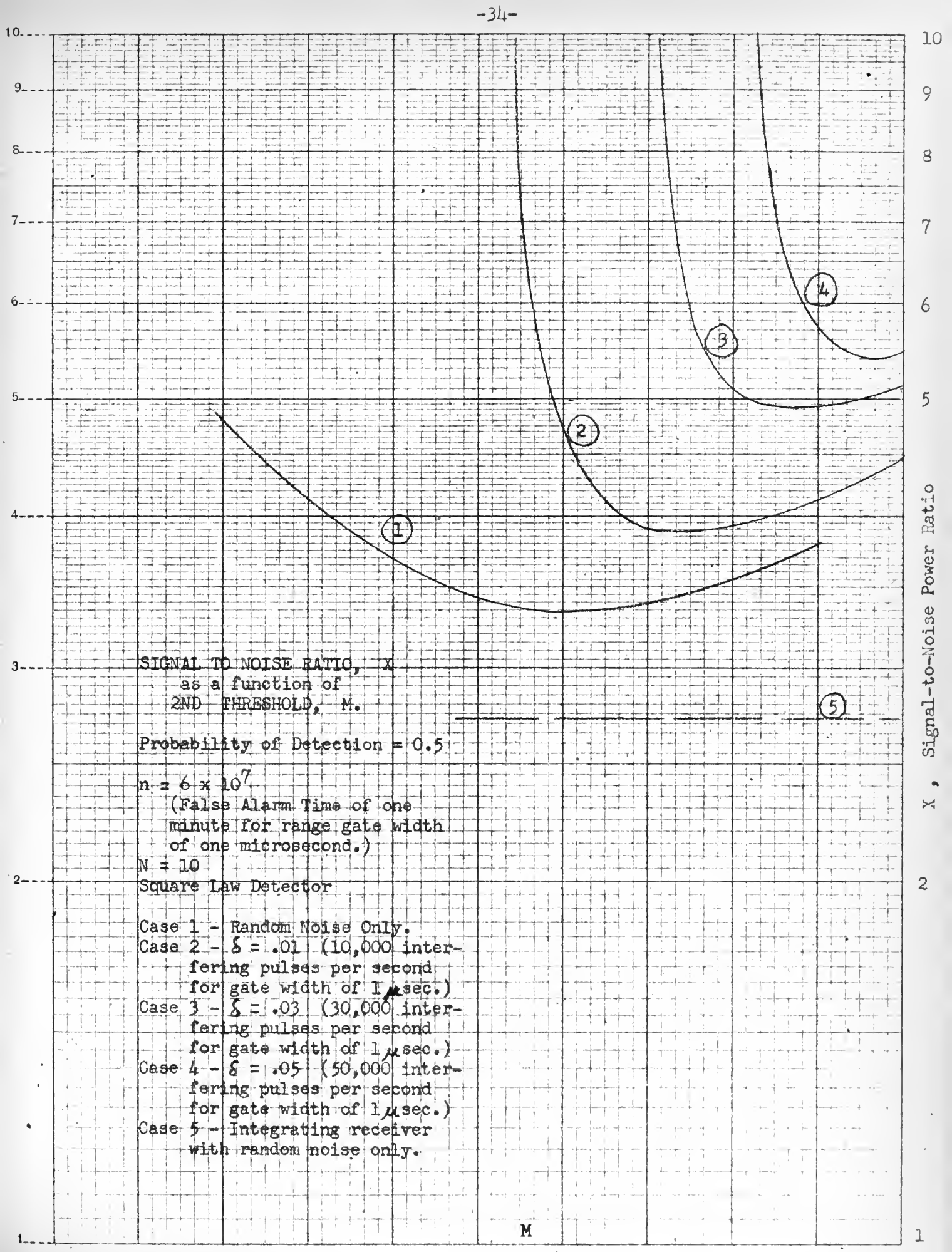
SIGNAL TO NOISE RATIO, X
as a function of
2ND THRESHOLD, M.
Probability of Detection = 0.5
n = 6 x 10^7
(False Alarm Time of one minute for range gate width of one microsecond.)
N = 10
Square Law Detector
Case 1 - Random Noise Only.
Case 2 - δ = .01 (10,000 interfering pulses per second for gate width of 1 μsec.)
Case 3 - δ = .03 (30,000 interfering pulses per second for gate width of 1 μsec.)
Case 4 - δ = .05 (50,000 interfering pulses per second for gate width of 1 μsec.)
Case 5 - Integrating receiver with random noise only.
1
2
3
4
5
M
X, Signal-to-Noise Power Ratio
0 1 2 3 4 5 6 7 8 9 10

FIGURE 3

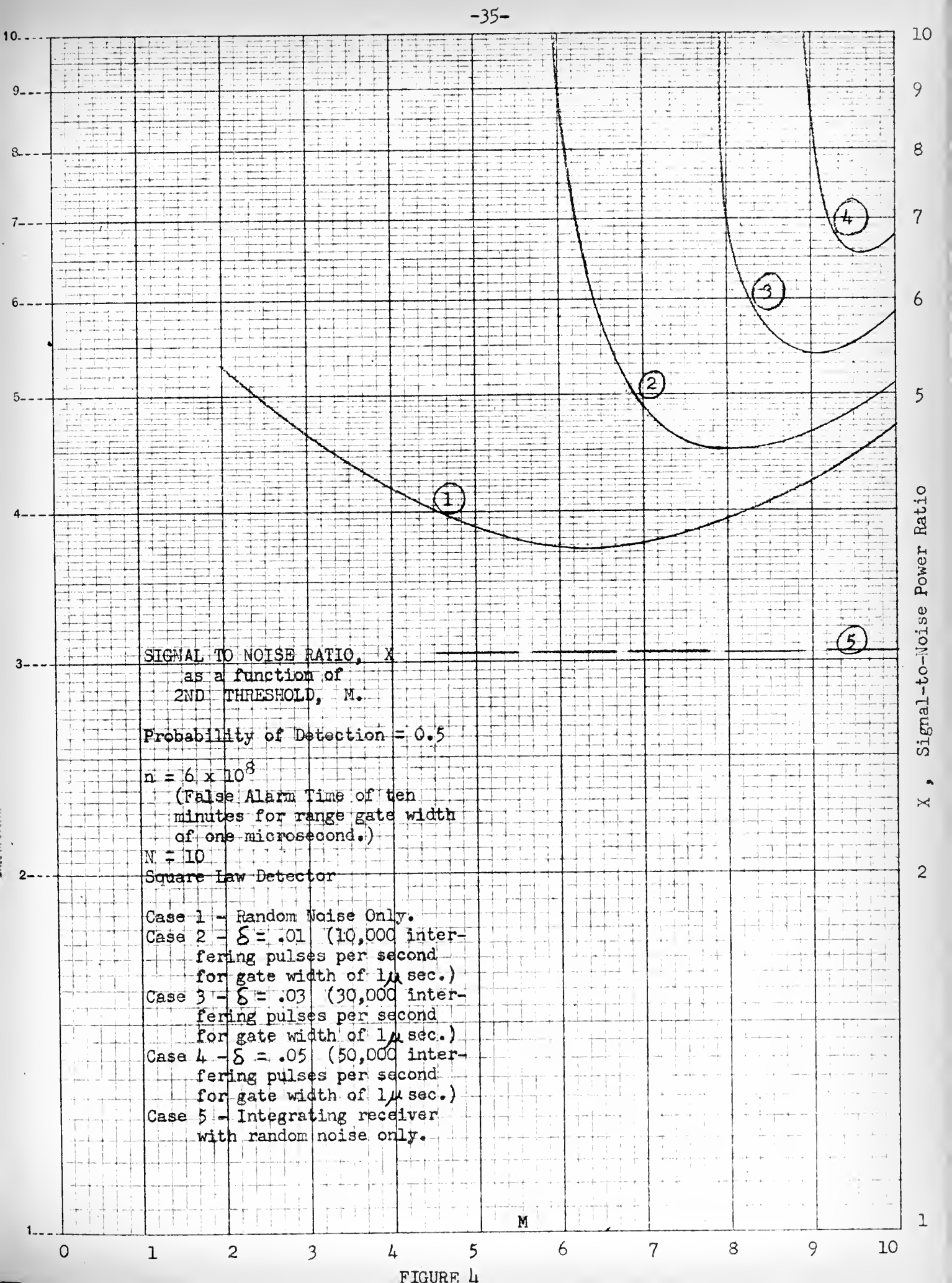
SIGNAL TO NOISE RATIO, X
as a function of
2ND THRESHOLD, M.
Probability of Detection = 0.5
n = 6 x 10^8
(False Alarm Time of ten minutes for range gate width of one microsecond.)
N = 10
Square Law Detector
Case 1 - Random Noise Only.
Case 2 - δ = .01 (10,000 interfering pulses per second for gate width of 1μ sec.)
Case 3 - δ = .03 (30,000 interfering pulses per second for gate width of 1μ sec.)
Case 4 - δ = .05 (50,000 interfering pulses per second for gate width of 1μ sec.)
Case 5 - Integrating receiver with random noise only.
1
2
3
4
5
M
X, Signal-to-Noise Power Ratio

FIGURE 4

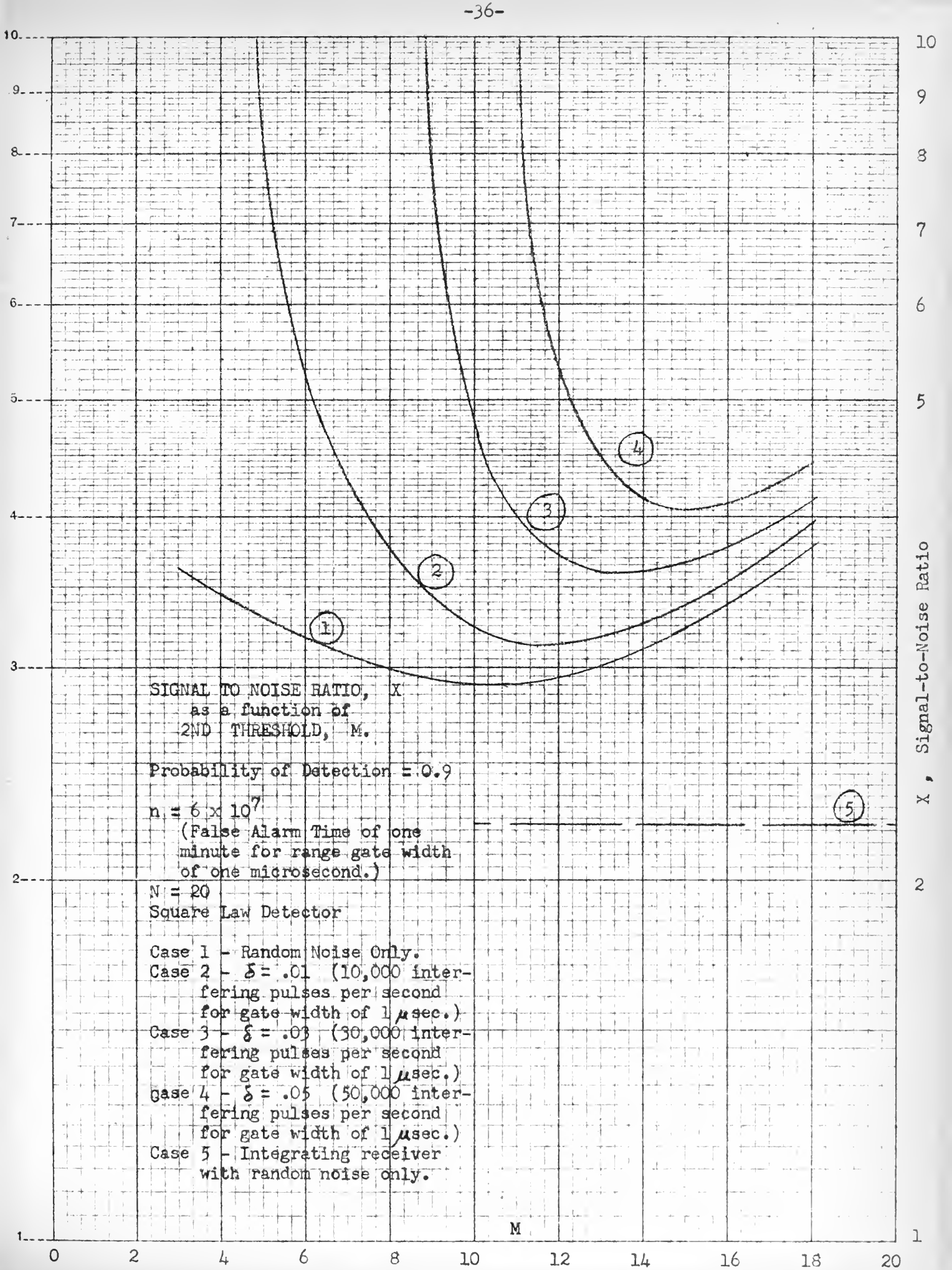
SIGNAL TO NOISE RATIO, X
as a function of
2ND THRESHOLD, M.
Probability of Detection = 0.9
n = 6 x 10^7
(False Alarm Time of one minute for range gate width of one microsecond.)
N = 20
Square Law Detector
Case 1 - Random Noise Only.
Case 2 - δ = .01 (10,000 interfering pulses per second for gate width of 1 μsec.)
Case 3 - δ = .03 (30,000 interfering pulses per second for gate width of 1 μsec.)
Case 4 - δ = .05 (50,000 interfering pulses per second for gate width of 1 μsec.)
Case 5 - Integrating receiver with random noise only.
1
2
3
4
5
M
X, Signal-to-Noise Ratio
0
2
4
6
8
10
12
14
16
18
20

FIGURE 5

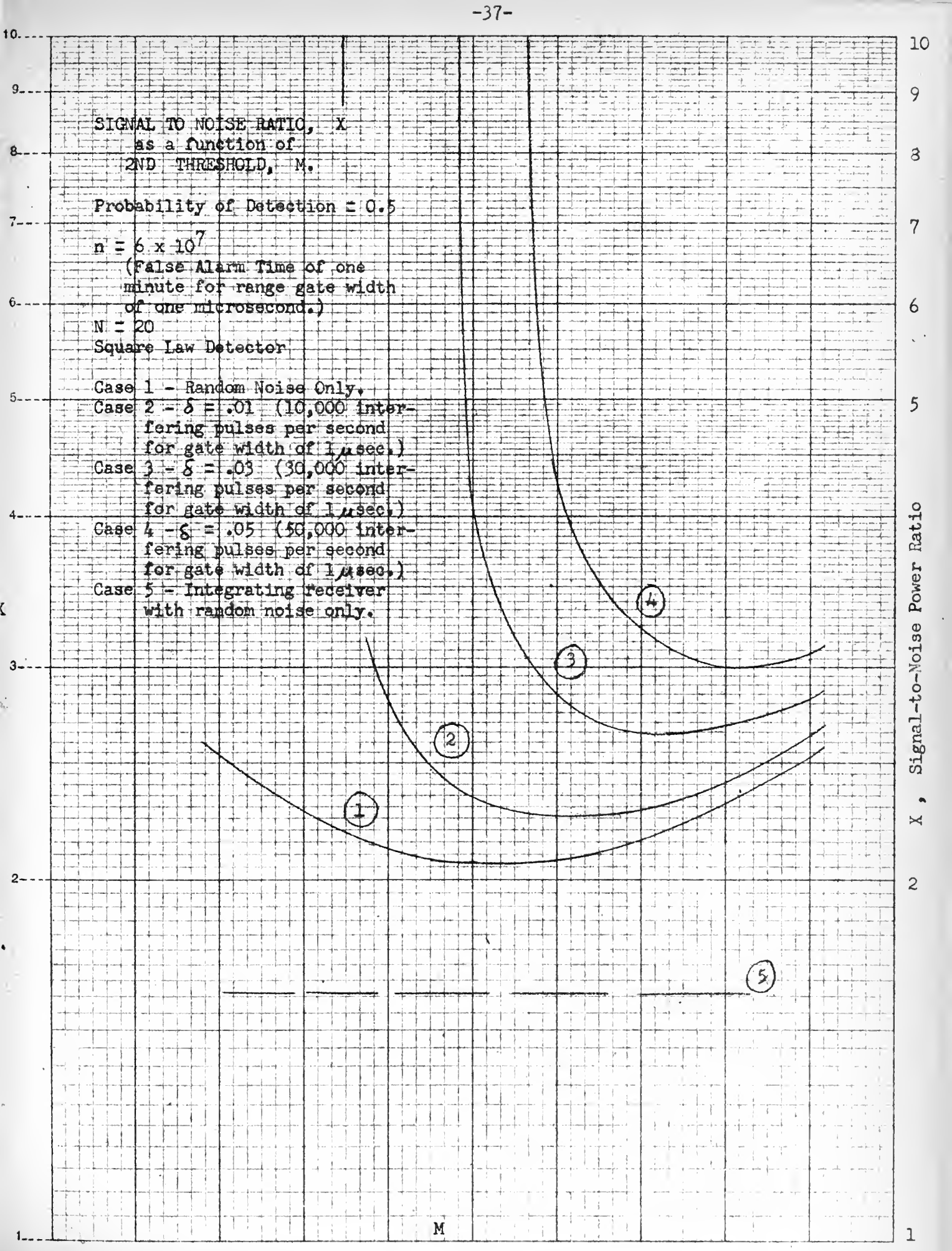
SIGNAL TO NOISE RATIO, X
as a function of
2ND THRESHOLD, M.
Probability of Detection = 0.5
n = 6 x 10^7
(False Alarm Time of one minute for range gate width of one microsecond.)
N = 20
Square Law Detector
Case 1 - Random Noise Only.
Case 2 - δ = .01 (10,000 interfering pulses per second for gate width of 1 μsec.)
Case 3 - δ = .03 (30,000 interfering pulses per second for gate width of 1 μsec.)
Case 4 - δ = .05 (50,000 interfering pulses per second for gate width of 1 μsec.)
Case 5 - Integrating receiver with random noise only.
1
2
3
4
5
M
X , Signal-to-Noise Power Ratio
0
2
4
6
8
10
12
14
16
18
20

FIGURE 6

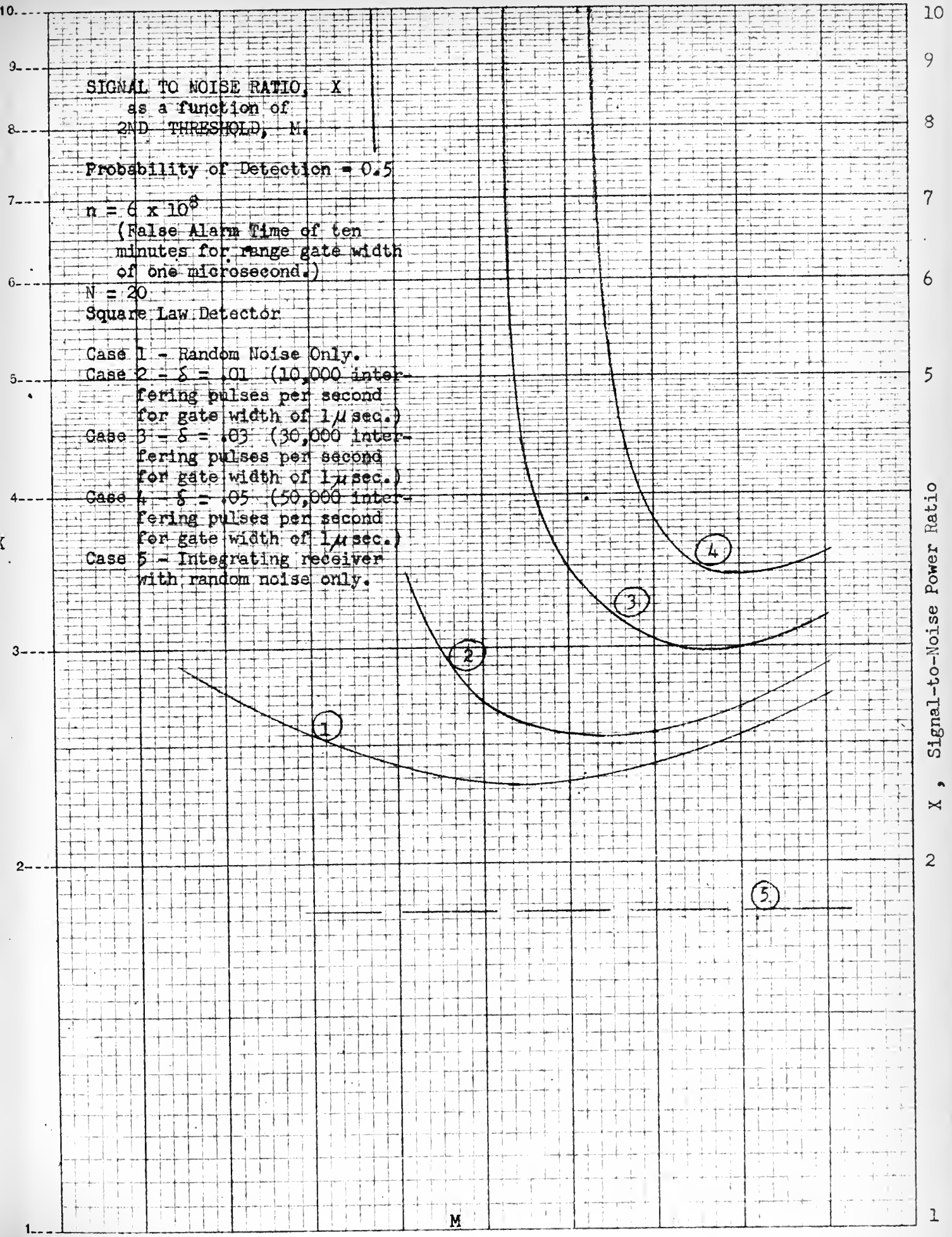
SIGNAL TO NOISE RATIO, X
as a function of
2ND THRESHOLD, M.
Probability of Detection = 0.5
n = 6 x 10^8
(False Alarm Time of ten minutes for range gate width of one microsecond.)
N = 20
Square Law Detector
Case 1 - Random Noise Only.
Case 2 - δ = .01 (10,000 interfering pulses per second for gate width of 1μ sec.)
Case 3 - δ = .03 (30,000 interfering pulses per second for gate width of 1μ sec.)
Case 4 - δ = .05 (50,000 interfering pulses per second for gate width of 1μ sec.)
Case 5 - Integrating receiver with random noise only.
1
2
3
4
5
M
X , Signal-to-Noise Power Ratio
0
2
4
6
8
10
12
14
16
18
20

FIGURE 7

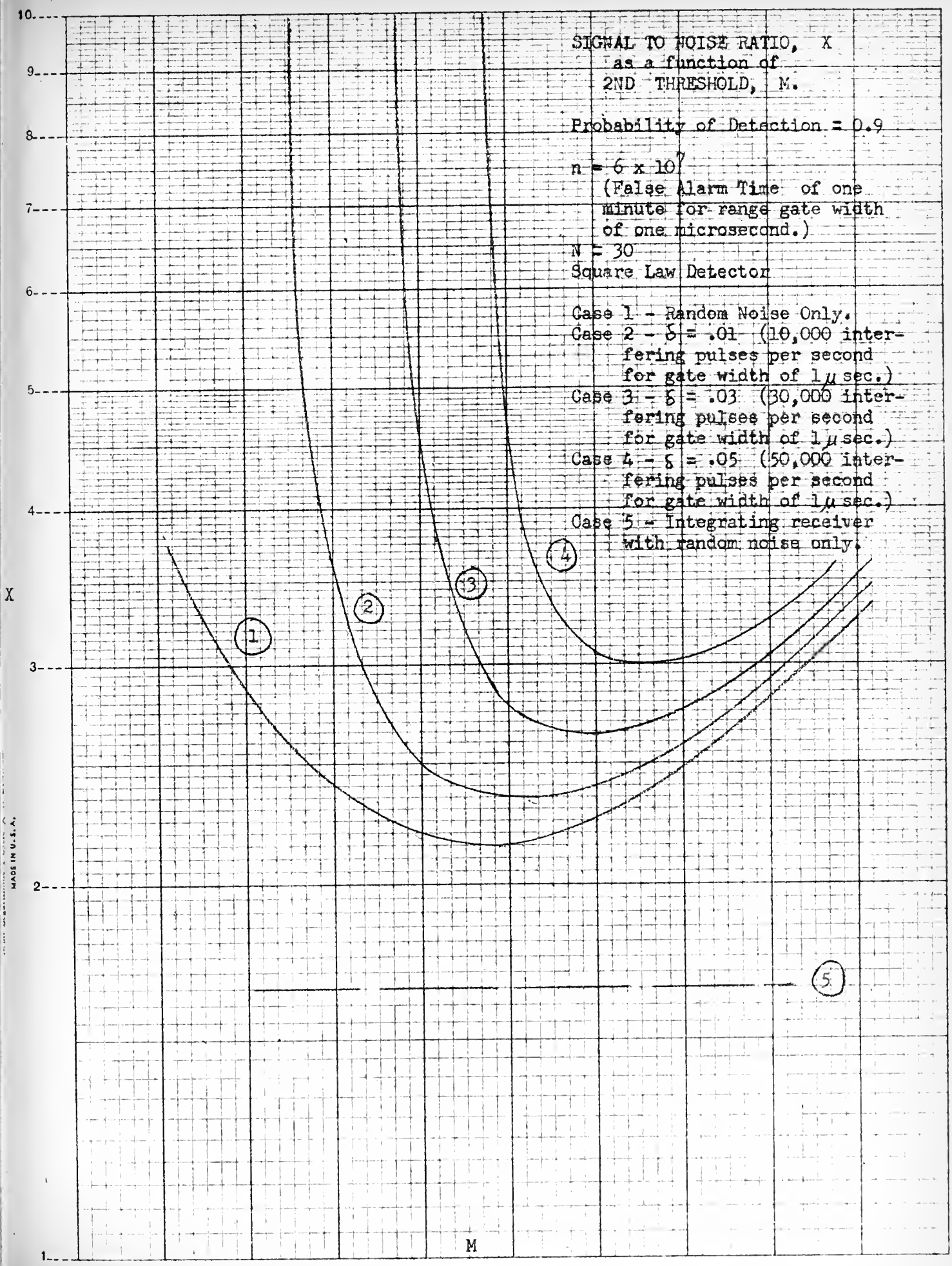
SIGNAL TO NOISE RATIO, X
as a function of
2ND THRESHOLD, M.
Probability of Detection = 0.9
n = 6 x 10^7
(False Alarm Time of one minute for range gate width of one microsecond.)
N = 30
Square Law Detector
Case 1 - Random Noise Only.
Case 2 - δ = .01 (10,000 interfering pulses per second for gate width of 1μ sec.)
Case 3 - δ = .03 (30,000 interfering pulsee per second for gate width of 1μ sec.)
Case 4 - δ = .05 (50,000 interfering pulses per second for gate width of 1μ sec.)
Case 5 - Integrating receiver with random noise only.
1
2
3
4
5
X
M
X , Signal-to-Noise Power Ratio
0
3
6
9
12
15
18
21
24
27
30
1
2
3
4
5
6
7
8
9
10

FIGURE 8

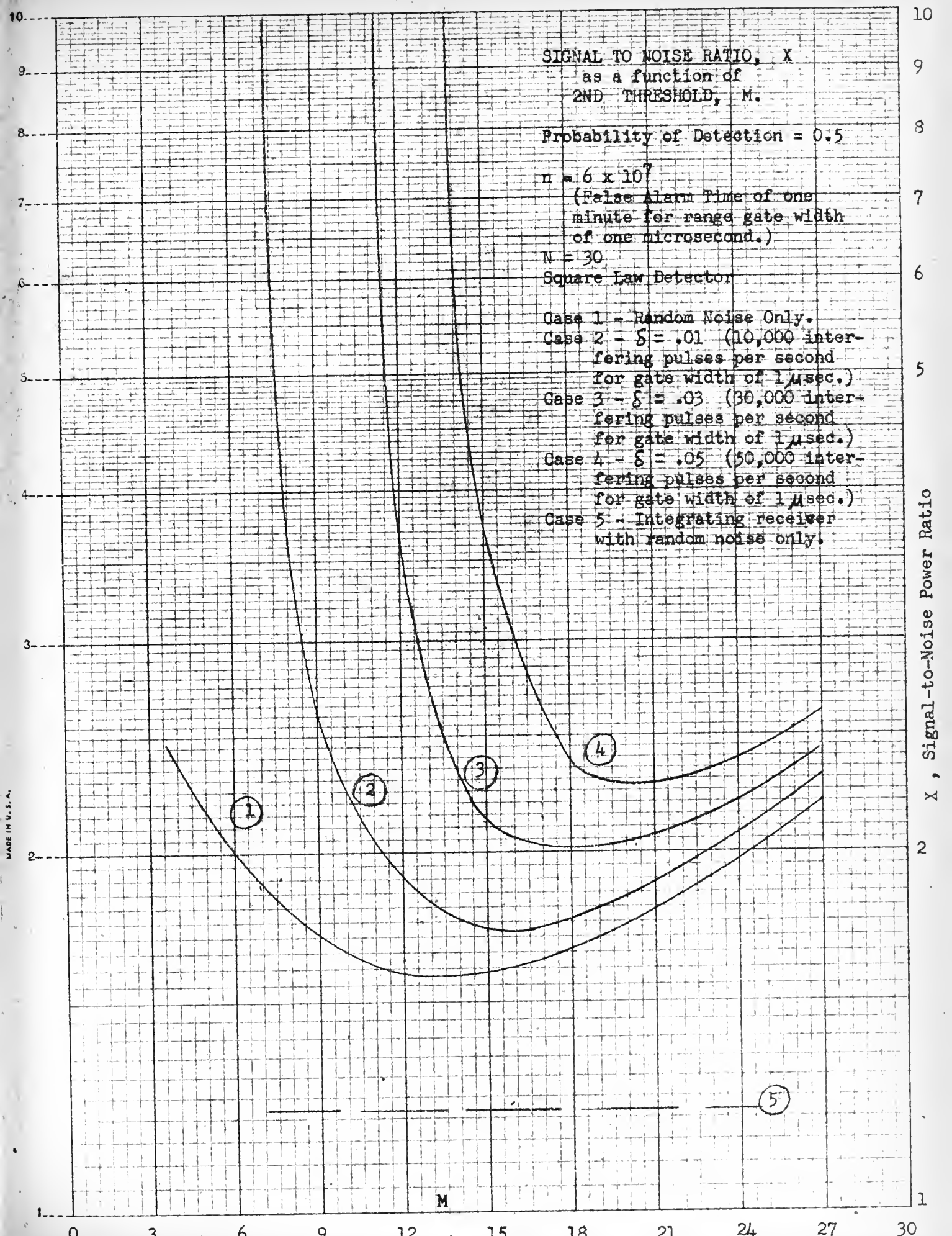
SIGNAL TO NOISE RATIO, X
as a function of
2ND THRESHOLD, M.
Probability of Detection = 0.5
n = 6 x 10^7
(False Alarm Time of one minute for range gate width of one microsecond.)
N = 30
Square Law Detector
Case 1 - Random Noise Only.
Case 2 - δ = .01 (10,000 interfering pulses per second for gate width of 1 μsec.)
Case 3 - δ = .03 (30,000 interfering pulses per second for gate width of 1 μsec.)
Case 4 - δ = .05 (50,000 interfering pulses per second for gate width of 1 μsec.)
Case 5 - Integrating receiver with random noise only.
1
2
3
4
5
M
X , Signal-to-Noise Power Ratio
0
3
6
9
12
15
18
21
24
27
30
1
2
3
4
5
6
7
8
9
10

FIGURE 9

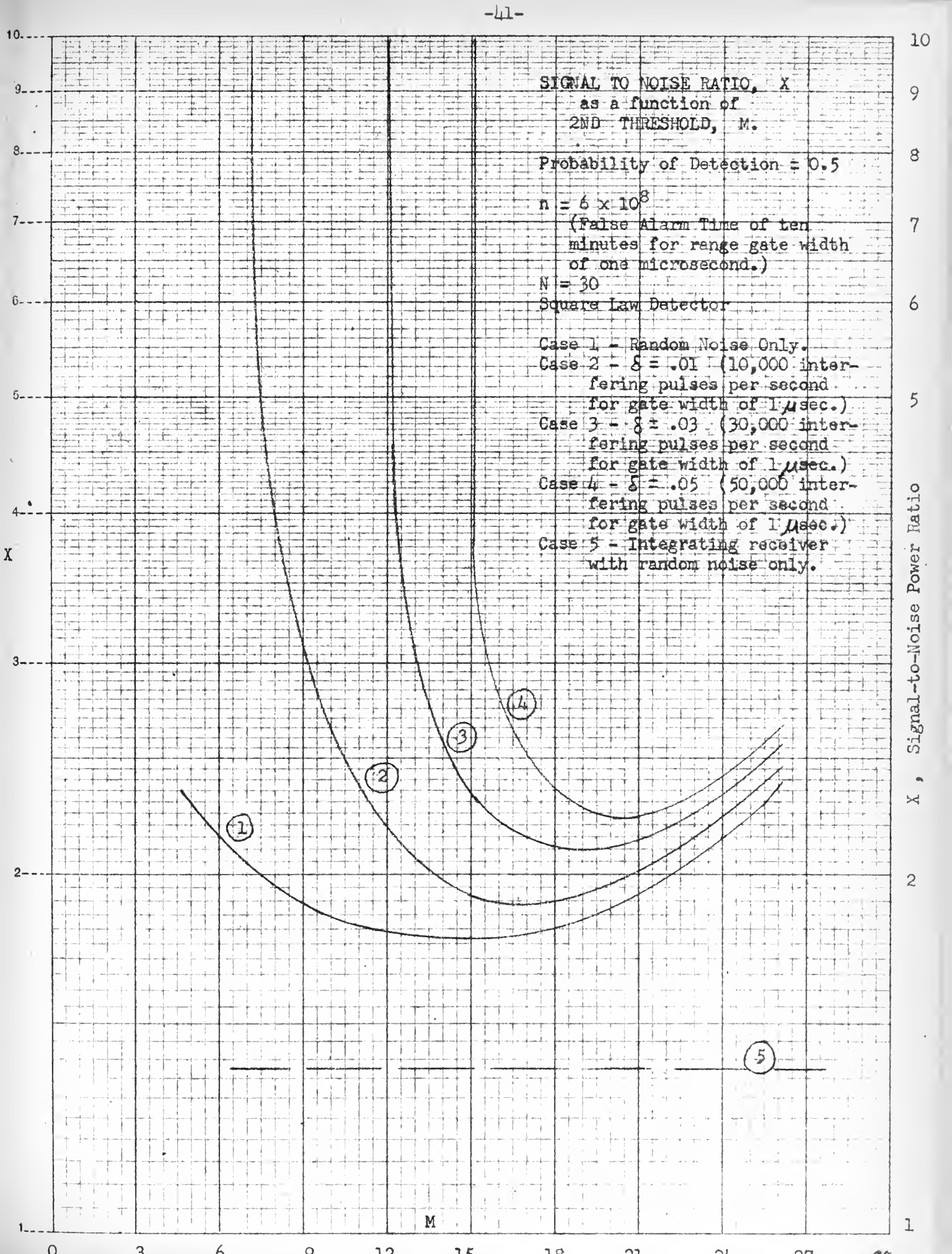
SIGNAL TO NOISE RATIO, X
as a function of
2ND THRESHOLD, M.
Probability of Detection = 0.5
n = 6 x 10^8
(False Alarm Time of ten minutes for range gate width of one microsecond.)
N = 30
Square Law Detector
Case 1 - Random Noise Only.
Case 2 - δ = .01 (10,000 interfering pulses per second for gate width of 1 μsec.)
Case 3 - δ = .03 (30,000 interfering pulses per second for gate width of 1 μsec.)
Case 4 - δ = .05 (50,000 interfering pulses per second for gate width of 1 μsec.)
Case 5 - Integrating receiver with random noise only.
X
M
X , Signal-to-Noise Power Ratio
1
2
3
4
5
10
9
8
7
6
5
4
3
2
1
0
3
6
9
12
15
18
21
24
27
30

FIGURE 10

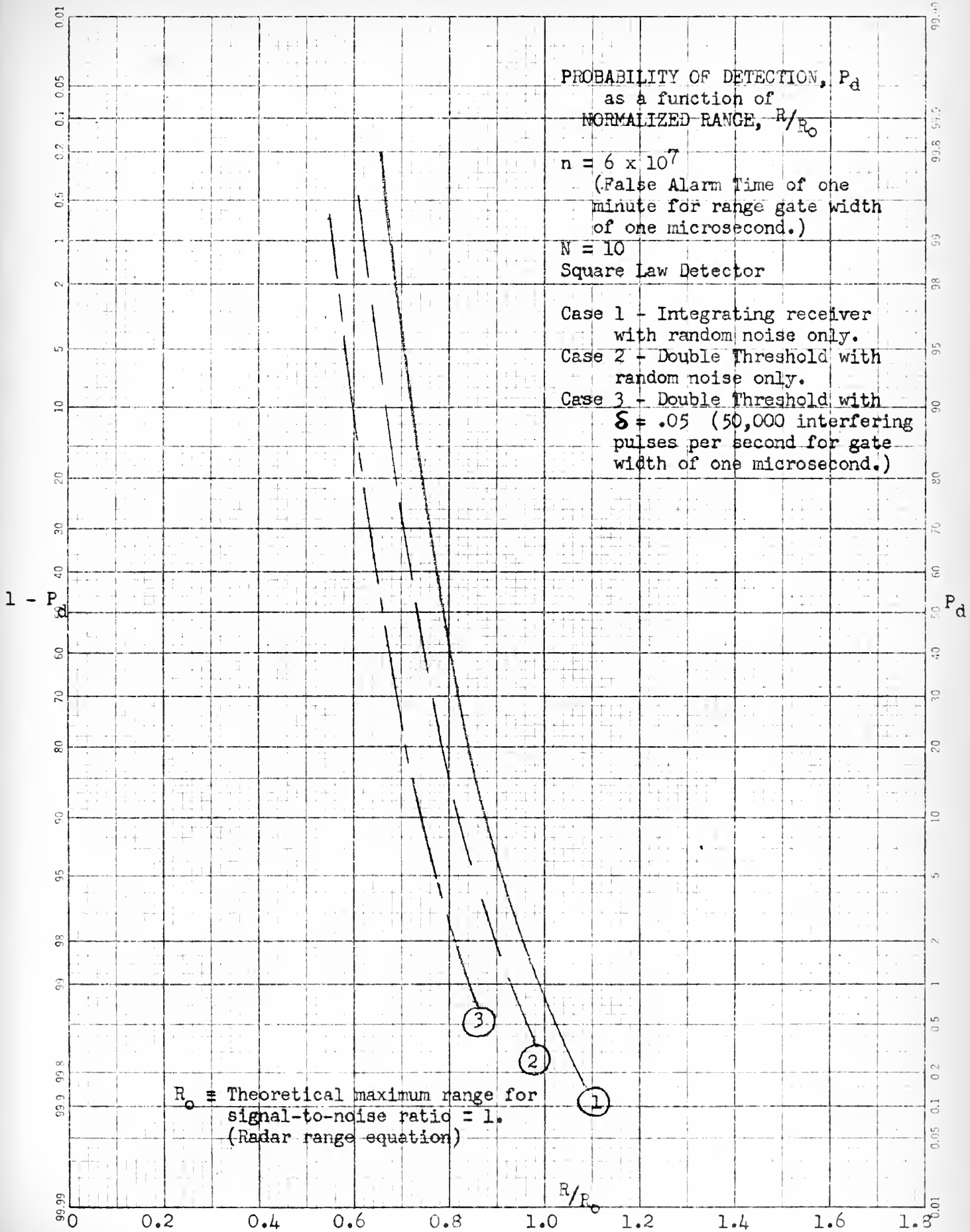
PROBABILITY OF DETECTION, P_d
as a function of
NORMALIZED RANGE, R/R_o
n = 6 x 10^7
(False Alarm Time of one minute for range gate width of one microsecond.)
N = 10
Square Law Detector
Case 1 - Integrating receiver with random noise only.
Case 2 - Double Threshold with random noise only.
Case 3 - Double Threshold with δ = .05 (50,000 interfering pulses per second for gate width of one microsecond.)
R_o ≡ Theoretical maximum range for signal-to-noise ratio = 1. (Radar range equation)
1 - P_d
P_d
R/R_o
0
0.2
0.4
0.6
0.8
1.0
1.2
1.4
1.6
1.8
0.01
0.05
0.1
0.2
0.5
1
2
5
10
20
30
40
50
60
70
80
90
95
98
99
99.8
99.99
1
2
3

FIGURE 11

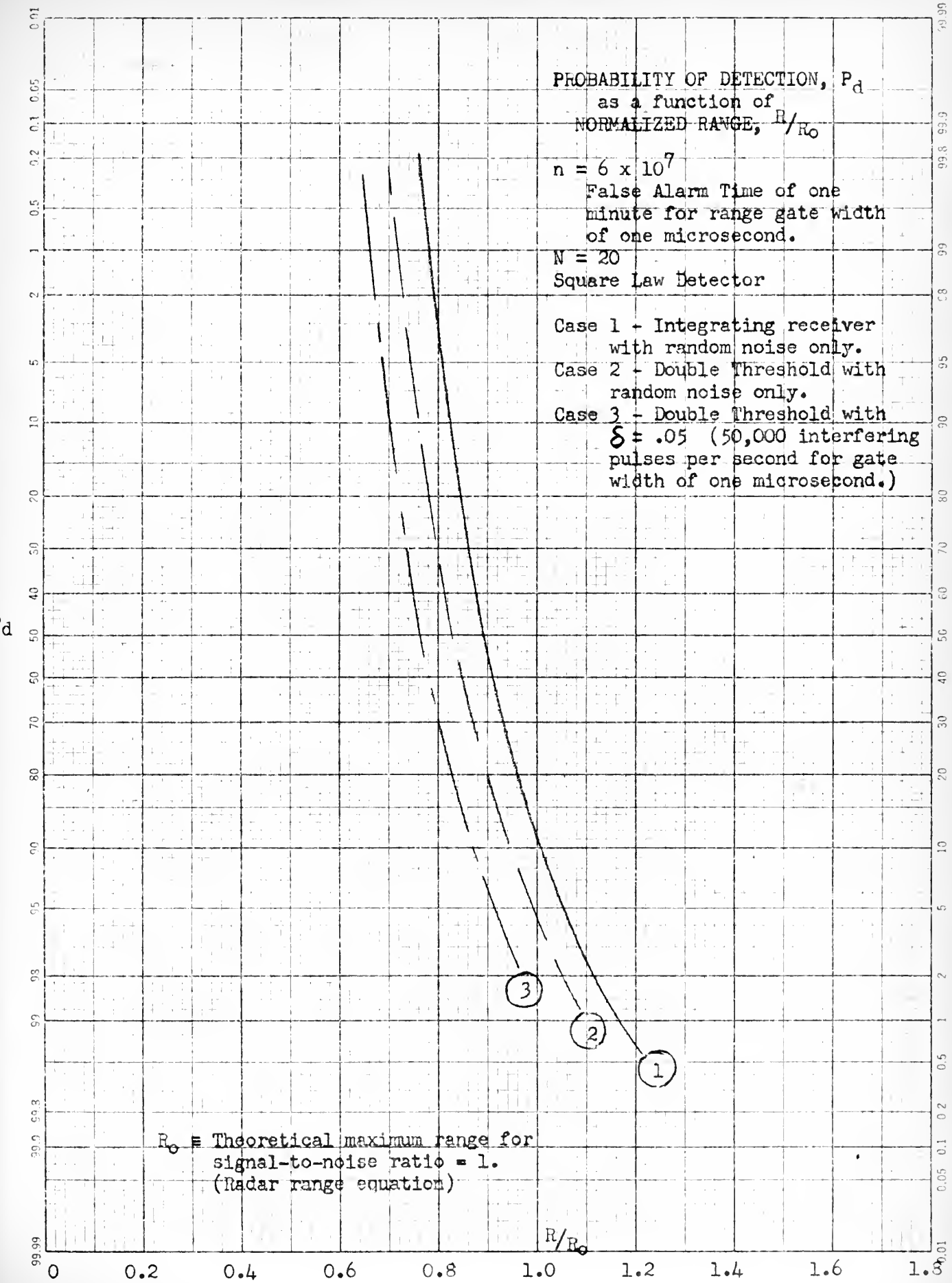
PROBABILITY OF DETECTION, P_d
as a function of
NORMALIZED RANGE, R/R_o
$n = 6 \times 10^7$
False Alarm Time of one minute for range gate width of one microsecond.
N = 20
Square Law Detector
Case 1 - Integrating receiver with random noise only.
Case 2 - Double Threshold with random noise only.
Case 3 - Double Threshold with $\delta = .05$ (50,000 interfering pulses per second for gate width of one microsecond.)
R_o ≡ Theoretical maximum range for signal-to-noise ratio = 1. (Radar range equation)
P_d
R/R_o
0
0.2
0.4
0.6
0.8
1.0
1.2
1.4
1.6
1.8
1
2
3

FIGURE 12

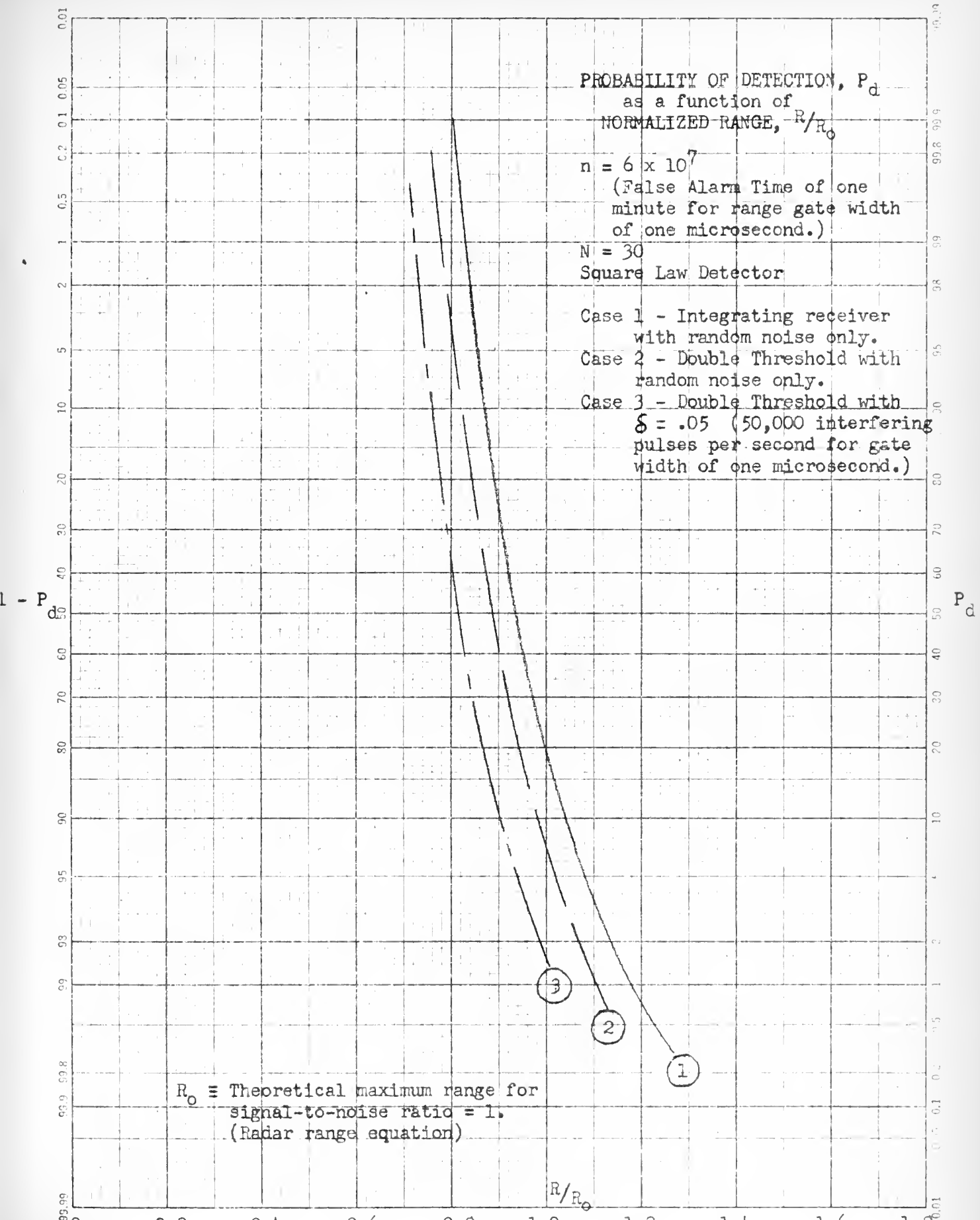
PROBABILITY OF DETECTION, P_d
as a function of
NORMALIZED RANGE, R/R_o
n = 6×10^7
(False Alarm Time of one minute for range gate width of one microsecond.)
N = 30
Square Law Detector
Case 1 - Integrating receiver with random noise only.
Case 2 - Double Threshold with random noise only.
Case 3 - Double Threshold with δ = .05 (50,000 interfering pulses per second for gate width of one microsecond.)
R_o ≡ Theoretical maximum range for signal-to-noise ratio = 1. (Radar range equation)
$1 - P_d$
P_d
R/R_o
0
0.2
0.4
0.6
0.8
1.0
1.2
1.4
1.6
1.8
1
2
3

FIGURE 13

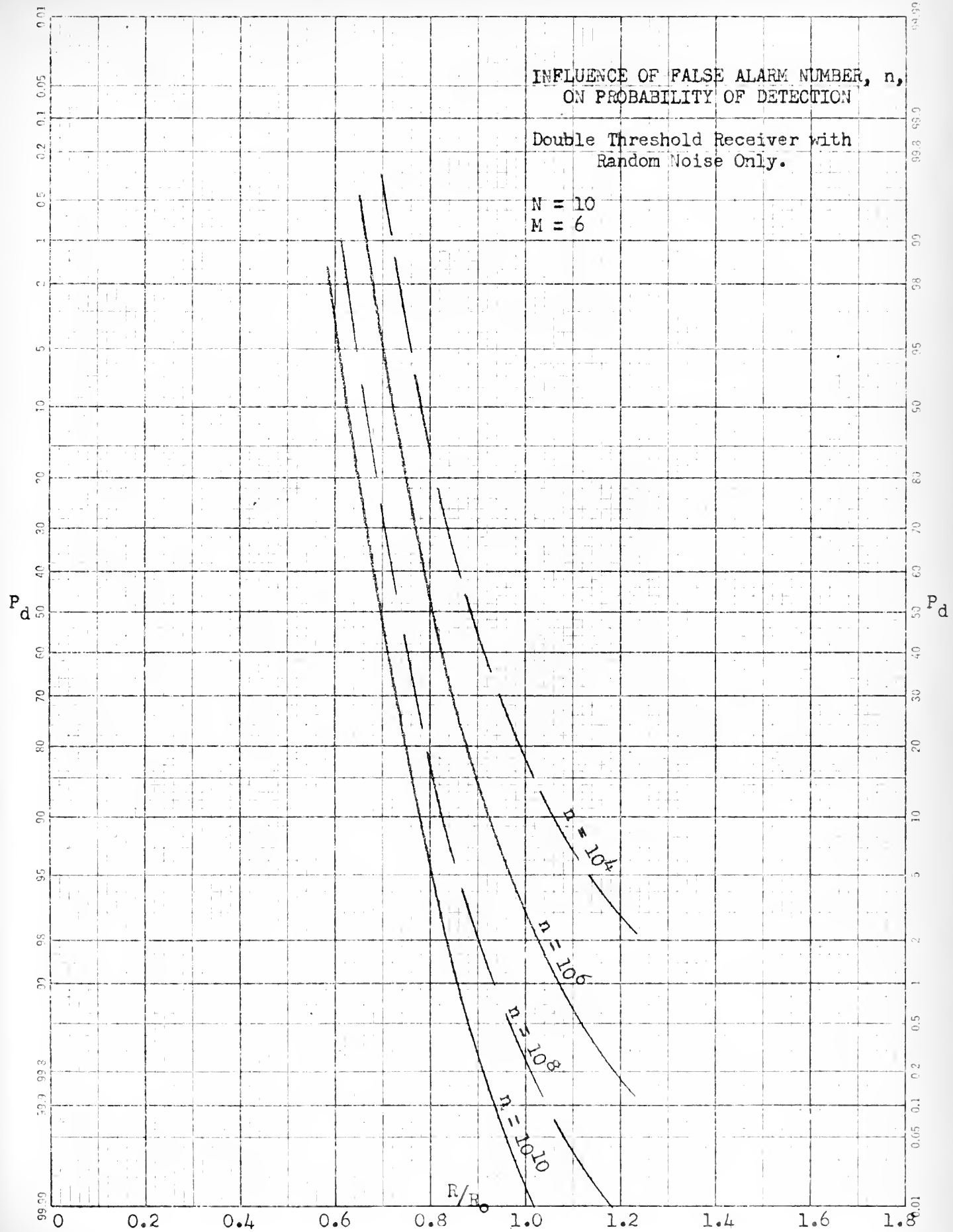
INFLUENCE OF FALSE ALARM NUMBER, n,
ON PROBABILITY OF DETECTION
Double Threshold Receiver with
Random Noise Only.
N = 10
M = 6
n = 10⁴
n = 10⁶
n = 10⁸
n = 10¹⁰
- Pd
Pd
R/Ro
0
0.2
0.4
0.6
0.8
1.0
1.2
1.4
1.6
1.8

FIGURE 14

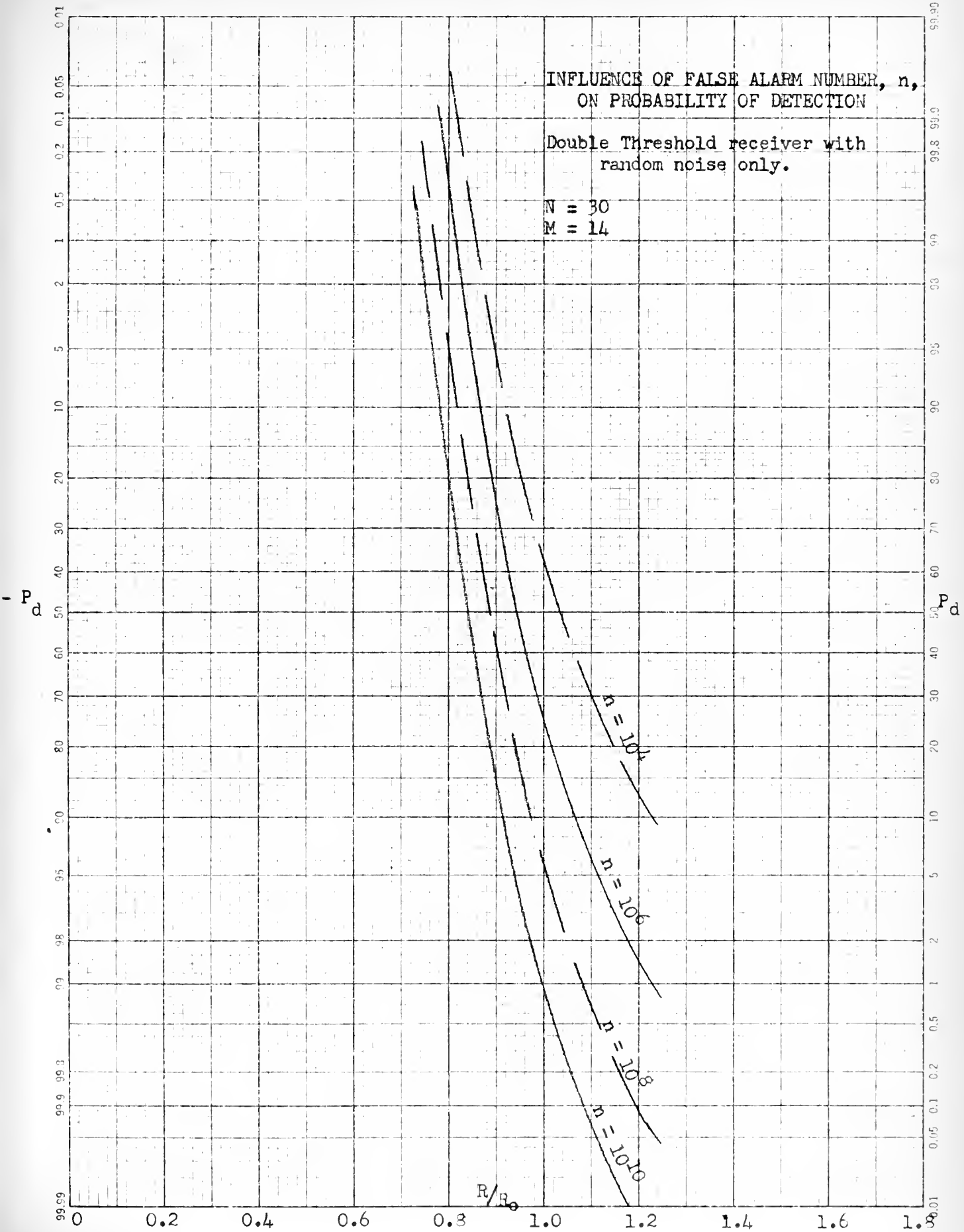
INFLUENCE OF FALSE ALARM NUMBER, n,
ON PROBABILITY OF DETECTION
Double Threshold receiver with
random noise only.
N = 30
M = 14
n = 10^4
n = 10^6
n = 10^8
n = 10^10
- Pd
Pd
R/Ro
0
0.2
0.4
0.6
0.8
1.0
1.2
1.4
1.6
1.8

FIGURE 15

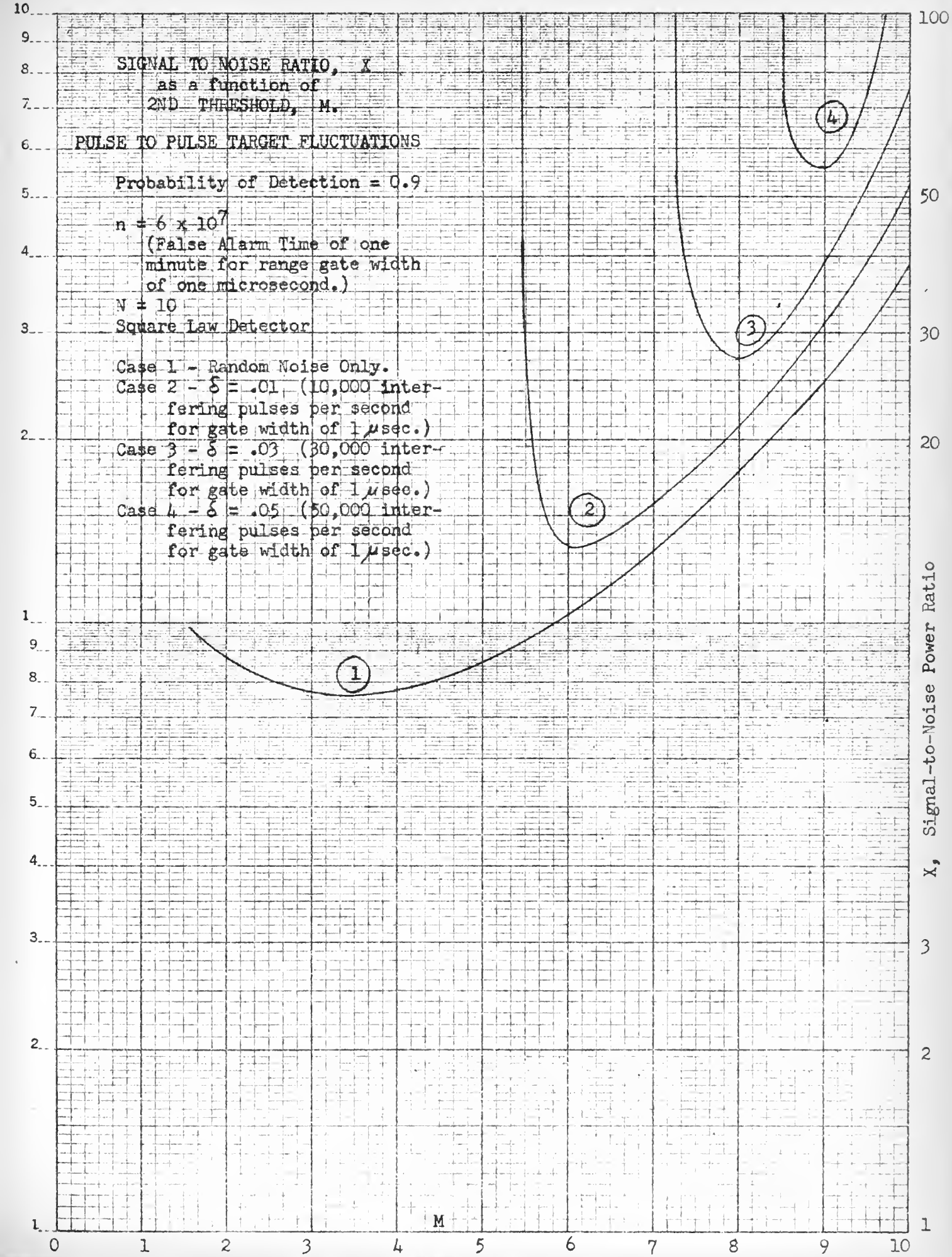
SIGNAL TO NOISE RATIO, X
as a function of
2ND THRESHOLD, M.
PULSE TO PULSE TARGET FLUCTUATIONS
Probability of Detection = 0.9
n = 6 x 10^7
(False Alarm Time of one minute for range gate width of one microsecond.)
N = 10
Square Law Detector
Case 1 - Random Noise Only.
Case 2 - δ = .01 (10,000 interfering pulses per second for gate width of 1 μsec.)
Case 3 - δ = .03 (30,000 interfering pulses per second for gate width of 1 μsec.)
Case 4 - δ = .05 (50,000 interfering pulses per second for gate width of 1 μsec.)
1
2
3
4
M
X, Signal-to-Noise Power Ratio

FIGURE 16

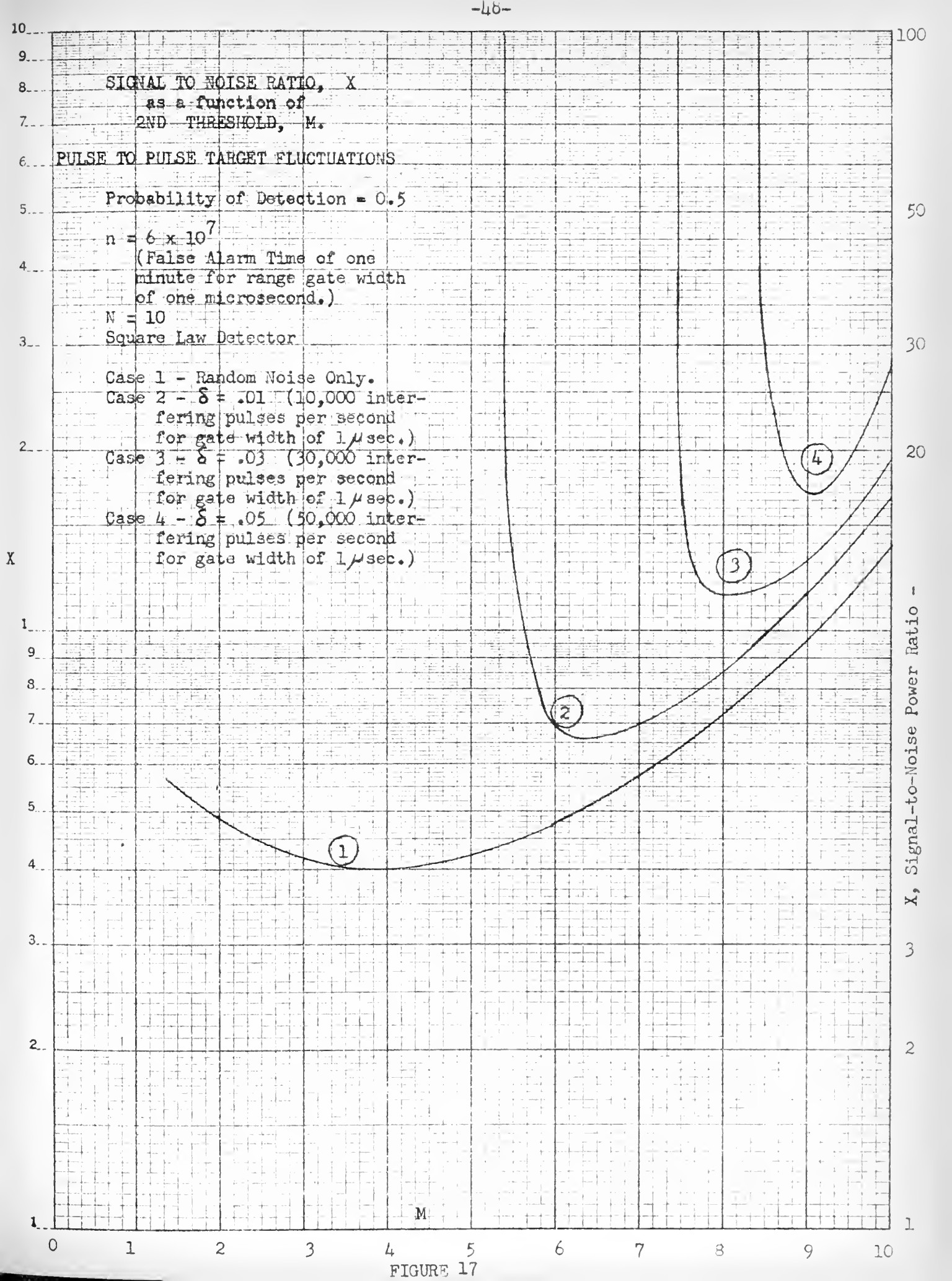
SIGNAL TO NOISE RATIO, X
as a function of
2ND THRESHOLD, M.
PULSE TO PULSE TARGET FLUCTUATIONS
Probability of Detection = 0.5
n = 6 x 10^7
(False Alarm Time of one minute for range gate width of one microsecond.)
N = 10
Square Law Detector
Case 1 - Random Noise Only.
Case 2 - δ = .01 (10,000 interfering pulses per second for gate width of 1 μsec.)
Case 3 - δ = .03 (30,000 interfering pulses per second for gate width of 1 μsec.)
Case 4 - δ = .05 (50,000 interfering pulses per second for gate width of 1 μsec.)
X
M
X, Signal-to-Noise Power Ratio -
1
2
3
4

FIGURE 17

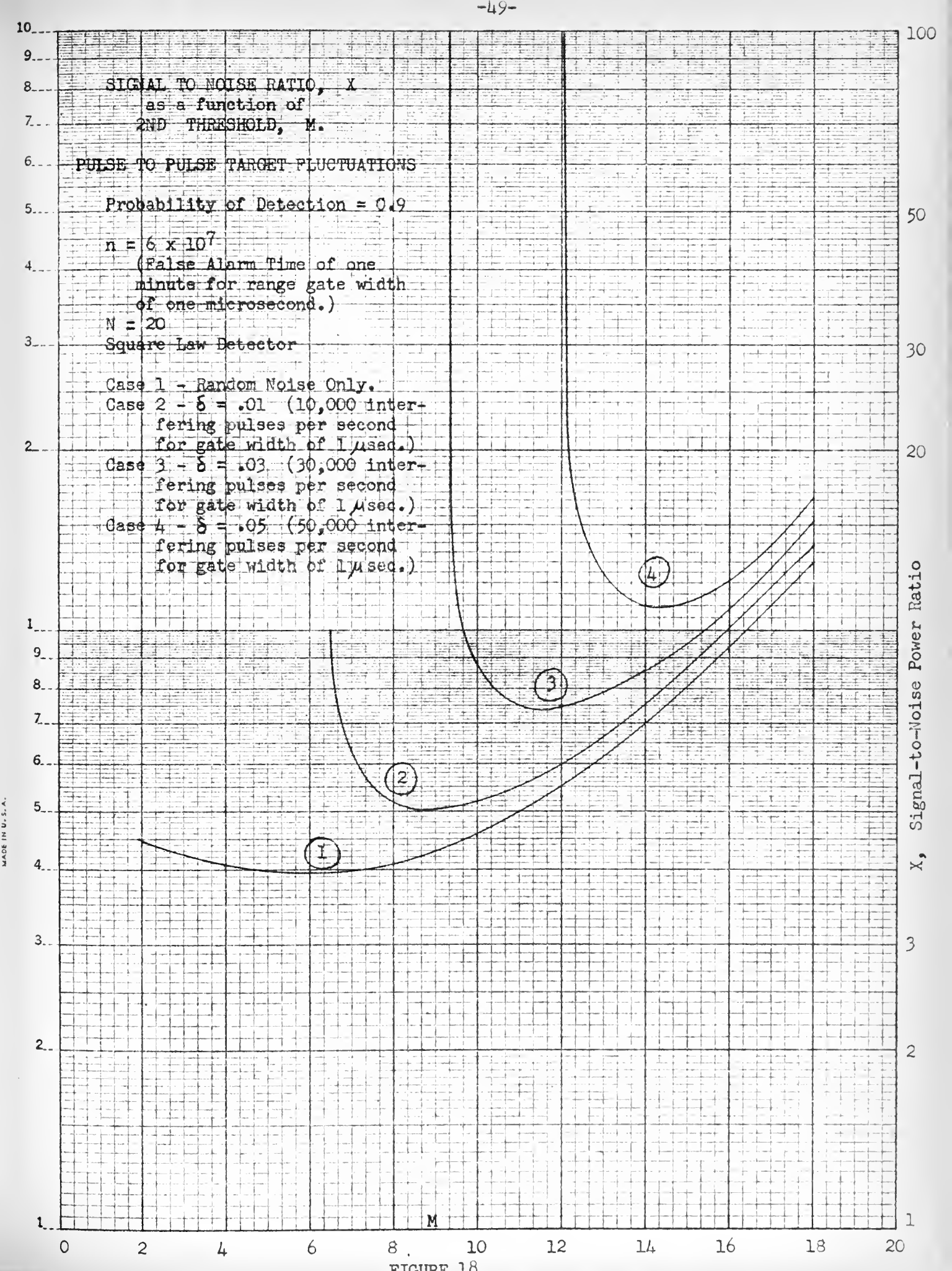
SIGNAL TO NOISE RATIO, X
as a function of
2ND THRESHOLD, M.
PULSE TO PULSE TARGET FLUCTUATIONS
Probability of Detection = 0.9
n = 6 x 10^7
(False Alarm Time of one minute for range gate width of one microsecond.)
N = 20
Square Law Detector
Case 1 - Random Noise Only.
Case 2 - δ = .01 (10,000 interfering pulses per second for gate width of 1 μsec.)
Case 3 - δ = .03 (30,000 interfering pulses per second for gate width of 1 μsec.)
Case 4 - δ = .05 (50,000 interfering pulses per second for gate width of 1 μsec.)
1
2
3
4
M
X, Signal-to-Noise Power Ratio
MADE IN U.S.A.

FIGURE 18

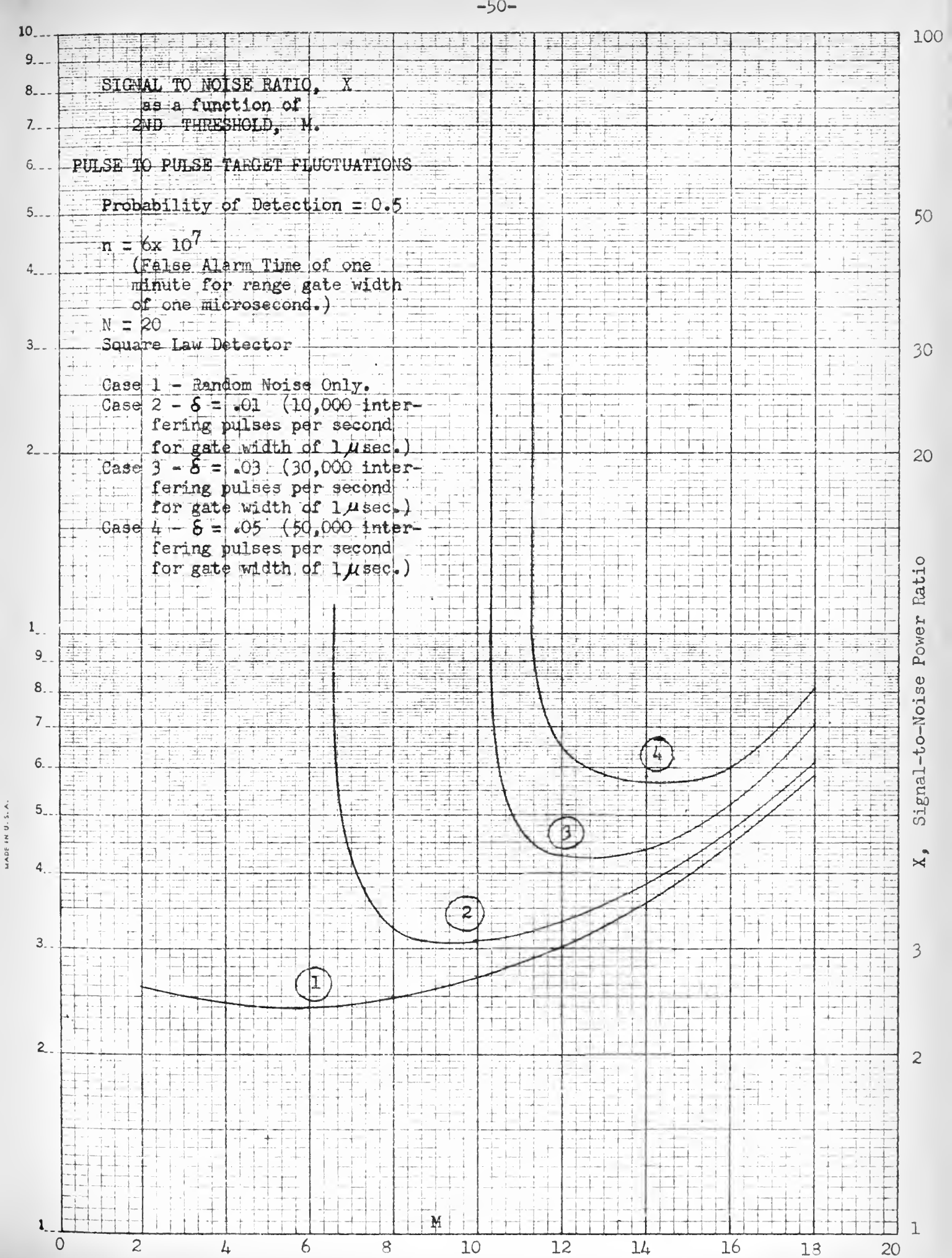
SIGNAL TO NOISE RATIO, X
as a function of
2ND THRESHOLD, M.
PULSE TO PULSE TARGET FLUCTUATIONS
Probability of Detection = 0.5
n = 6x 10^7
(False Alarm Time of one minute for range gate width of one microsecond.)
N = 20
Square Law Detector
Case 1 - Random Noise Only.
Case 2 - δ = .01 (10,000 interfering pulses per second for gate width of 1μsec.)
Case 3 - δ = .03 (30,000 interfering pulses per second for gate width of 1μsec.)
Case 4 - δ = .05 (50,000 interfering pulses per second for gate width of 1μsec.)
1
2
3
4
M
X, Signal-to-Noise Power Ratio
0
2
4
6
8
10
12
14
16
18
20
1
2
3
4
5
6
7
8
9
10
20
30
50
100

FIGURE 19

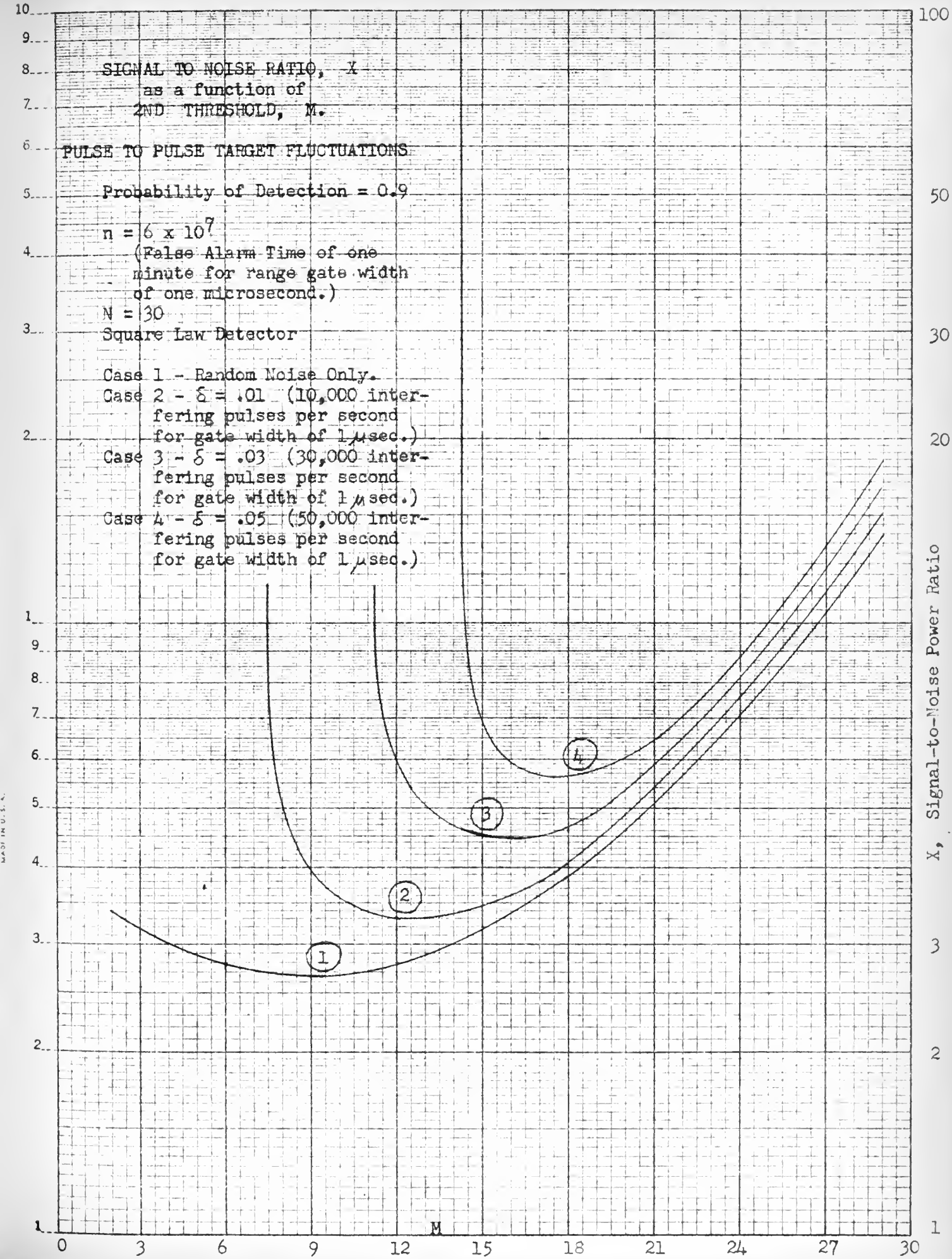
SIGNAL TO NOISE RATIO, X
as a function of
2ND THRESHOLD, M.
PULSE TO PULSE TARGET FLUCTUATIONS
Probability of Detection = 0.9
n = 6 x 10^7
(False Alarm Time of one minute for range gate width of one microsecond.)
N = 30
Square Law Detector
Case 1 - Random Noise Only.
Case 2 - δ = .01 (10,000 interfering pulses per second for gate width of 1 μsec.)
Case 3 - δ = .03 (30,000 interfering pulses per second for gate width of 1 μsec.)
Case 4 - δ = .05 (50,000 interfering pulses per second for gate width of 1 μsec.)
1
2
3
4
M
0
3
6
9
12
15
18
21
24
27
30
X, Signal-to-Noise Power Ratio
100
50
30
20
10
9
8
7
6
5
4
3
2
1

FIGURE 20

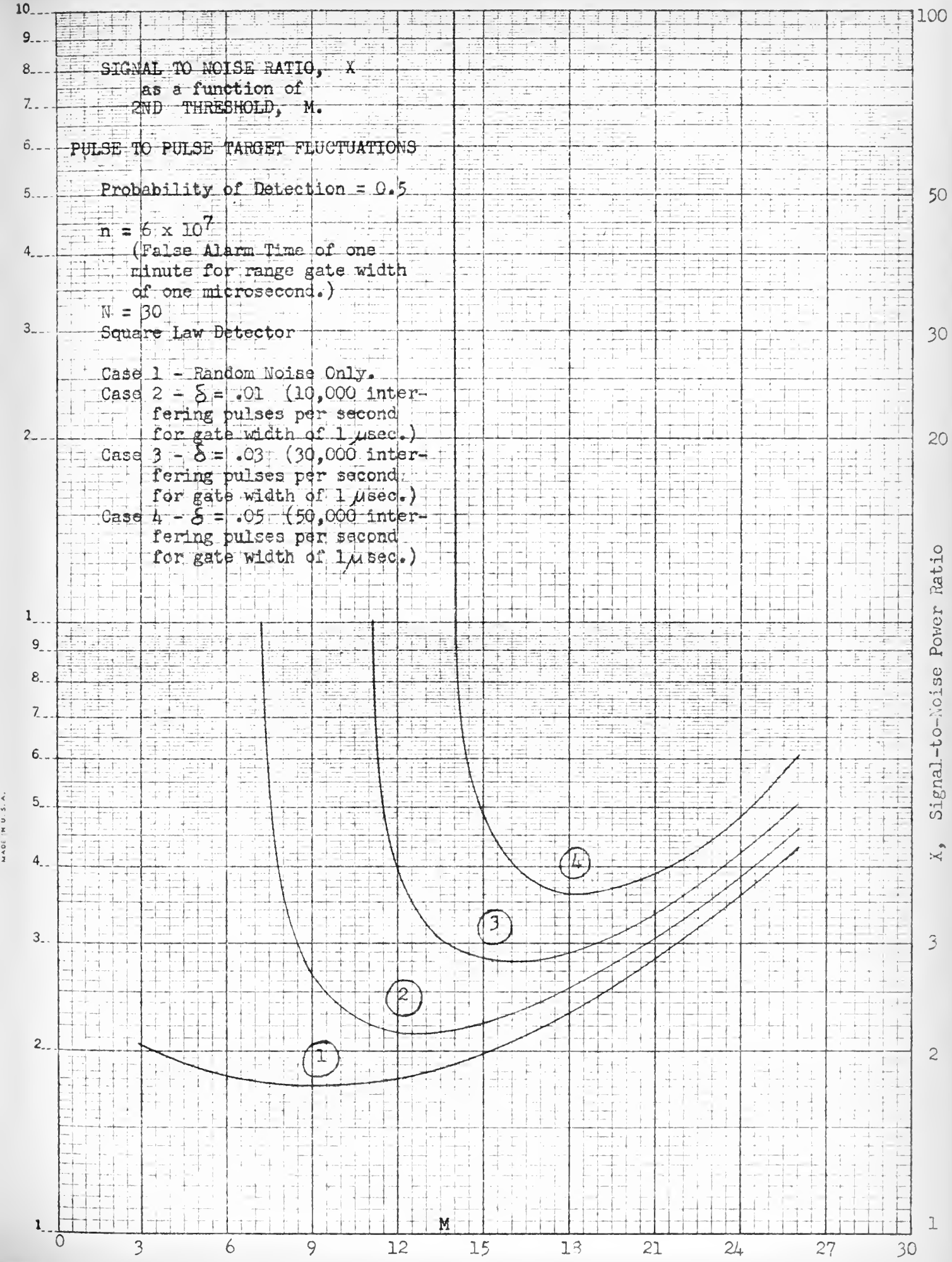
SIGNAL TO NOISE RATIO, X
as a function of
2ND THRESHOLD, M.
PULSE TO PULSE TARGET FLUCTUATIONS
Probability of Detection = 0.5
n = 6 x 10^7
(False Alarm Time of one minute for range gate width of one microsecond.)
N = 30
Square Law Detector
Case 1 - Random Noise Only.
Case 2 - δ = .01 (10,000 interfering pulses per second for gate width of 1 μsec.)
Case 3 - δ = .03 (30,000 interfering pulses per second for gate width of 1 μsec.)
Case 4 - δ = .05 (50,000 interfering pulses per second for gate width of 1 μsec.)
X, Signal-to-Noise Power Ratio
M
0
3
6
9
12
15
18
21
24
27
30
1
2
3
4
10
9
8
7
6
5
4
3
2
1
100
50
30
20
3
2
1
MADE IN U.S.A.

FIGURE 21

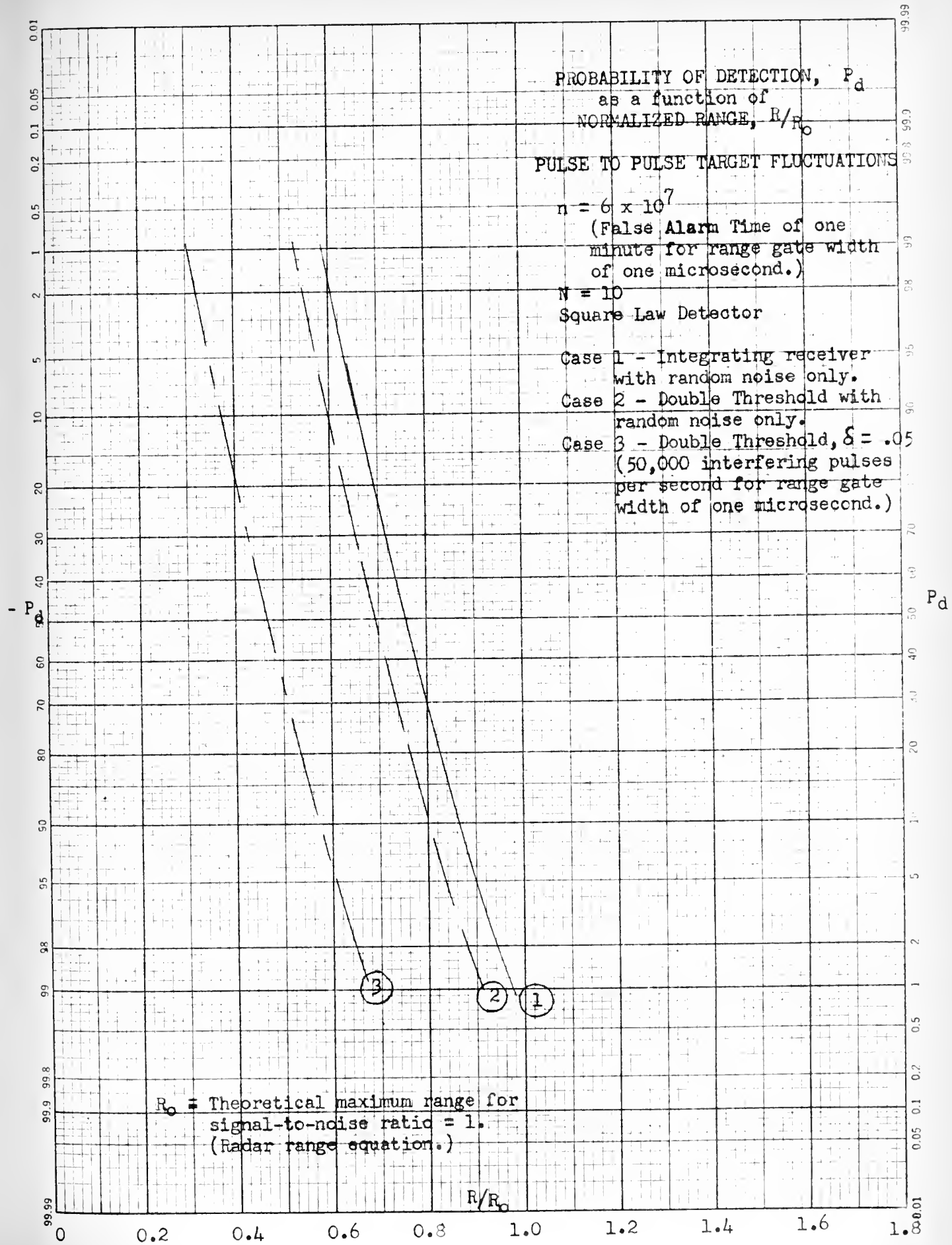
PROBABILITY OF DETECTION, P_d
as a function of
NORMALIZED RANGE, R/R_o
PULSE TO PULSE TARGET FLUCTUATIONS
$n = 6 \times 10^7$
(False Alarm Time of one minute for range gate width of one microsecond.)
N = 10
Square Law Detector
Case 1 - Integrating receiver with random noise only.
Case 2 - Double Threshold with random noise only.
Case 3 - Double Threshold, $\delta = .05$
(50,000 interfering pulses per second for range gate width of one microsecond.)
R_o = Theoretical maximum range for signal-to-noise ratio = 1. (Radar range equation.)
P_d
R/R_o
0
0.2
0.4
0.6
0.8
1.0
1.2
1.4
1.6
1.8
3
2
1

FIGURE 22

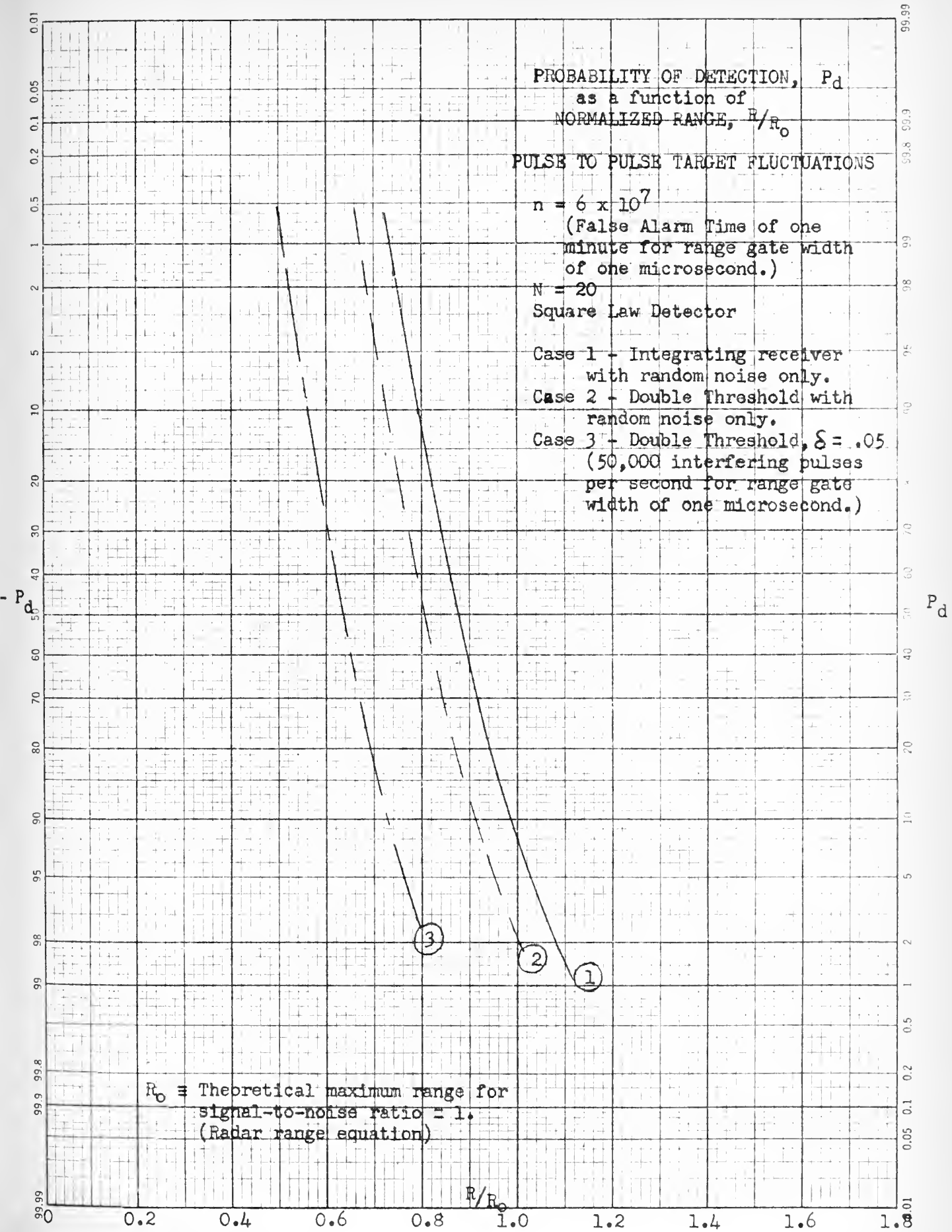
PROBABILITY OF DETECTION, P_d
as a function of
NORMALIZED RANGE, R/R_o
PULSE TO PULSE TARGET FLUCTUATIONS
$n = 6 \times 10^7$
(False Alarm Time of one minute for range gate width of one microsecond.)
N = 20
Square Law Detector
Case 1 - Integrating receiver with random noise only.
Case 2 - Double Threshold with random noise only.
Case 3 - Double Threshold, $\delta = .05$
(50,000 interfering pulses per second for range gate width of one microsecond.)
$R_o \equiv$ Theoretical maximum range for signal-to-noise ratio = 1. (Radar range equation)
P_d
$1 - P_d$
R/R_o
0
0.2
0.4
0.6
0.8
1.0
1.2
1.4
1.6
1.8
1
2
3

FIGURE 23

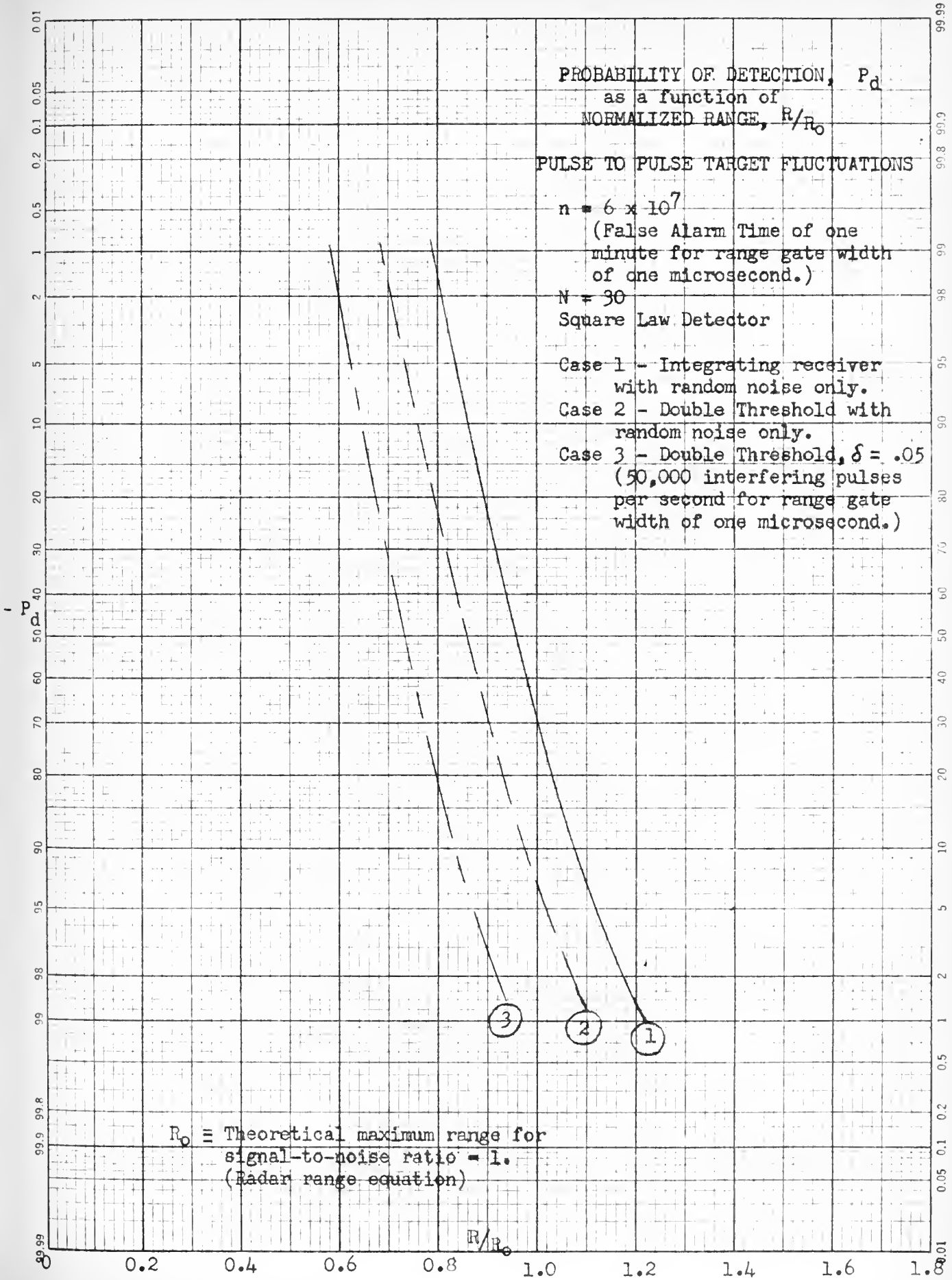
PROBABILITY OF DETECTION, P_d
as a function of
NORMALIZED RANGE, R/R_o
PULSE TO PULSE TARGET FLUCTUATIONS
$n = 6 \times 10^7$
(False Alarm Time of one minute for range gate width of one microsecond.)
N = 30
Square Law Detector
Case 1 - Integrating receiver with random noise only.
Case 2 - Double Threshold with random noise only.
Case 3 - Double Threshold, $\delta = .05$ (50,000 interfering pulses per second for range gate width of one microsecond.)
P_d
R_o ≡ Theoretical maximum range for signal-to-noise ratio = 1. (Radar range equation)
R/R_o
0
0.2
0.4
0.6
0.8
1.0
1.2
1.4
1.6
1.8
3
2
1

FIGURE 24

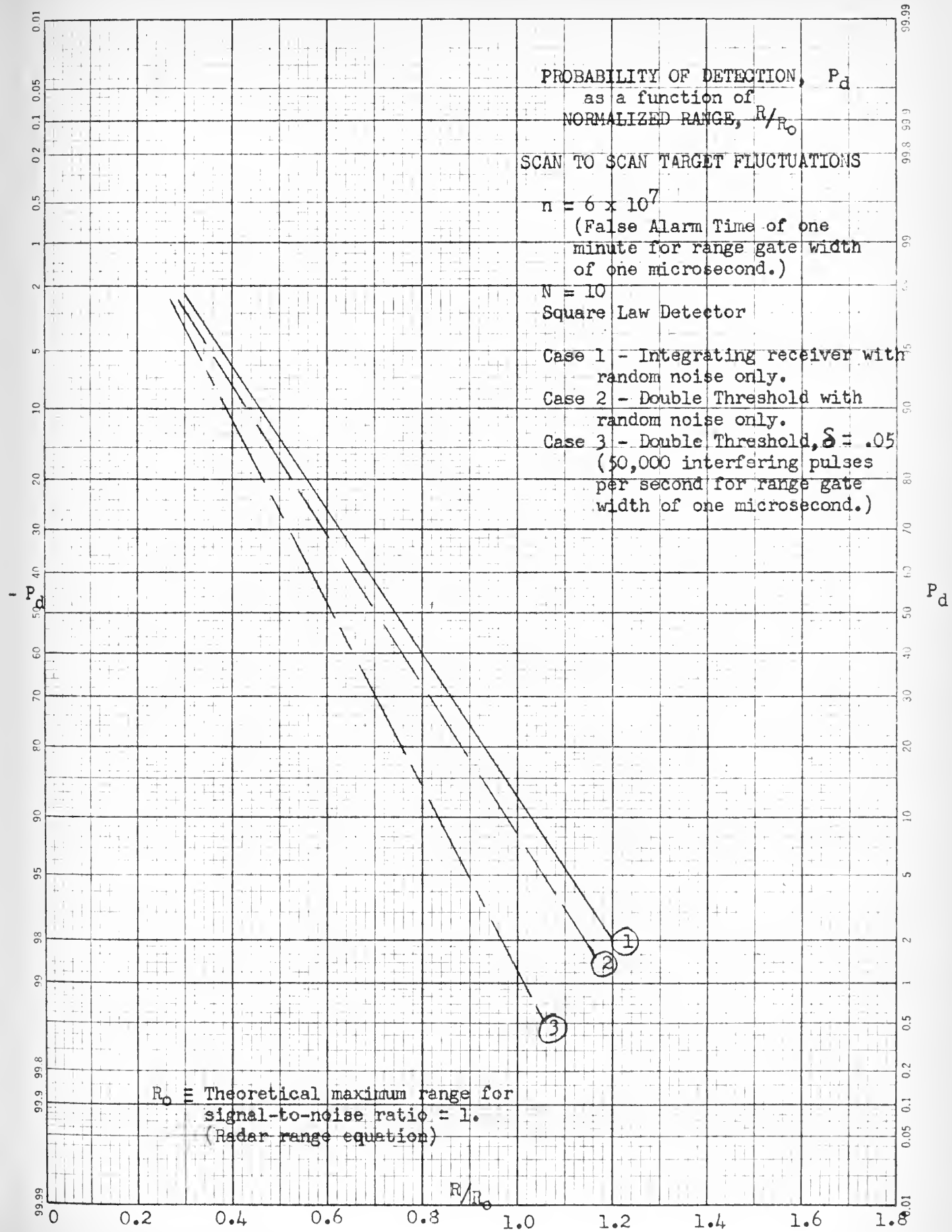
PROBABILITY OF DETECTION, P_d
as a function of
NORMALIZED RANGE, R/R_o
SCAN TO SCAN TARGET FLUCTUATIONS
$n = 6 \times 10^7$
(False Alarm Time of one minute for range gate width of one microsecond.)
N = 10
Square Law Detector
Case 1 - Integrating receiver with random noise only.
Case 2 - Double Threshold with random noise only.
Case 3 - Double Threshold, $\delta = .05$ (50,000 interfering pulses per second for range gate width of one microsecond.)
$R_o \equiv$ Theoretical maximum range for signal-to-noise ratio = 1. (Radar range equation)
P_d
R/R_o
0
0.2
0.4
0.6
0.8
1.0
1.2
1.4
1.6
1.8
1
2
3

FIGURE 25

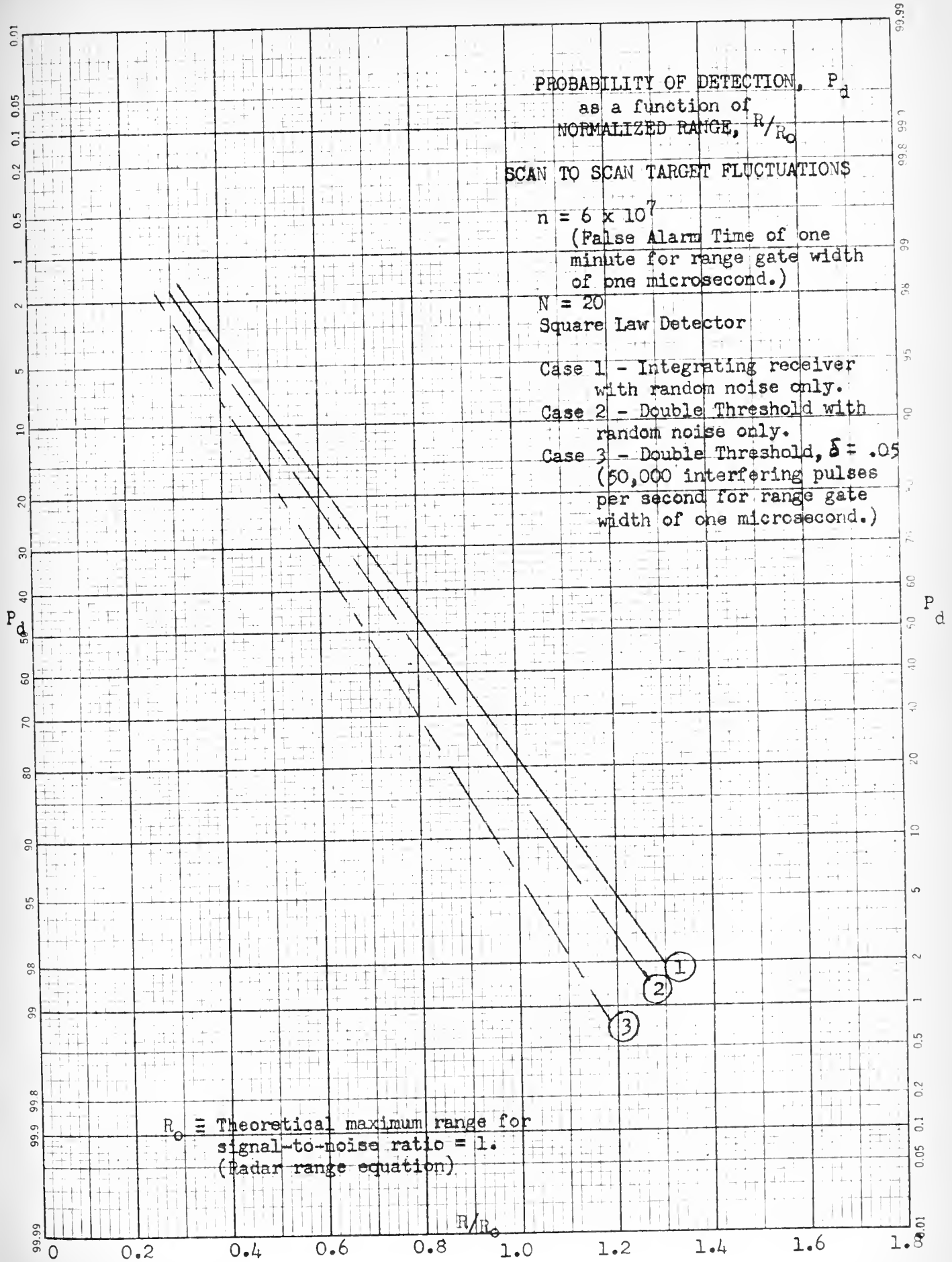
PROBABILITY OF DETECTION, P_d
as a function of
NORMALIZED RANGE, R/R_o
SCAN TO SCAN TARGET FLUCTUATIONS
$n = 6 \times 10^7$
(False Alarm Time of one minute for range gate width of one microsecond.)
N = 20
Square Law Detector
Case 1 - Integrating receiver with random noise only.
Case 2 - Double Threshold with random noise only.
Case 3 - Double Threshold, $\delta = .05$
(50,000 interfering pulses per second for range gate width of one microsecond.)
$R_o \equiv$ Theoretical maximum range for signal-to-noise ratio = 1. (Radar range equation)
$- P_d$
P_d
R/R_o
0
0.2
0.4
0.6
0.8
1.0
1.2
1.4
1.6
1.8
1
2
3

FIGURE 26

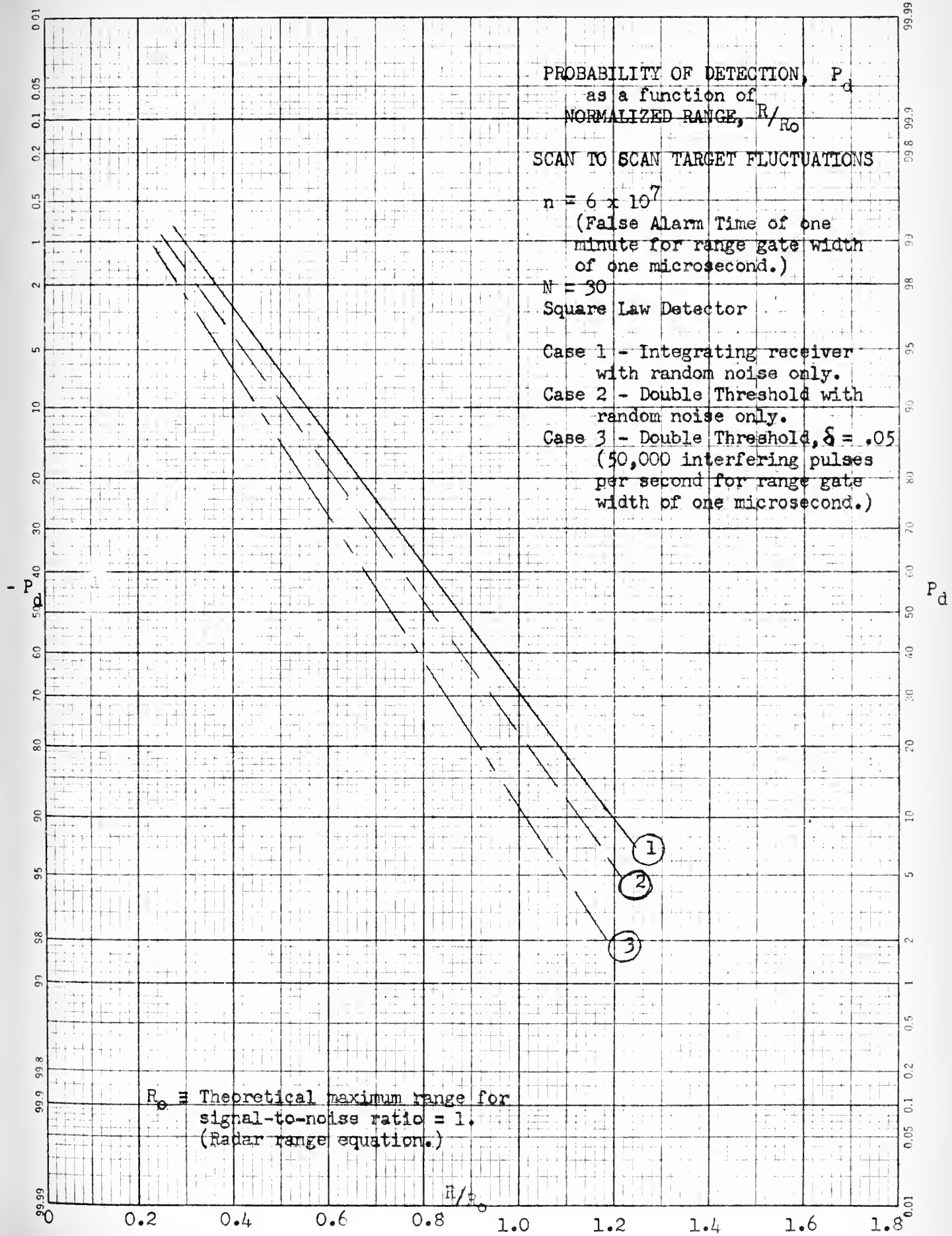
PROBABILITY OF DETECTION, P_d
as a function of
NORMALIZED RANGE, R/R_o
SCAN TO SCAN TARGET FLUCTUATIONS
$n = 6 \times 10^7$
(False Alarm Time of one minute for range gate width of one microsecond.)
N = 30
Square Law Detector
Case 1 - Integrating receiver with random noise only.
Case 2 - Double Threshold with random noise only.
Case 3 - Double Threshold, $\delta = .05$ (50,000 interfering pulses per second for range gate width of one microsecond.)
P_d
$R_o \equiv$ Theoretical maximum range for signal-to-noise ratio = 1. (Radar range equation.)
R/R_o
0
0.2
0.4
0.6
0.8
1.0
1.2
1.4
1.6
1.8
1
2
3

FIGURE 27

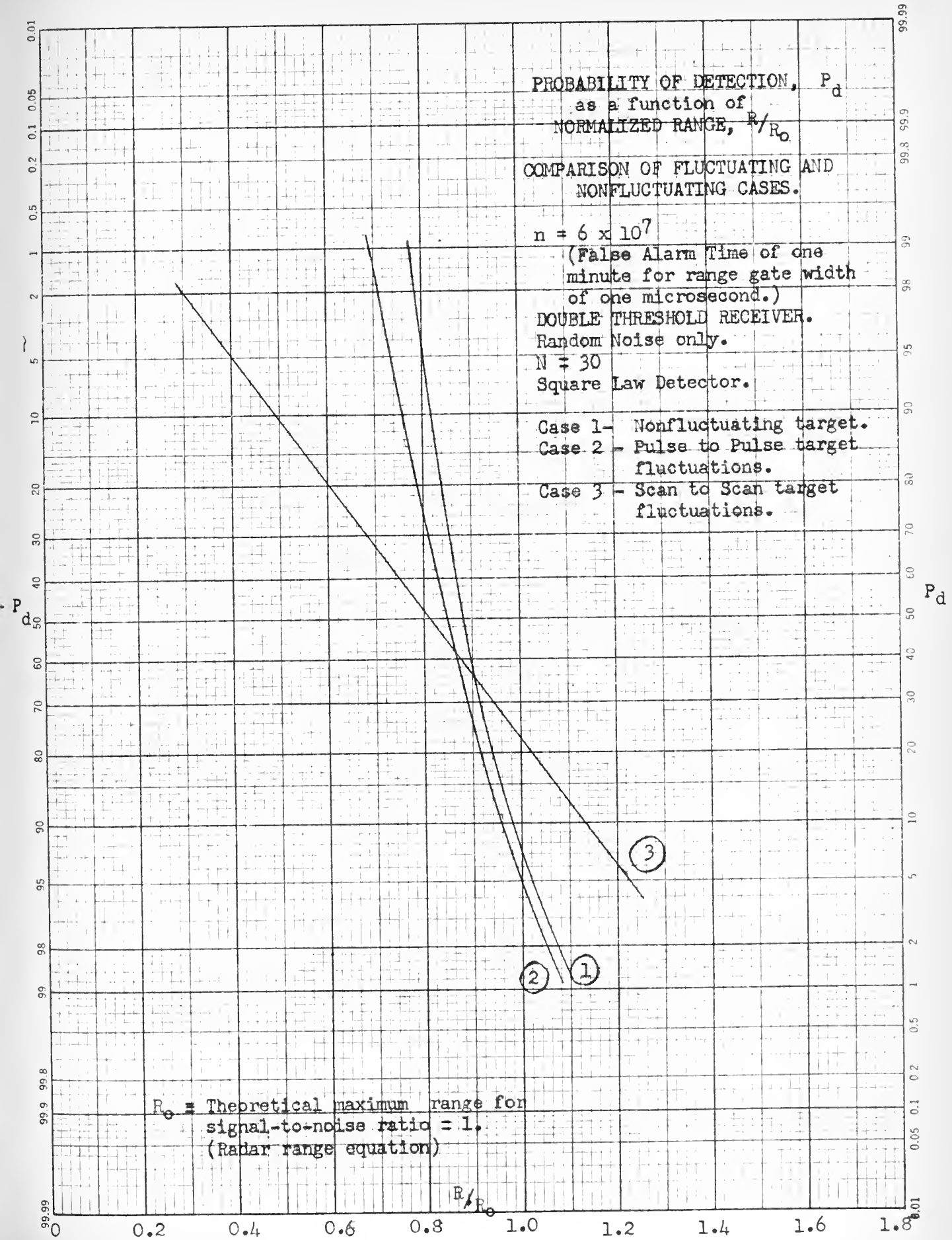
PROBABILITY OF DETECTION, P_d
as a function of
NORMALIZED RANGE, R/R_o
COMPARISON OF FLUCTUATING AND NONFLUCTUATING CASES.
$n = 6 \times 10^7$
(False Alarm Time of one minute for range gate width of one microsecond.)
DOUBLE THRESHOLD RECEIVER.
Random Noise only.
N = 30
Square Law Detector.
Case 1- Nonfluctuating target.
Case 2 - Pulse to Pulse target fluctuations.
Case 3 - Scan to Scan target fluctuations.
P_d
R/R_o
R_o = Theoretical maximum range for signal-to-noise ratio = 1. (Radar range equation)
0
0.2
0.4
0.6
0.8
1.0
1.2
1.4
1.6
1.8
3
2
1

FIGURE 28

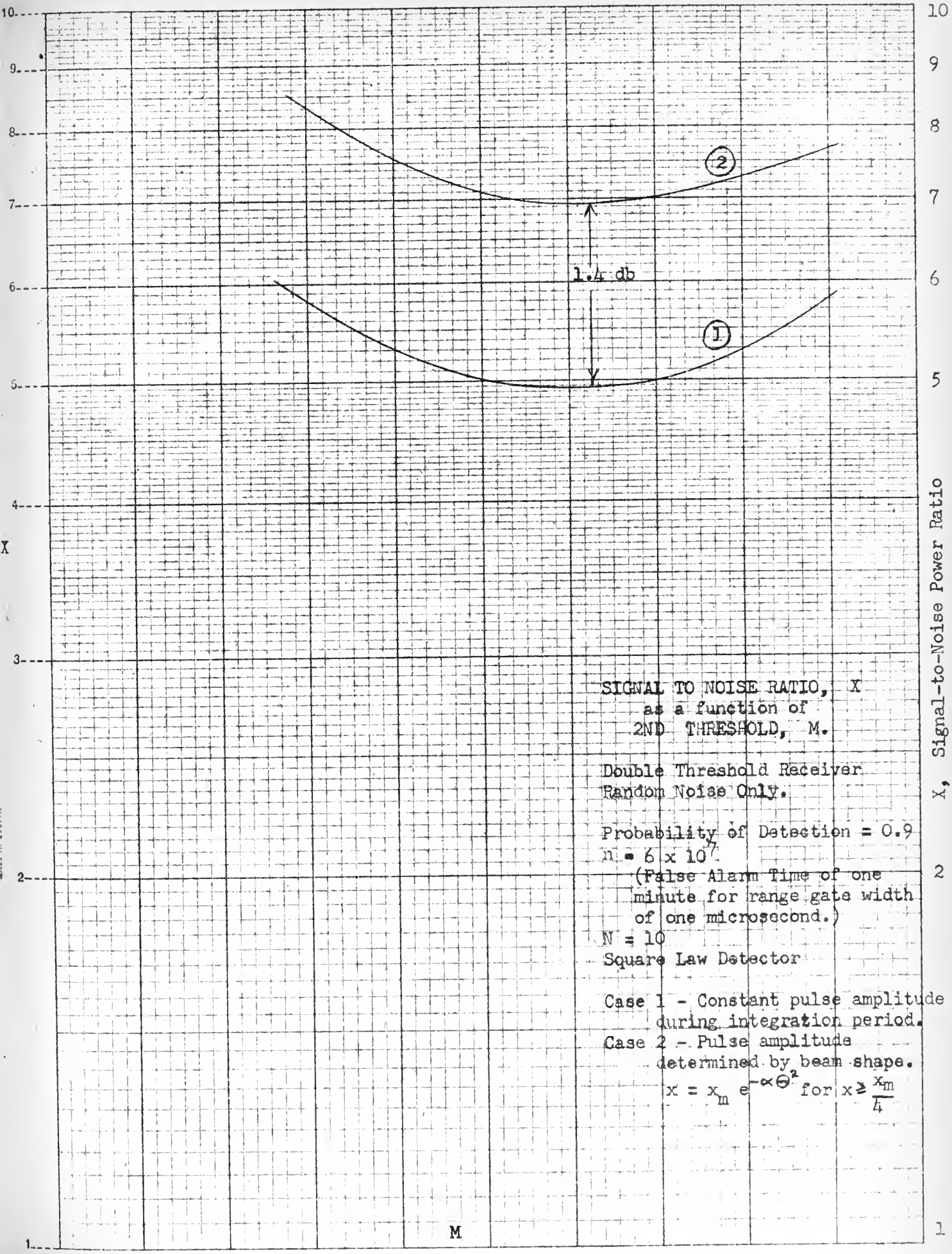
10
9
8
7
6
5
4
3
2
1
X
2
1.4 db
1
M
0 1 2 3 4 5 6 7 8 9 10
X, Signal-to-Noise Power Ratio
SIGNAL TO NOISE RATIO, X
as a function of
2ND THRESHOLD, M.
Double Threshold Receiver
Random Noise Only.
Probability of Detection = 0.9
n = 6 x 10^7
(False Alarm Time of one minute for range gate width of one microsecond.)
N = 10
Square Law Detector
Case 1 - Constant pulse amplitude during integration period.
Case 2 - Pulse amplitude determined by beam shape.
$x = x_m e^{-\alpha\theta^2}$ for $x \geq \frac{x_m}{4}$

FIGURE 29

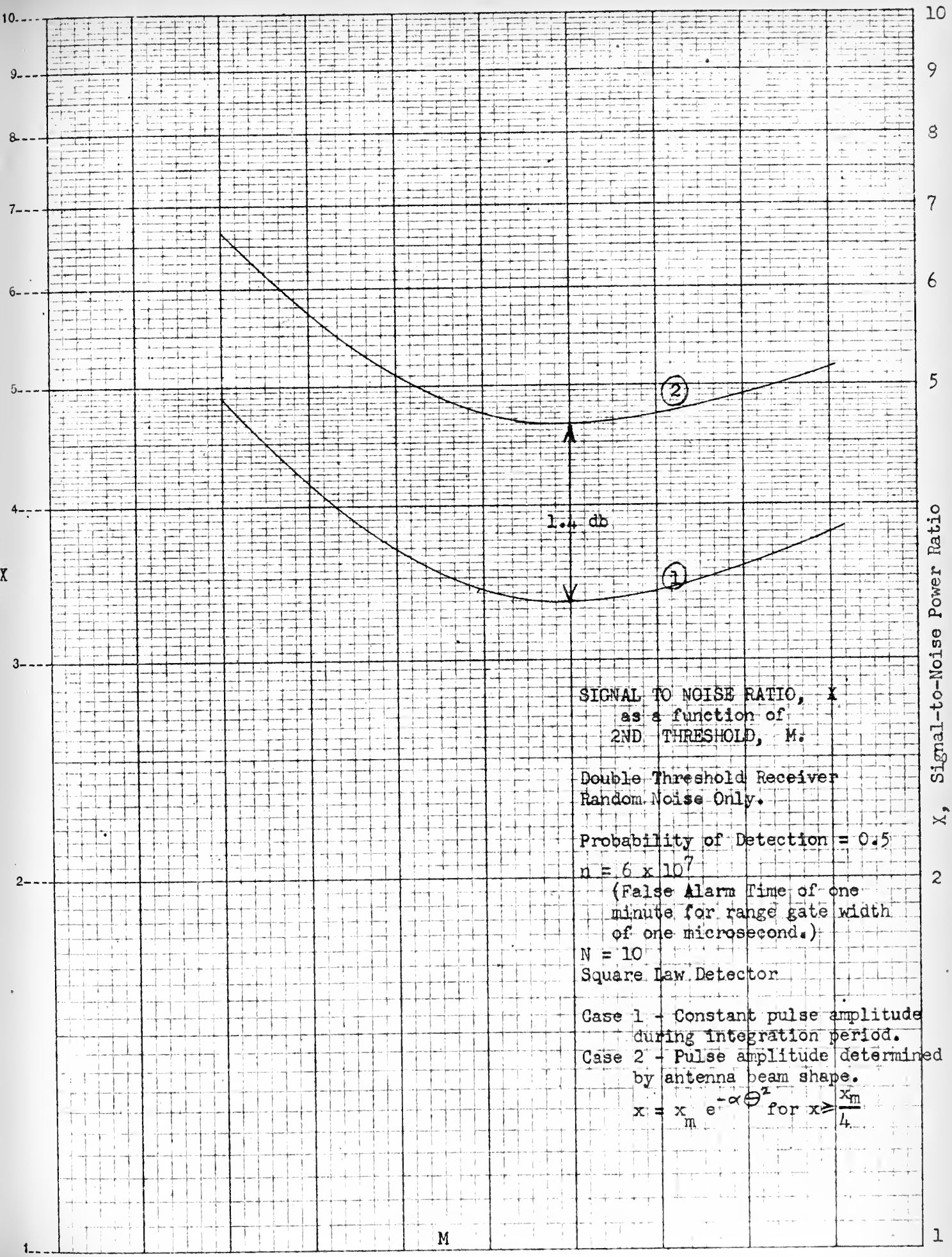
10
9
8
7
6
5
4
3
2
1
X
0
1
2
3
4
5
6
7
8
9
10
M
X, Signal-to-Noise Power Ratio
1.4 db
2
1
SIGNAL TO NOISE RATIO, X
as a function of
2ND THRESHOLD, M.
Double Threshold Receiver
Random Noise Only.
Probability of Detection = 0.5
n = 6 x 10^7
(False Alarm Time of one minute for range gate width of one microsecond.)
N = 10
Square Law Detector
Case 1 - Constant pulse amplitude during integration period.
Case 2 - Pulse amplitude determined by antenna beam shape.
x = x_m e^{-α Θ^2} for x ≥ x_m/4

FIGURE 30

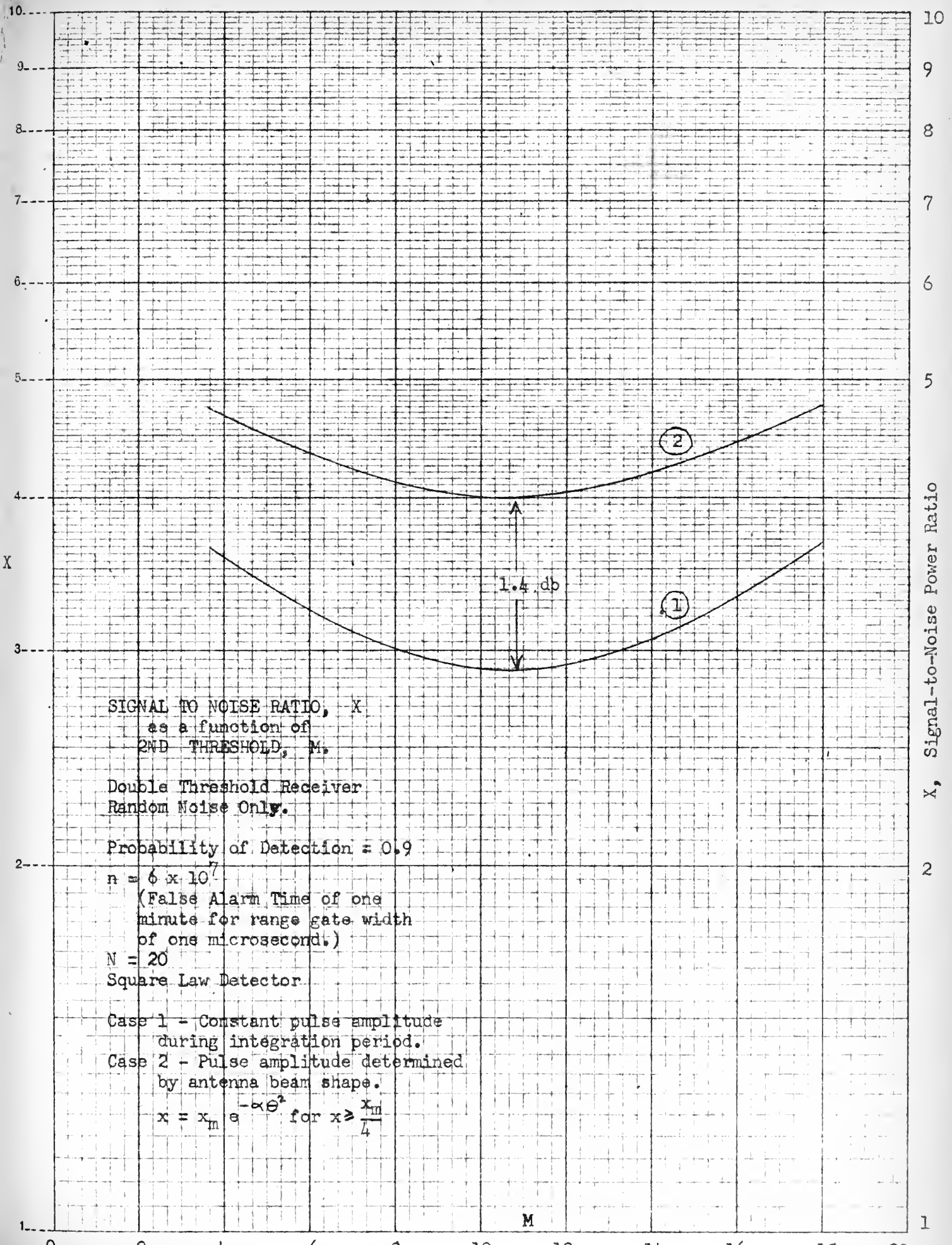
10
9
8
7
6
5
4
3
2
1
X
X, Signal-to-Noise Power Ratio
1.4 db
2
1
SIGNAL TO NOISE RATIO, X
as a function of
2ND THRESHOLD, M.
Double Threshold Receiver
Random Noise Only.
Probability of Detection = 0.9
n = 6 x 10^7
(False Alarm Time of one minute for range gate width of one microsecond.)
N = 20
Square Law Detector
Case 1 - Constant pulse amplitude during integration period.
Case 2 - Pulse amplitude determined by antenna beam shape.
x = x_m e^{-∝θ^2} for x ≥ x_m/4
M
0
2
4
6
8
10
12
14
16
18
20

FIGURE 31

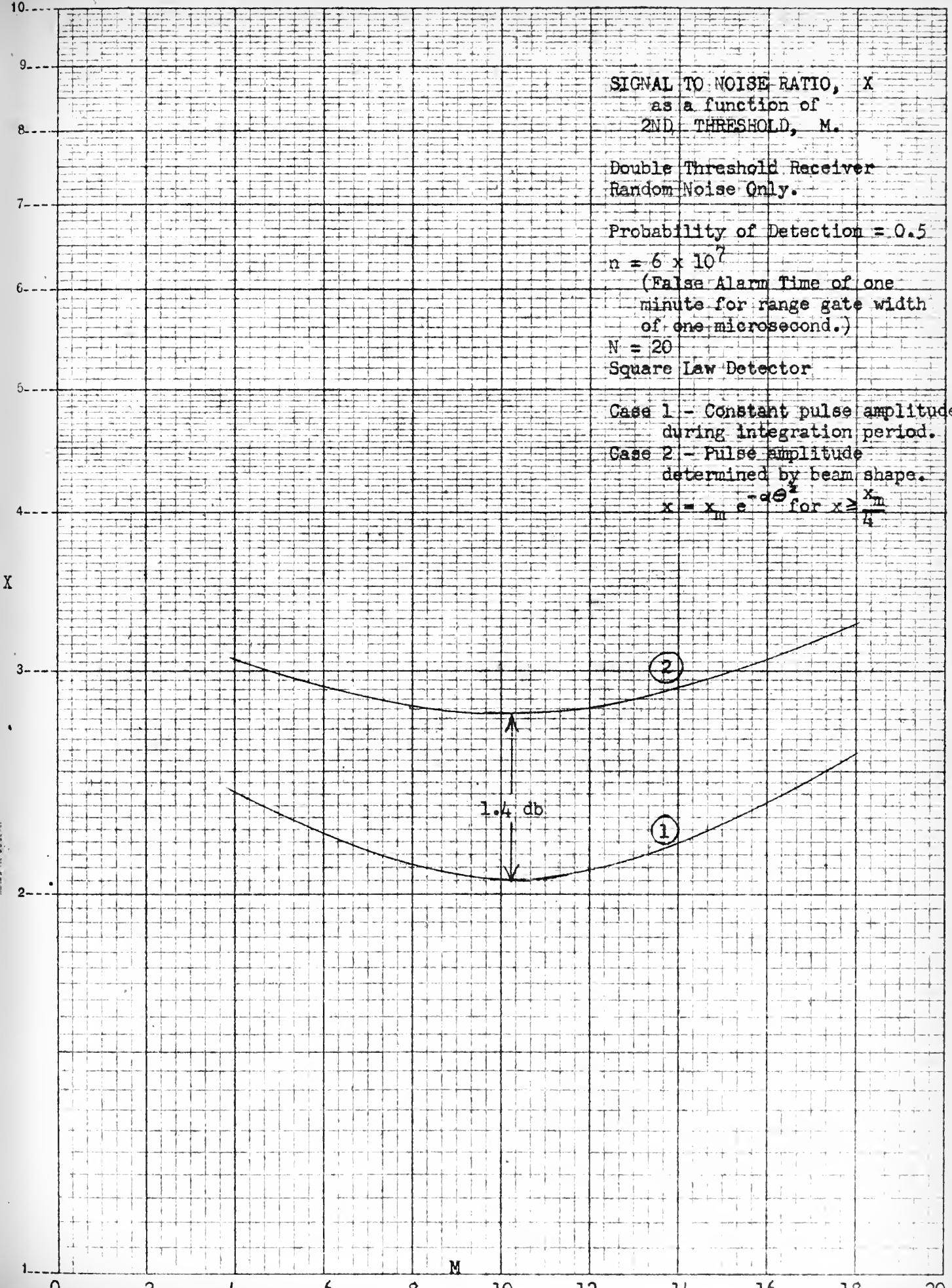
SIGNAL TO NOISE RATIO, X
as a function of
2ND THRESHOLD, M.
Double Threshold Receiver
Random Noise Only.
Probability of Detection = 0.5
n = 6 x 10^7
(False Alarm Time of one minute for range gate width of one microsecond.)
N = 20
Square Law Detector
Case 1 - Constant pulse amplitude during integration period.
Case 2 - Pulse amplitude determined by beam shape.
x = x_m e^{-αθ^2} for x ≥ x_m/4
1.4 db
1
2
X
M
X, Signal-to-Noise Power Ratio
0
2
4
6
8
10
12
14
16
18
20
1
2
3
4
5
6
7
8
9
10

FIGURE 32

BINOMIAL EXPANSION -- PARTIAL SUMS

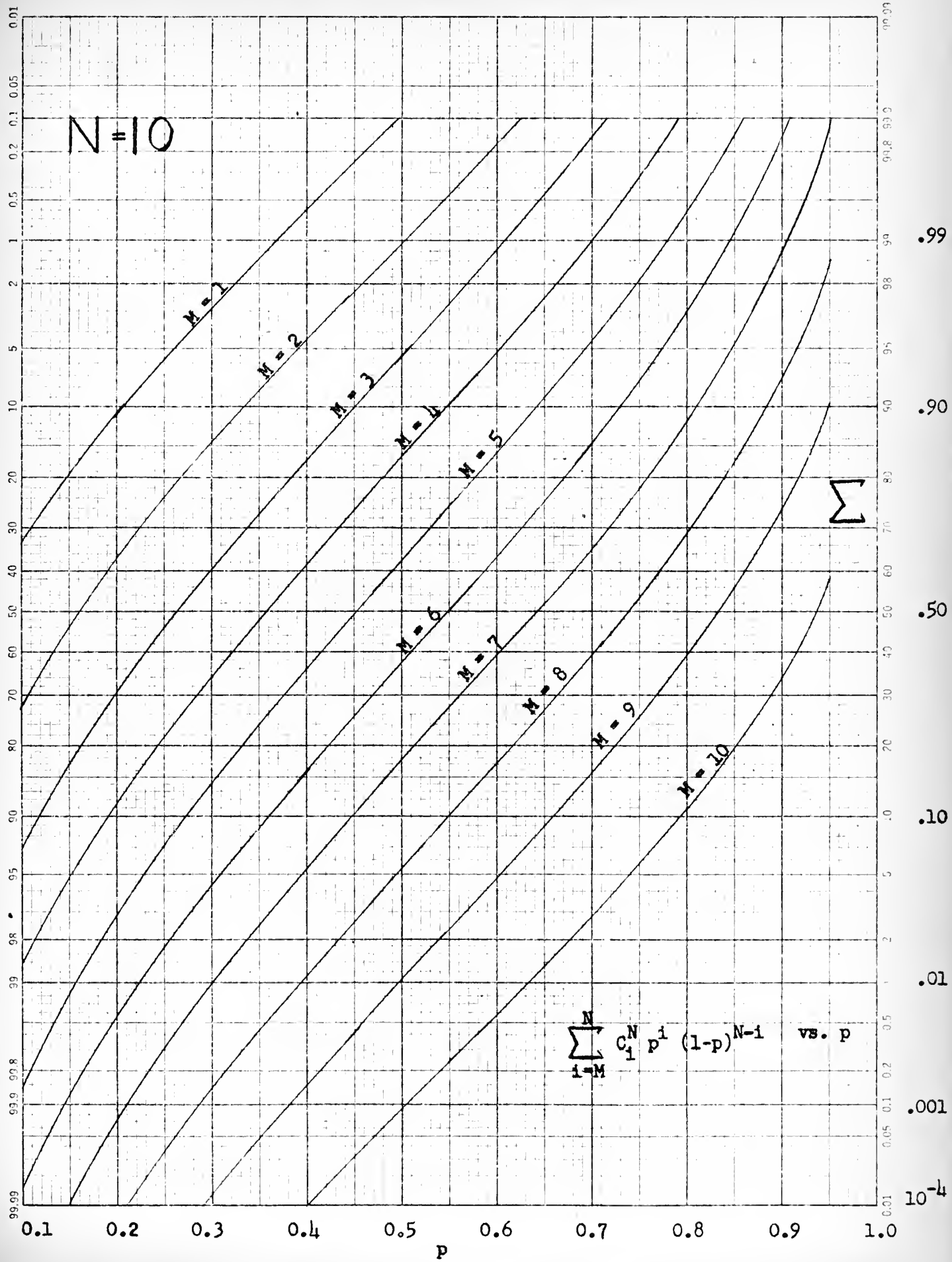

FIGURE 33

BINOMIAL DISTRIBUTION -- PARTIAL SUMS

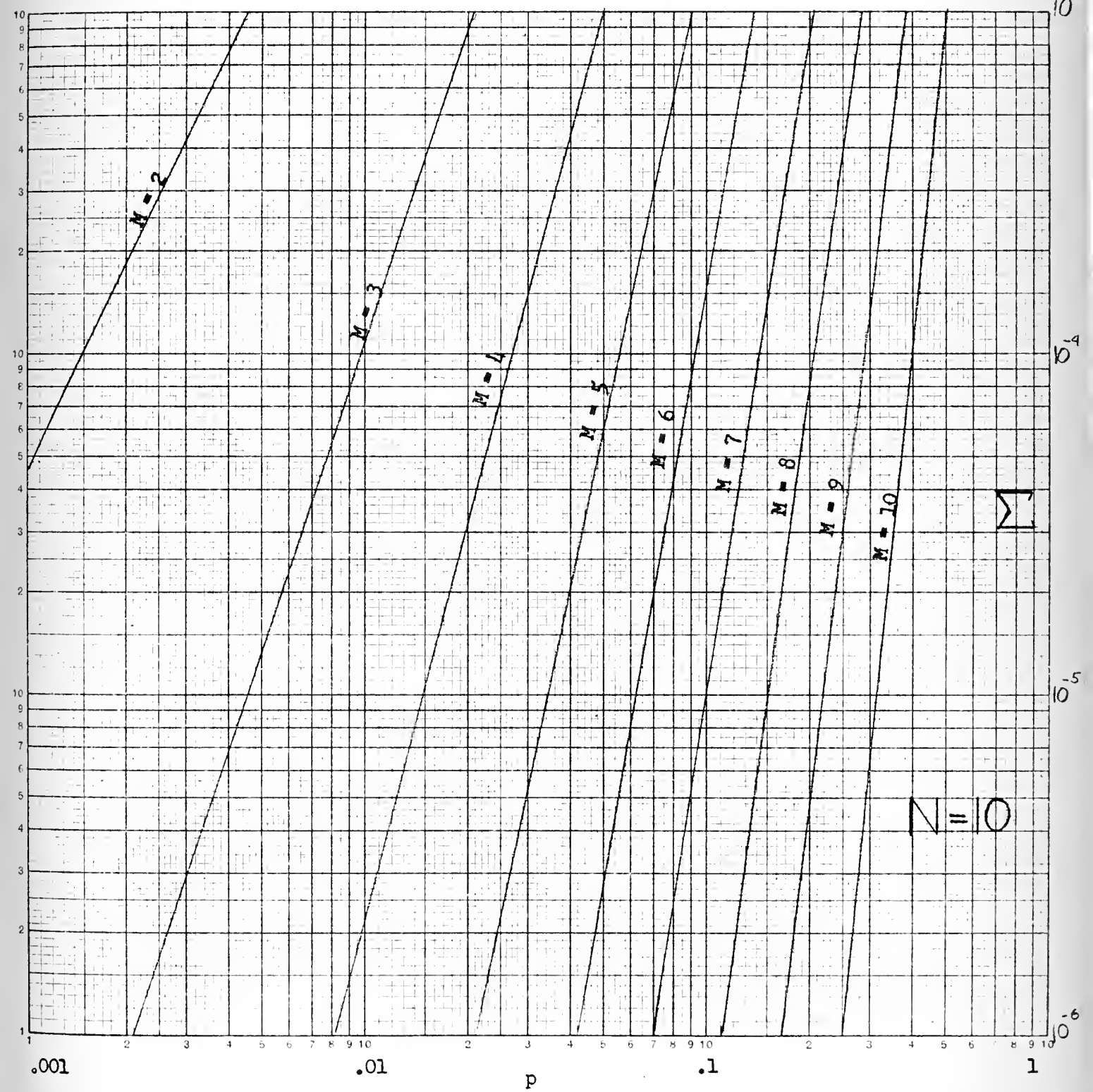

$$\sum_{i=M}^{N} C_i^N \, p^i \, (1-p)^{N-i} \quad \text{vs. } p$$

FIGURE 34

BINOMIAL DISTRIBUTION -- PARTIAL SUMS

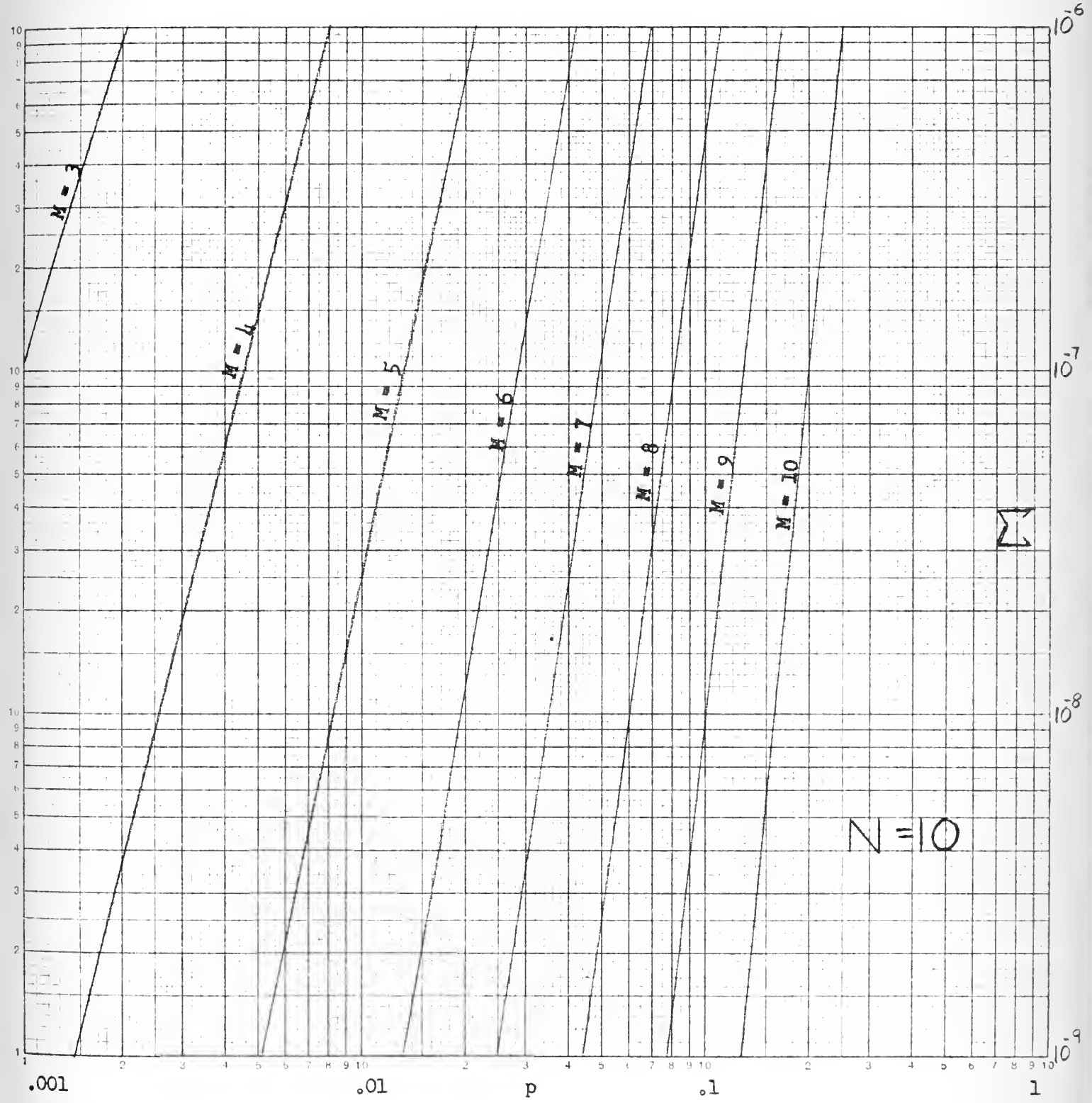

$$\sum_{i=M}^{N} C_i^N \, p^i \, (1-p)^{N-i} \quad \text{vs. p}$$

FIGURE 35

BINOMIAL EXPANSION -- PARTIAL SUMS

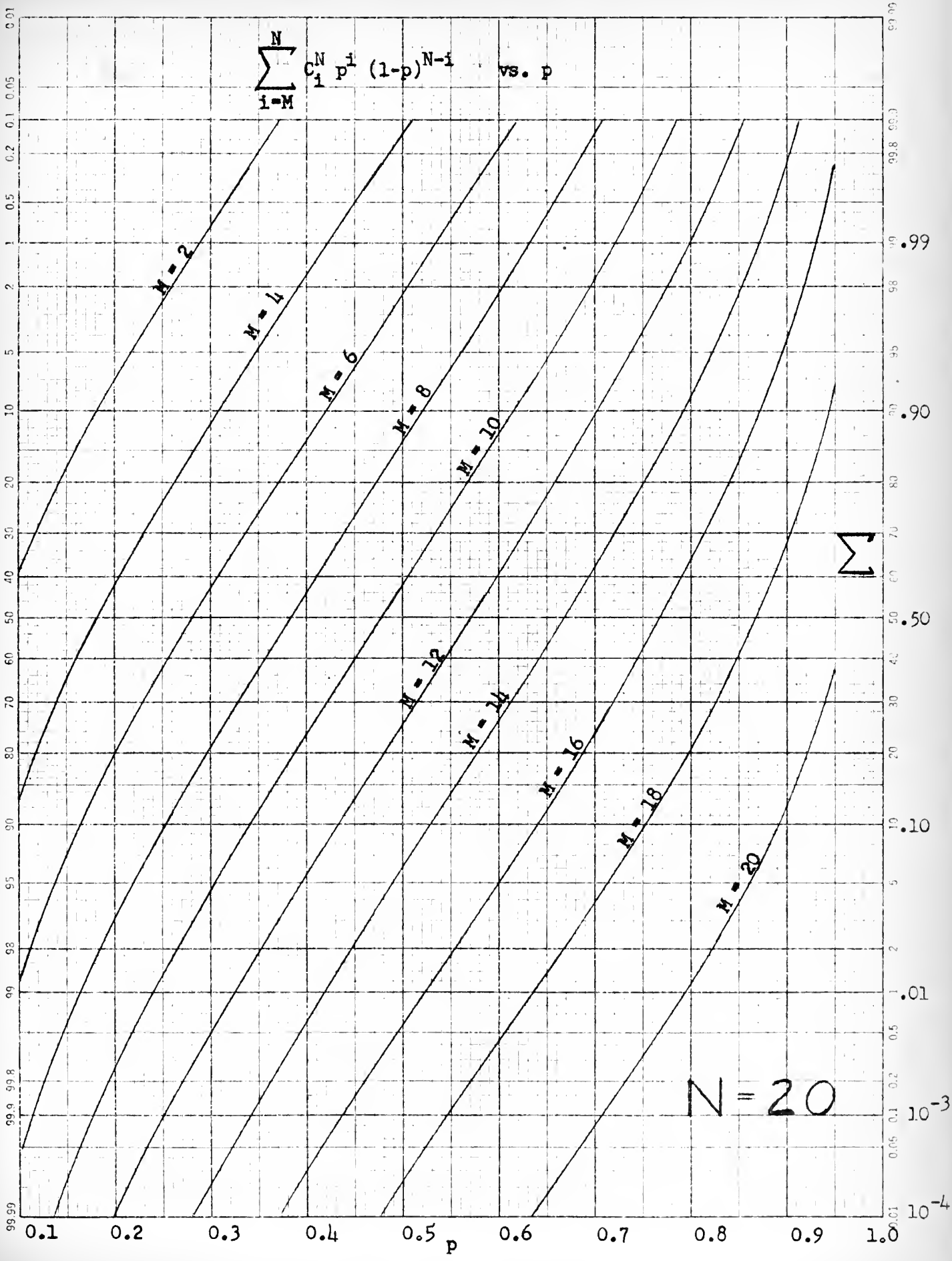

FIGURE 36

BINOMIAL EXPANSION -- PARTIAL SUMS

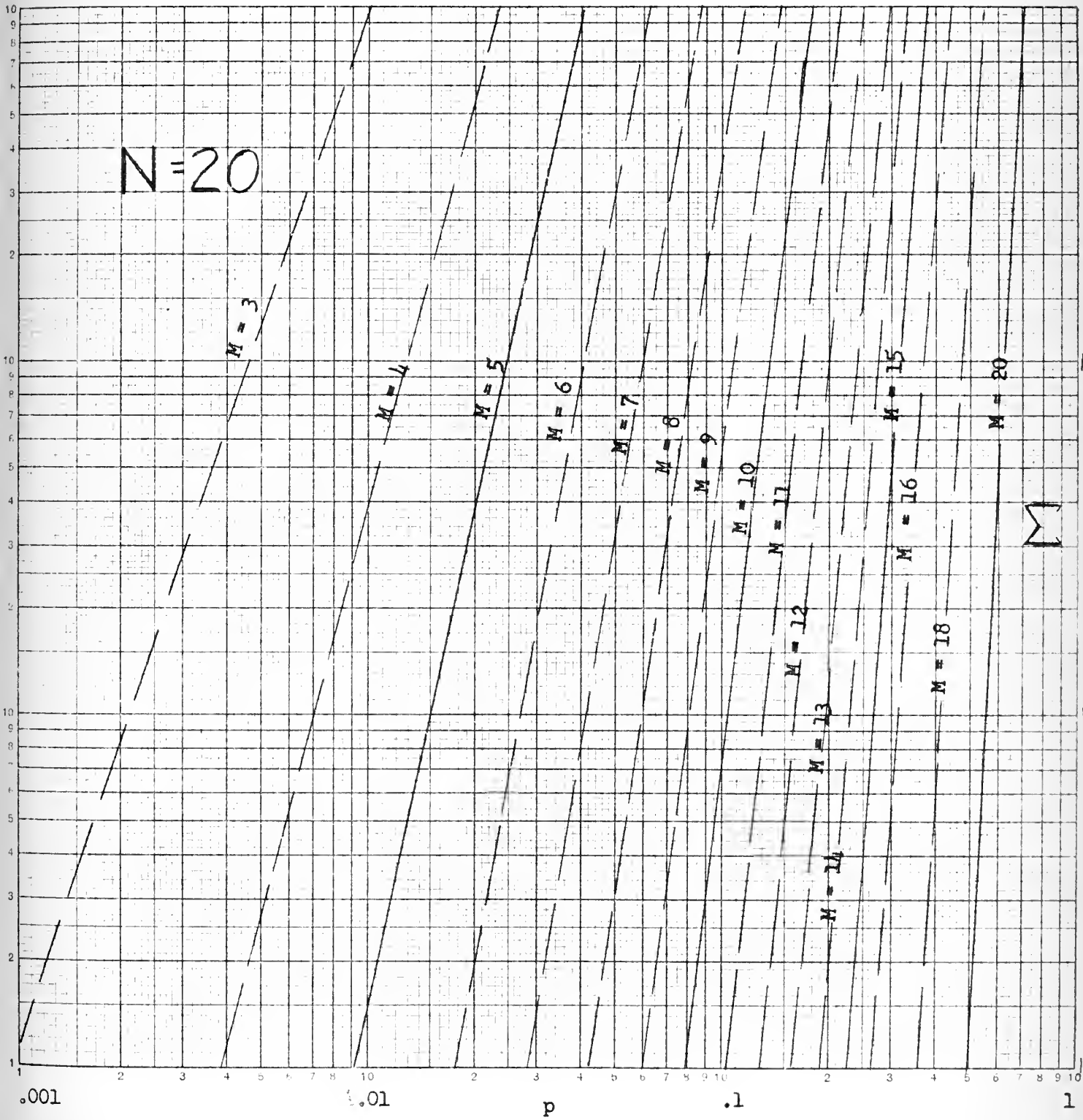

$$\sum_{i=M}^{N} C_i^N \, p^i \, (1-p)^{N-i} \qquad \text{vs. p}$$

FIGURE 37

BINOMIAL DISTRIBUTION -- PARTIAL SUMS

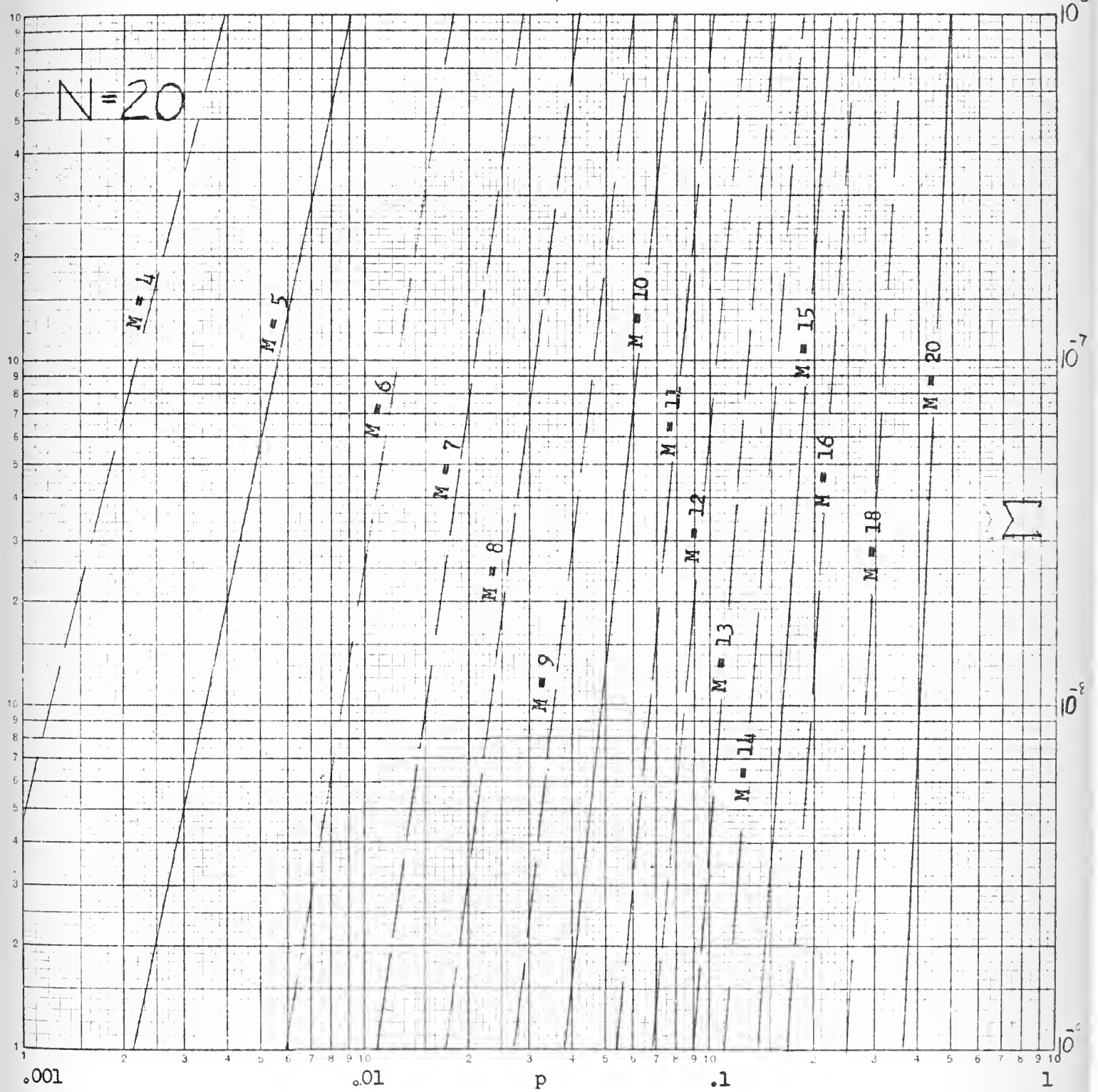

$$\sum_{i=M}^{N} C_i^N \, p^i \, (1-p)^{N-i} \quad \text{vs. p}$$

FIGURE 38

BINOMIAL EXPANSION -- PARTIAL SUMS

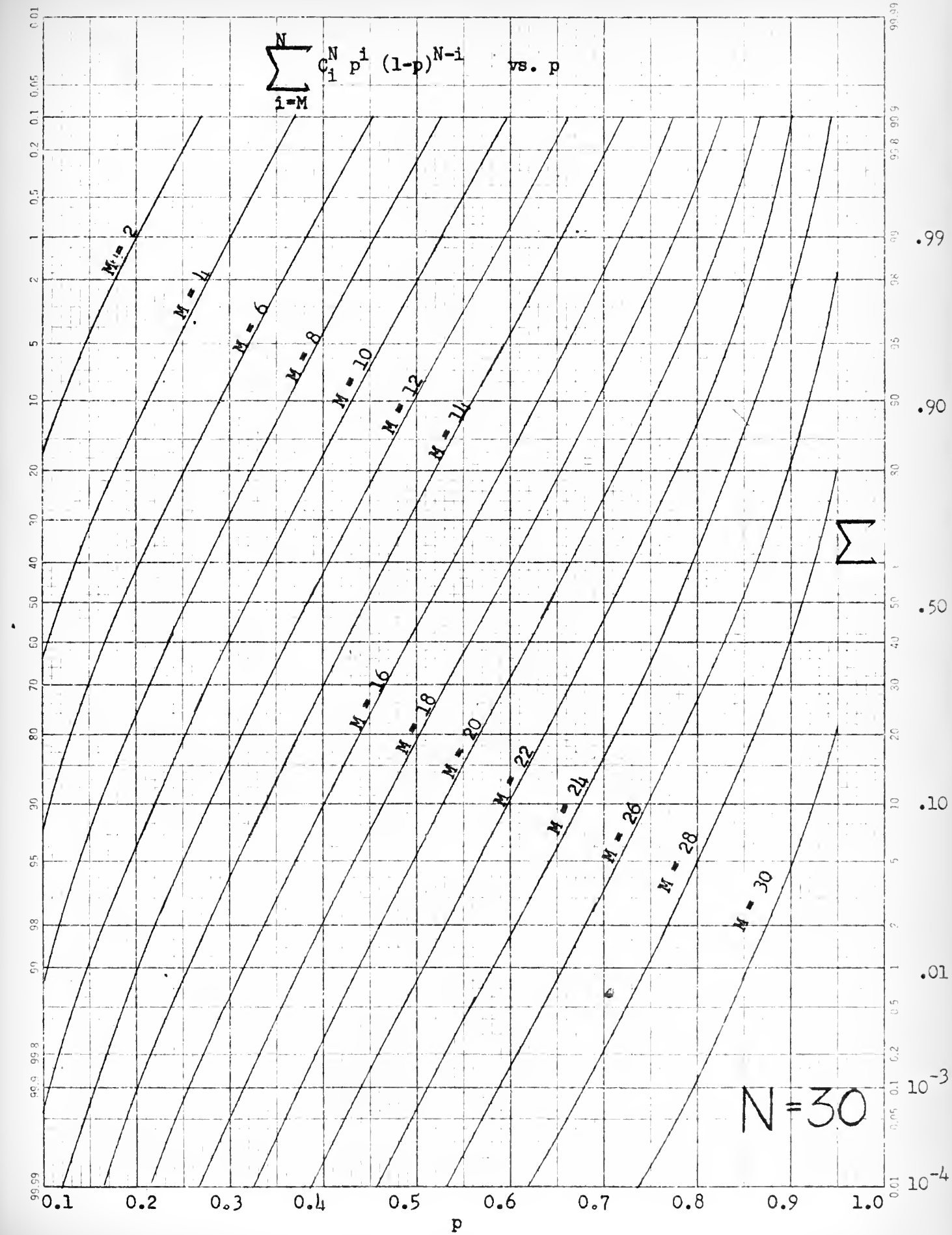

FIGURE 39

BINOMIAL DISTRIBUTION -- PARTIAL SUMS

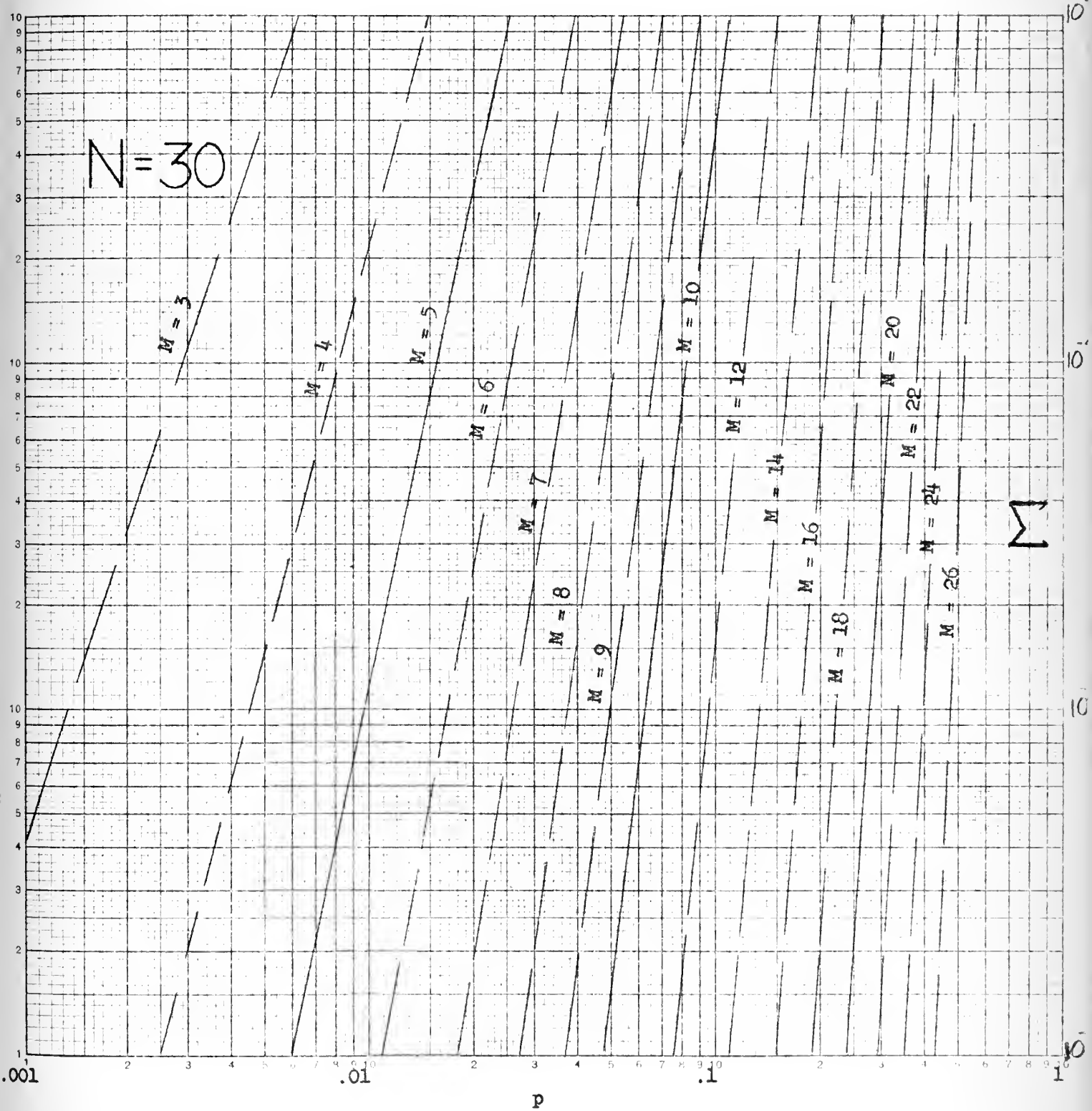

$$\sum_{i=M}^{N} C_i^N \, p^i \, (1-p)^{N-i} \quad \text{vs. } p$$

FIGURE 40

BINOMIAL DISTRIBUTION -- PARTIAL SUMS

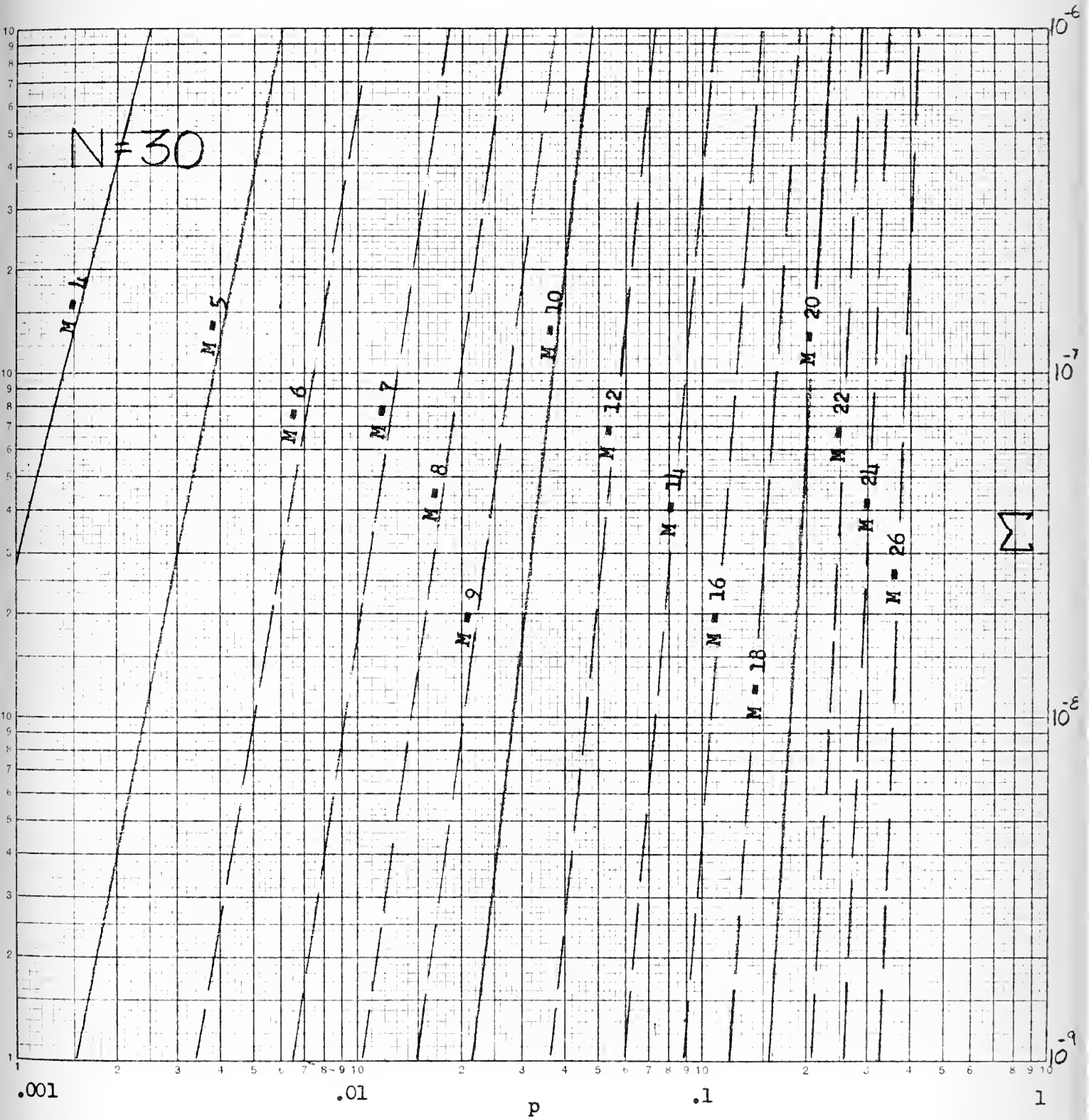

$$\sum_{i=M}^{N} C_i^N \, p^i \, (1-p)^{N-i} \qquad \text{vs. p}$$

FIGURE 41

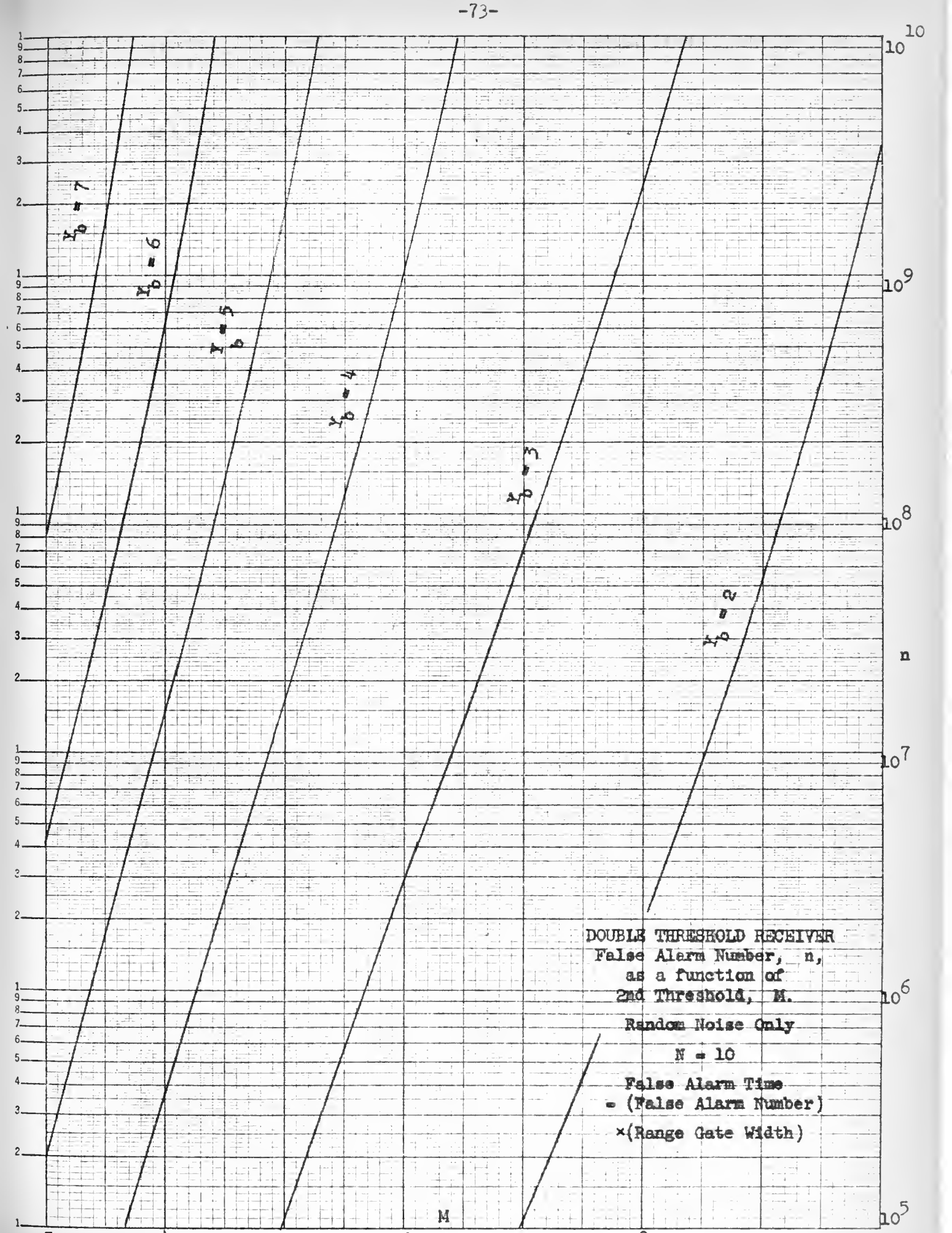
DOUBLE THRESHOLD RECEIVER
False Alarm Number, n,
as a function of
2nd Threshold, M.
Random Noise Only
N = 10
False Alarm Time
= (False Alarm Number)
×(Range Gate Width)
$P_b = 7$
$P_b = 6$
$P_b = 5$
$P_b = 4$
$P_b = 3$
$P_b = 2$
n
M
10^{10}
10^9
10^8
10^7
10^6
10^5
3
4
5
6
7
8
9
10

FIGURE 42

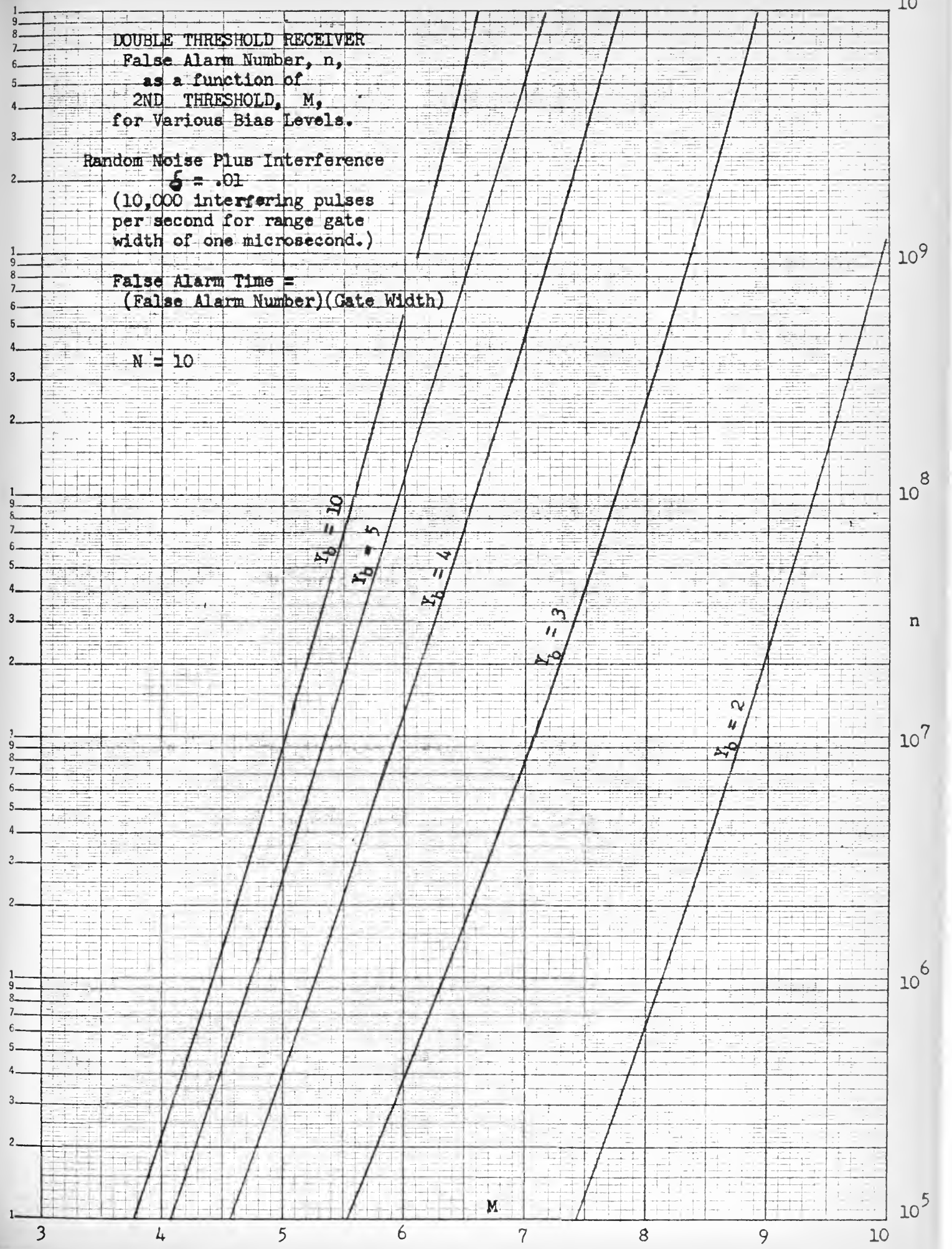
DOUBLE THRESHOLD RECEIVER
False Alarm Number, n,
as a function of
2ND THRESHOLD, M,
for Various Bias Levels.
Random Noise Plus Interference
δ = .01
(10,000 interfering pulses
per second for range gate
width of one microsecond.)
False Alarm Time =
(False Alarm Number)(Gate Width)
N = 10
$Y_b = 10$
$Y_b = 5$
$Y_b = 4$
$Y_b = 3$
$Y_b = 2$
n
M
10^{10}
10^9
10^8
10^7
10^6
10^5
3
4
5
6
7
8
9
10

FIGURE 13

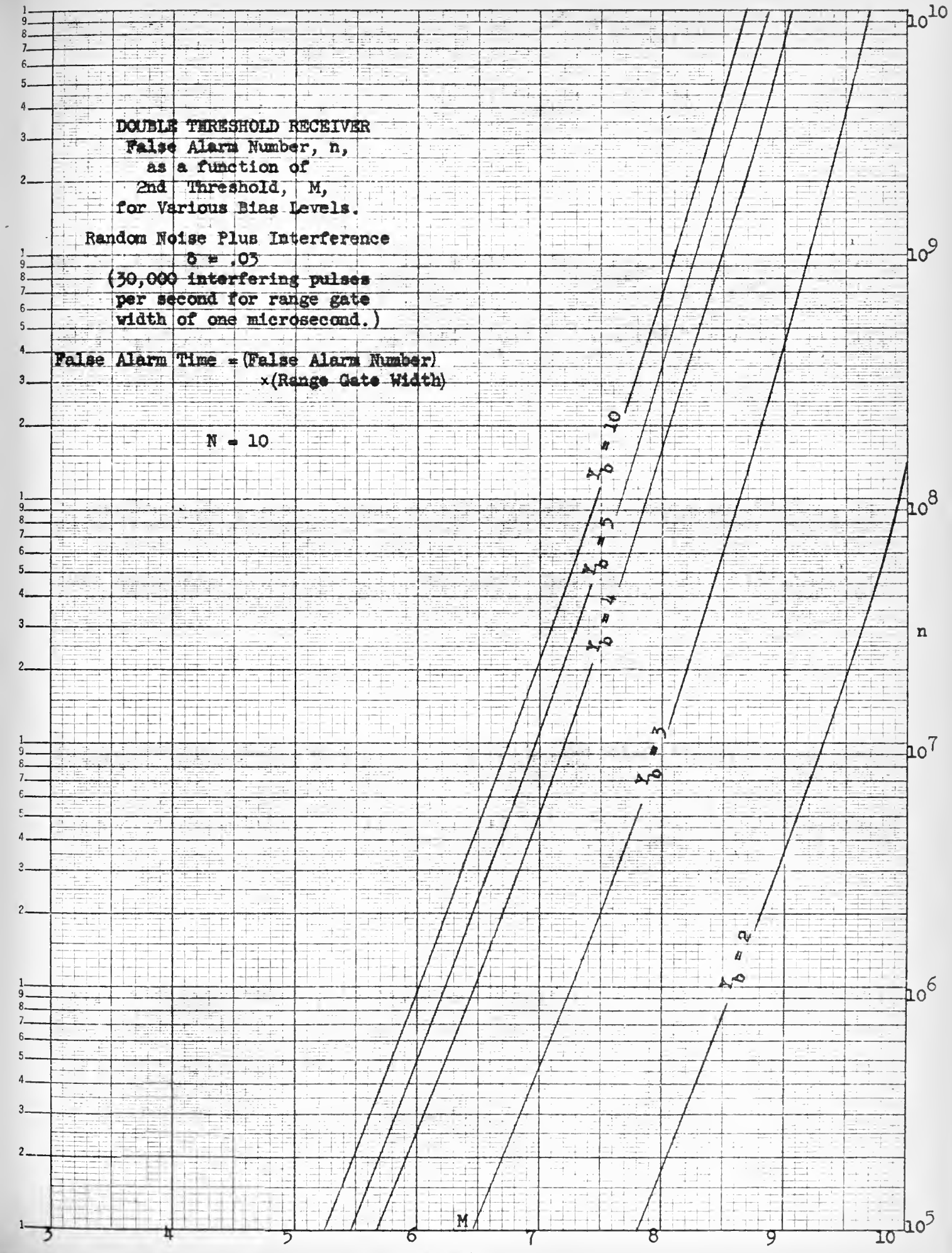
DOUBLE THRESHOLD RECEIVER
False Alarm Number, n,
as a function of
2nd Threshold, M,
for Various Bias Levels.
Random Noise Plus Interference
δ = .03
(30,000 interfering pulses
per second for range gate
width of one microsecond.)
False Alarm Time = (False Alarm Number)
×(Range Gate Width)
N = 10
$Y_b = 10$
$Y_b = 5$
$Y_b = 4$
$Y_b = 3$
$Y_b = 2$
n
M
10^{10}
10^9
10^8
10^7
10^6
10^5
3
4
5
6
7
8
9
10

FIGURE 44

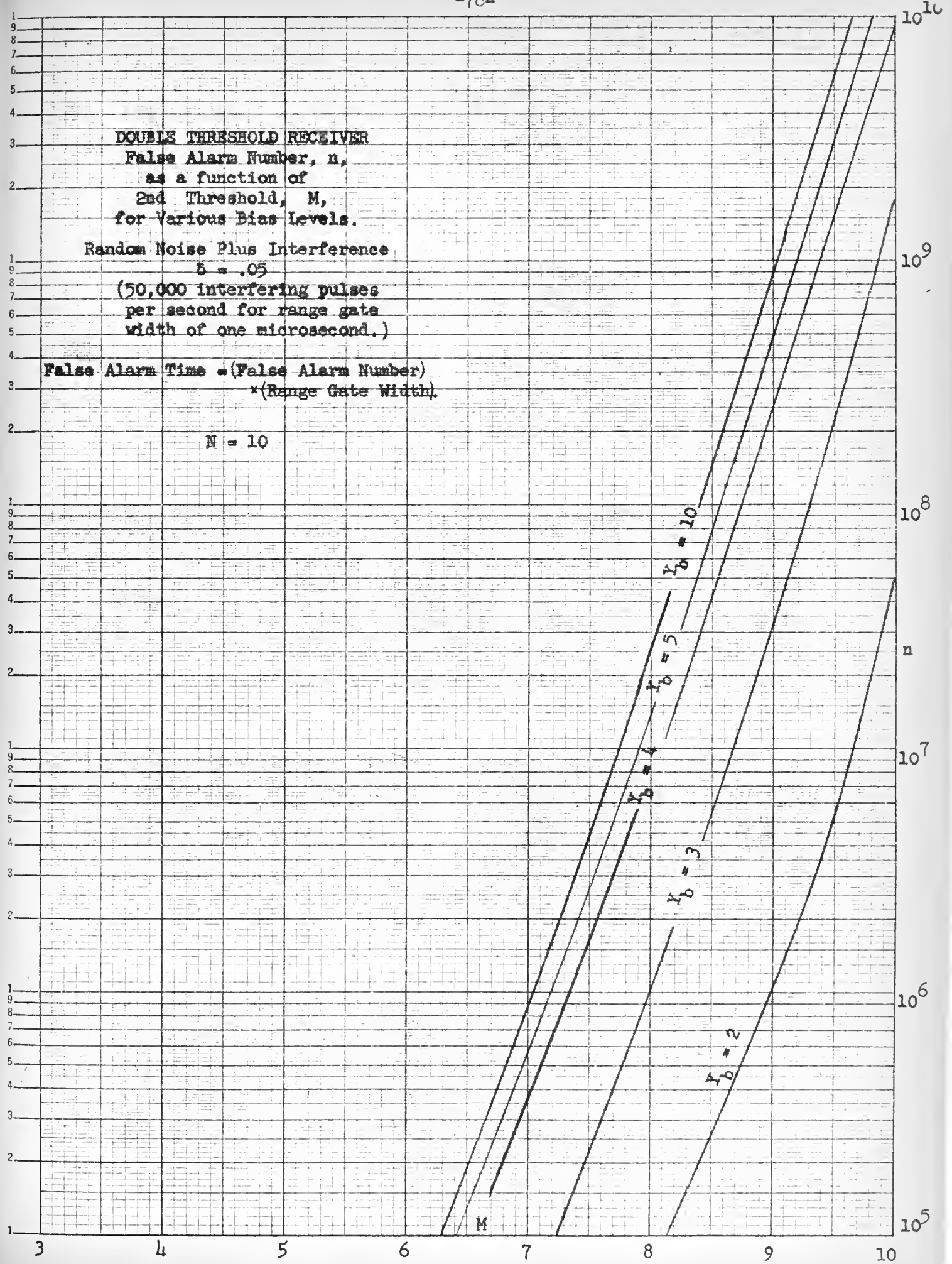
DOUBLE THRESHOLD RECEIVER
False Alarm Number, n,
as a function of
2nd Threshold, M,
for Various Bias Levels.
Random Noise Plus Interference
δ = .05
(50,000 interfering pulses
per second for range gate
width of one microsecond.)
False Alarm Time = (False Alarm Number)
×(Range Gate Width).
N = 10
Y_b = 10
Y_b = 5
Y_b = 4
Y_b = 3
Y_b = 2
n
M
10^{10}
10^9
10^8
10^7
10^6
10^5
3
4
5
6
7
8
9
10

FIGURE 45

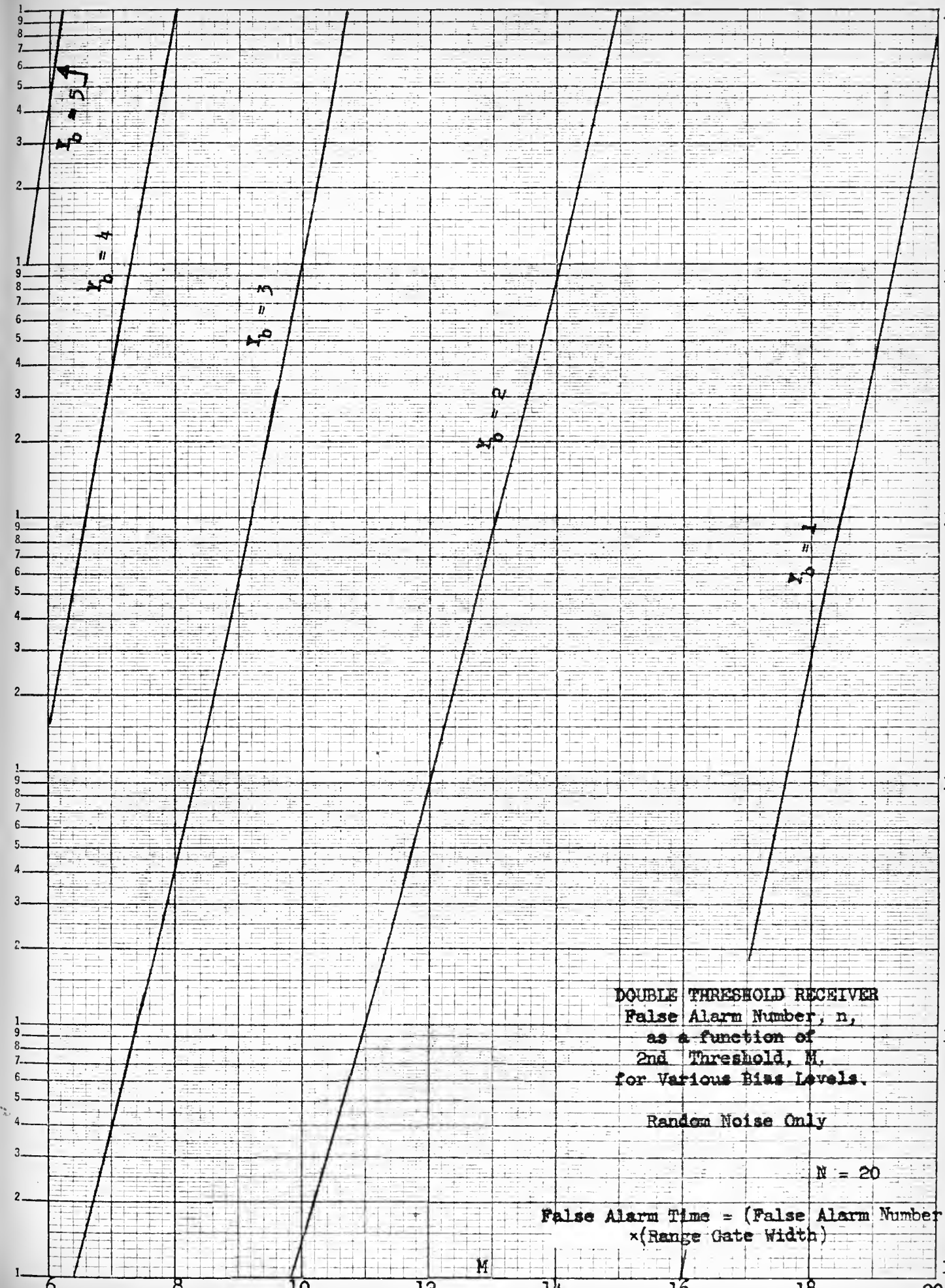
$x_b = 5$
$x_b = 4$
$x_b = 3$
$x_b = 2$
$x_b = 1$
10^9
10^8
10^7
10^6
10^5
n
M
6
8
10
12
14
16
18
20
DOUBLE THRESHOLD RECEIVER
False Alarm Number, n,
as a function of
2nd Threshold, M,
for Various Bias Levels.
Random Noise Only
N = 20
False Alarm Time = (False Alarm Number)
×(Range Gate Width)

FIGURE 4.6

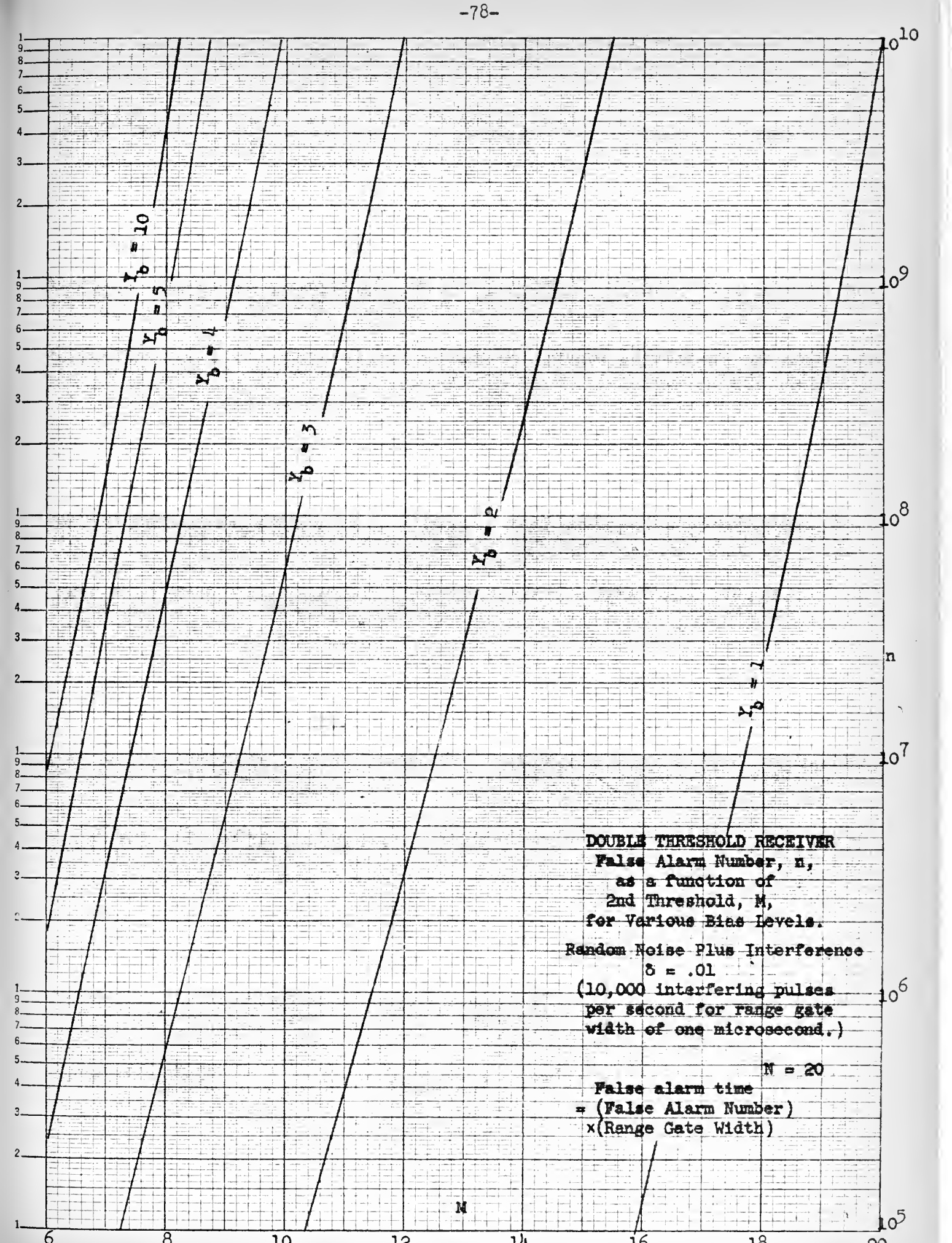
$Y_b = 10$
$Y_b = 5$
$Y_b = 4$
$Y_b = 3$
$Y_b = 2$
$Y_b = 1$
10^{10}
10^9
10^8
10^7
10^6
10^5
n
M
6
8
10
12
14
16
18
20
DOUBLE THRESHOLD RECEIVER
False Alarm Number, n,
as a function of
2nd Threshold, M,
for Various Bias Levels.
Random Noise Plus Interference
δ = .01
(10,000 interfering pulses
per second for range gate
width of one microsecond.)
N = 20
False alarm time
= (False Alarm Number)
x(Range Gate Width)

FIGURE 47

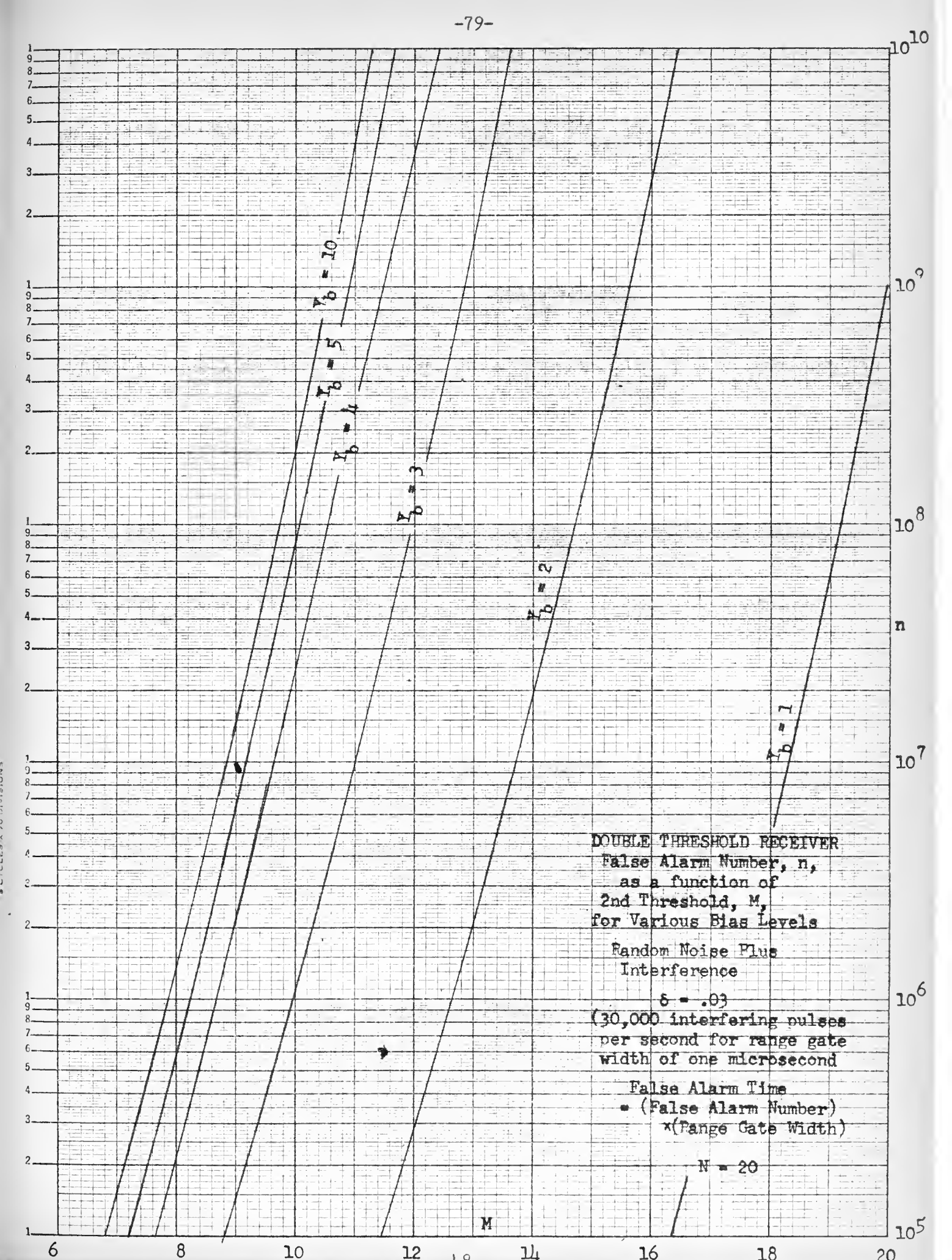
$Y_b = 10$
$Y_b = 5$
$Y_b = 4$
$Y_b = 3$
$Y_b = 2$
$Y_b = 1$
10^{10}
10^9
10^8
10^7
10^6
10^5
n
M
6
8
10
12
14
16
18
20
DOUBLE THRESHOLD RECEIVER
False Alarm Number, n,
as a function of
2nd Threshold, M,
for Various Bias Levels
Random Noise Plus
Interference
δ = .03
(30,000 interfering pulses
per second for range gate
width of one microsecond
False Alarm Time
= (False Alarm Number)
×(Range Gate Width)
N = 20

FIGURE 48

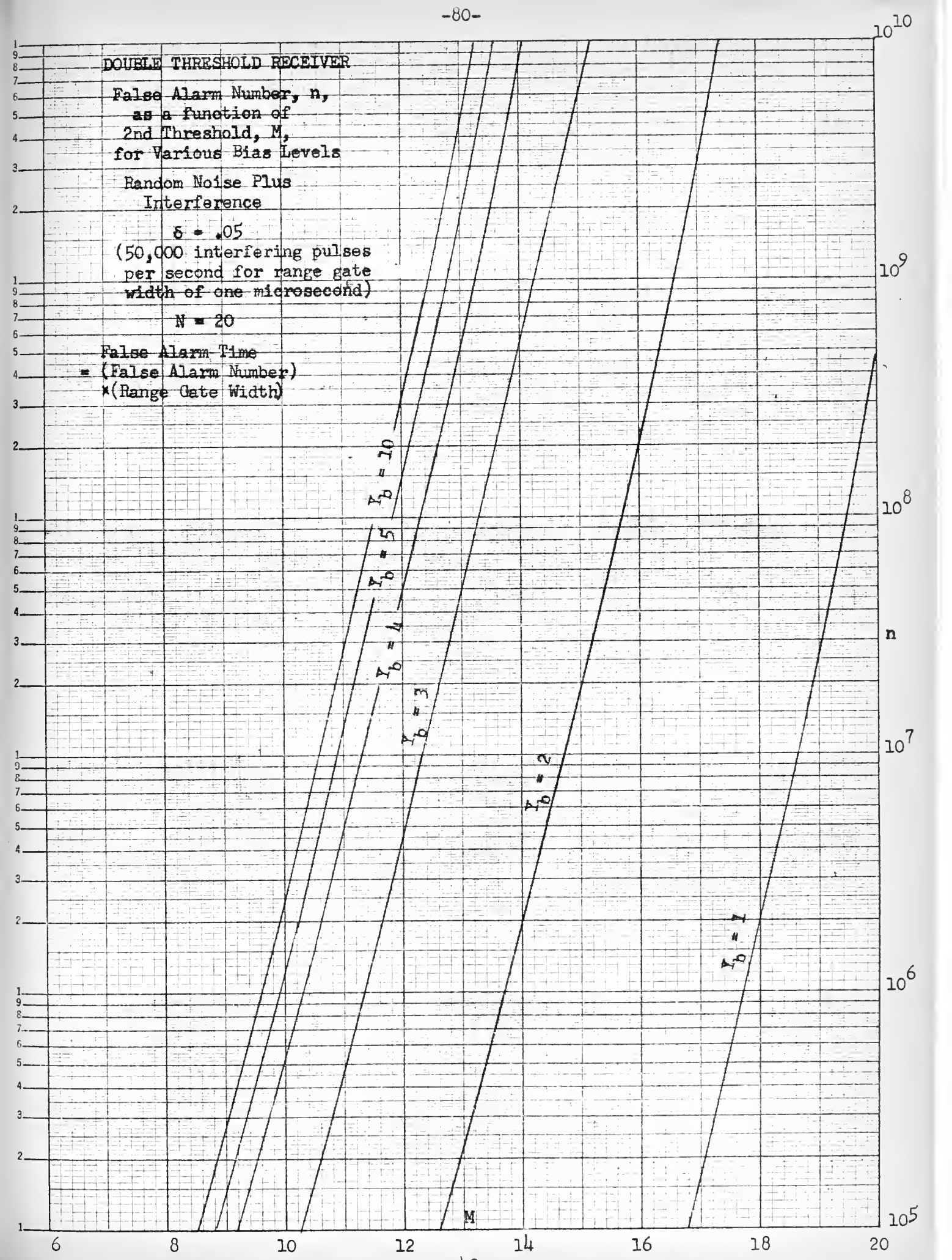
DOUBLE THRESHOLD RECEIVER
False Alarm Number, n,
as a function of
2nd Threshold, M,
for Various Bias Levels
Random Noise Plus
Interference
δ = .05
(50,000 interfering pulses
per second for range gate
width of one microsecond)
N = 20
False Alarm Time
= (False Alarm Number)
*(Range Gate Width)
$Y_b = 10$
$Y_b = 5$
$Y_b = 4$
$Y_b = 3$
$Y_b = 2$
$Y_b = 1$
n
M
10^{10}
10^9
10^8
10^7
10^6
10^5
6
8
10
12
14
16
18
20

FIGURE 49

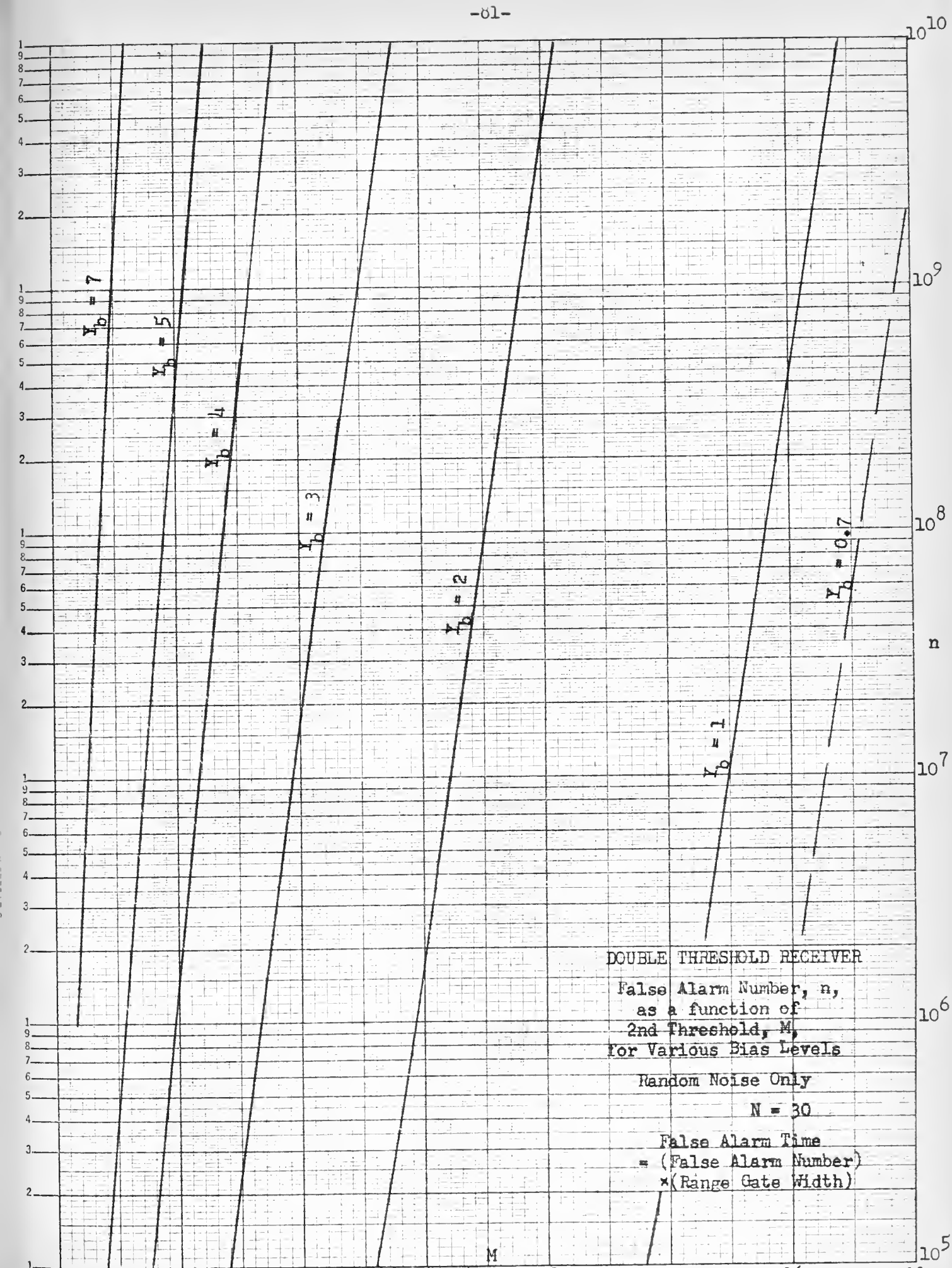
$Y_b = 7$
$Y_b = 5$
$Y_b = 4$
$Y_b = 3$
$Y_b = 2$
$Y_b = 1$
$Y_b = 0.7$
n
M
10^{10}
10^{9}
10^{8}
10^{7}
10^{6}
10^{5}
2
6
10
14
18
22
26
30
DOUBLE THRESHOLD RECEIVER
False Alarm Number, n,
as a function of
2nd Threshold, M,
for Various Bias Levels
Random Noise Only
N = 30
False Alarm Time
= (False Alarm Number)
*(Range Gate Width)

FIGURE 50

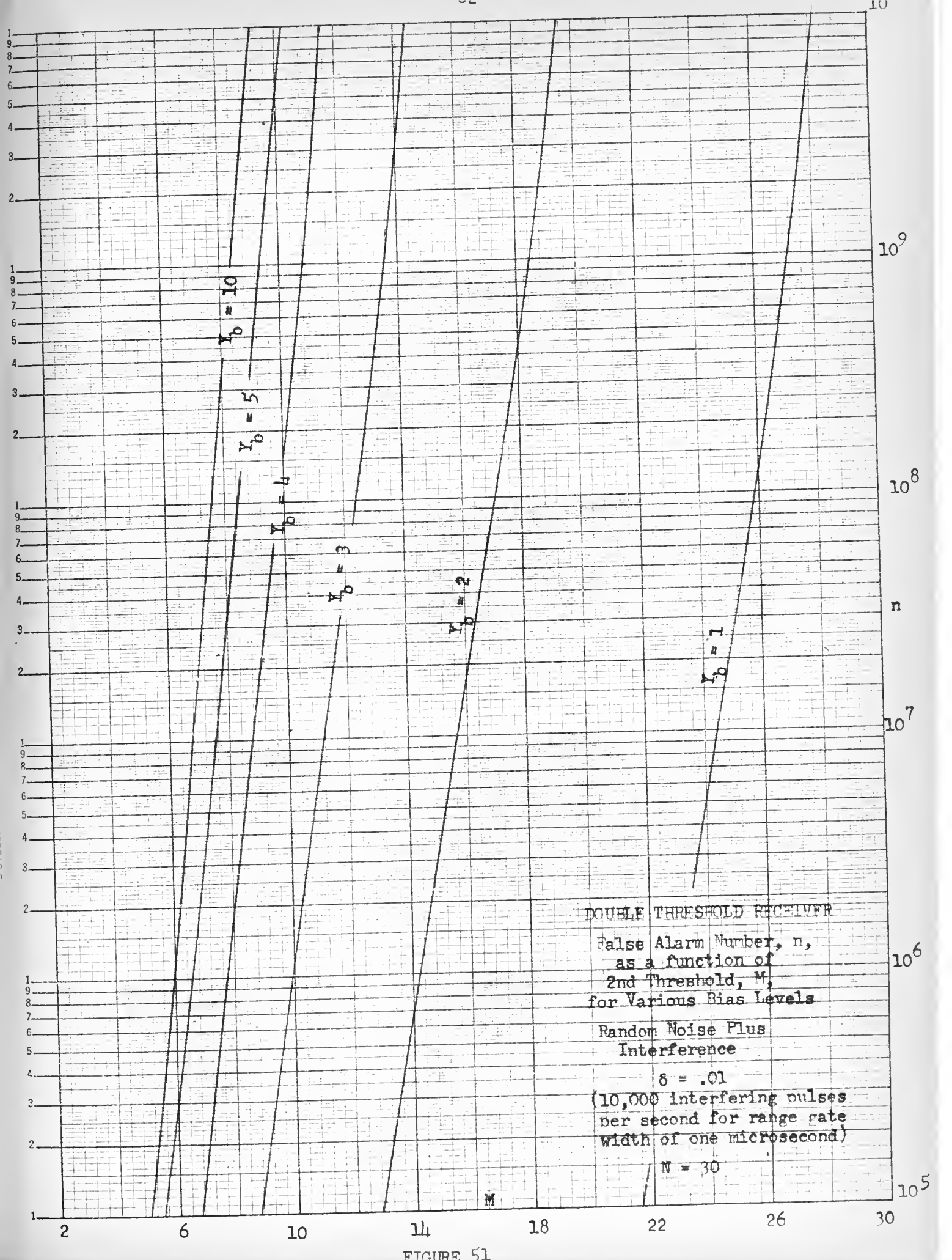
$Y_b = 10$
$Y_b = 5$
$Y_b = 4$
$Y_b = 3$
$Y_b = 2$
$Y_b = 1$
10^9
10^8
10^7
10^6
10^5
n
M
2
6
10
14
18
22
26
30
DOUBLE THRESHOLD RECEIVER
False Alarm Number, n,
as a function of
2nd Threshold, M,
for Various Bias Levels
Random Noise Plus
Interference
δ = .01
(10,000 interfering pulses
per second for range gate
width of one microsecond)
N = 30

FIGURE 51

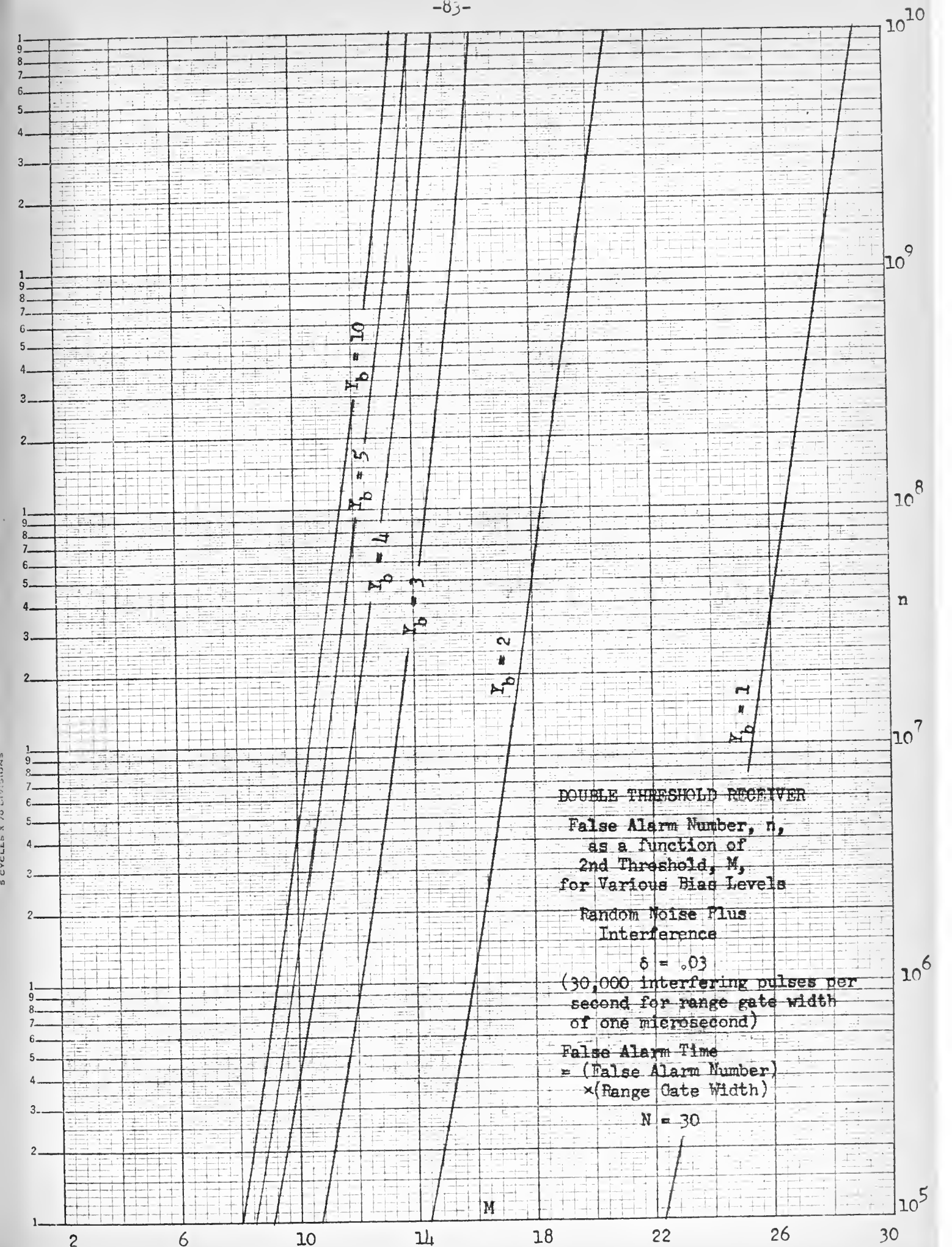
10^{10}
10^{9}
10^{8}
10^{7}
10^{6}
10^{5}
n
$I_b = 10$
$I_b = 5$
$I_b = 4$
$I_b = 3$
$I_b = 2$
$I_b = 1$
M
2
6
10
14
18
22
26
30
DOUBLE THRESHOLD RECEIVER
False Alarm Number, n,
as a function of
2nd Threshold, M,
for Various Bias Levels
Random Noise Plus
Interference
δ = .03
(30,000 interfering pulses per
second for range gate width
of one microsecond)
False Alarm Time
= (False Alarm Number)
×(Range Gate Width)
N = 30

FIGURE 52

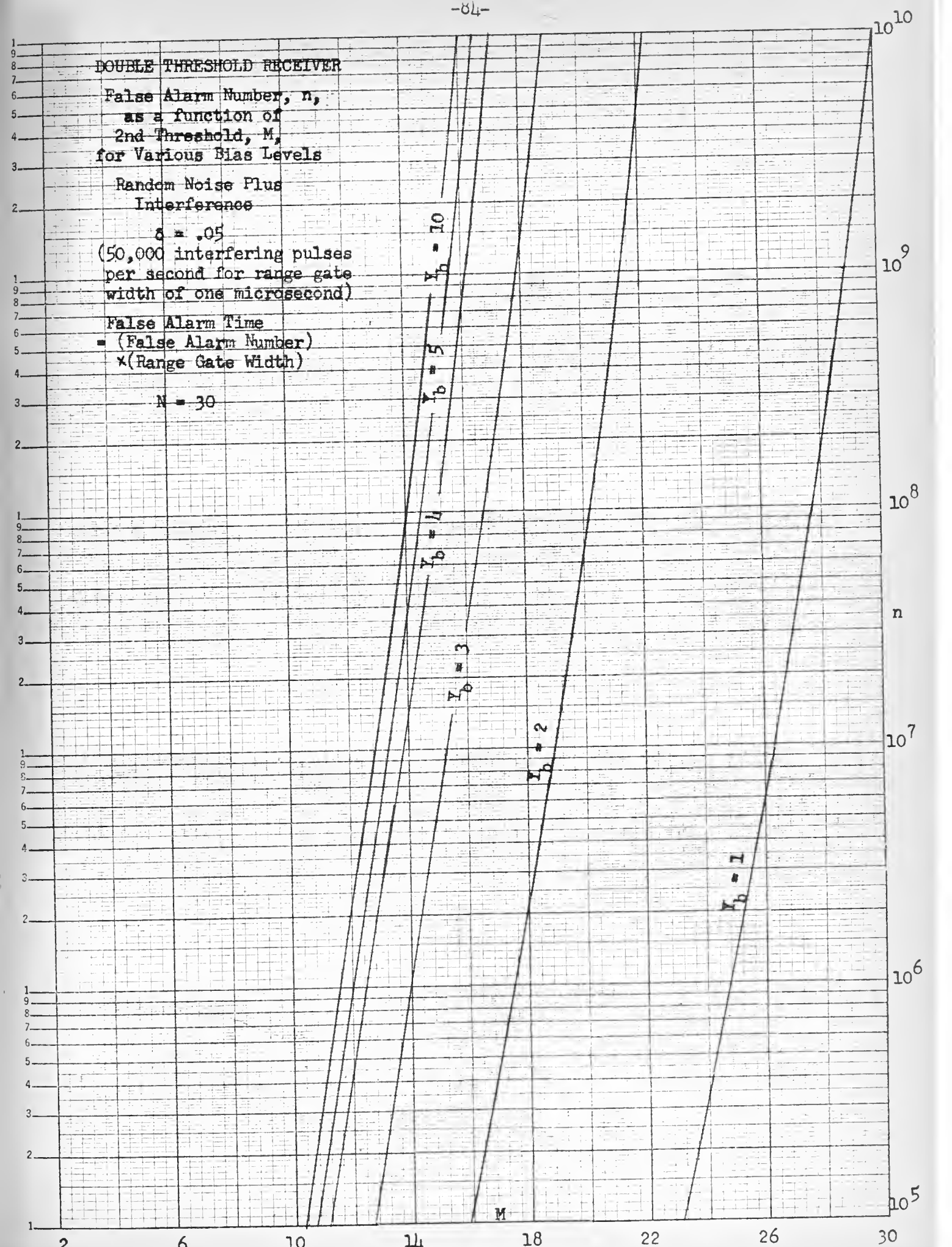
DOUBLE THRESHOLD RECEIVER
False Alarm Number, n,
as a function of
2nd Threshold, M,
for Various Bias Levels
Random Noise Plus
Interference
δ = .05
(50,000 interfering pulses
per second for range gate
width of one microsecond)
False Alarm Time
= (False Alarm Number)
×(Range Gate Width)
N = 30
Y_b = 10
Y_b = 5
Y_b = 4
Y_b = 3
Y_b = 2
Y_b = 1
n
M
10^{10}
10^9
10^8
10^7
10^6
10^5
2
6
10
14
18
22
26
30

FIGURE 53

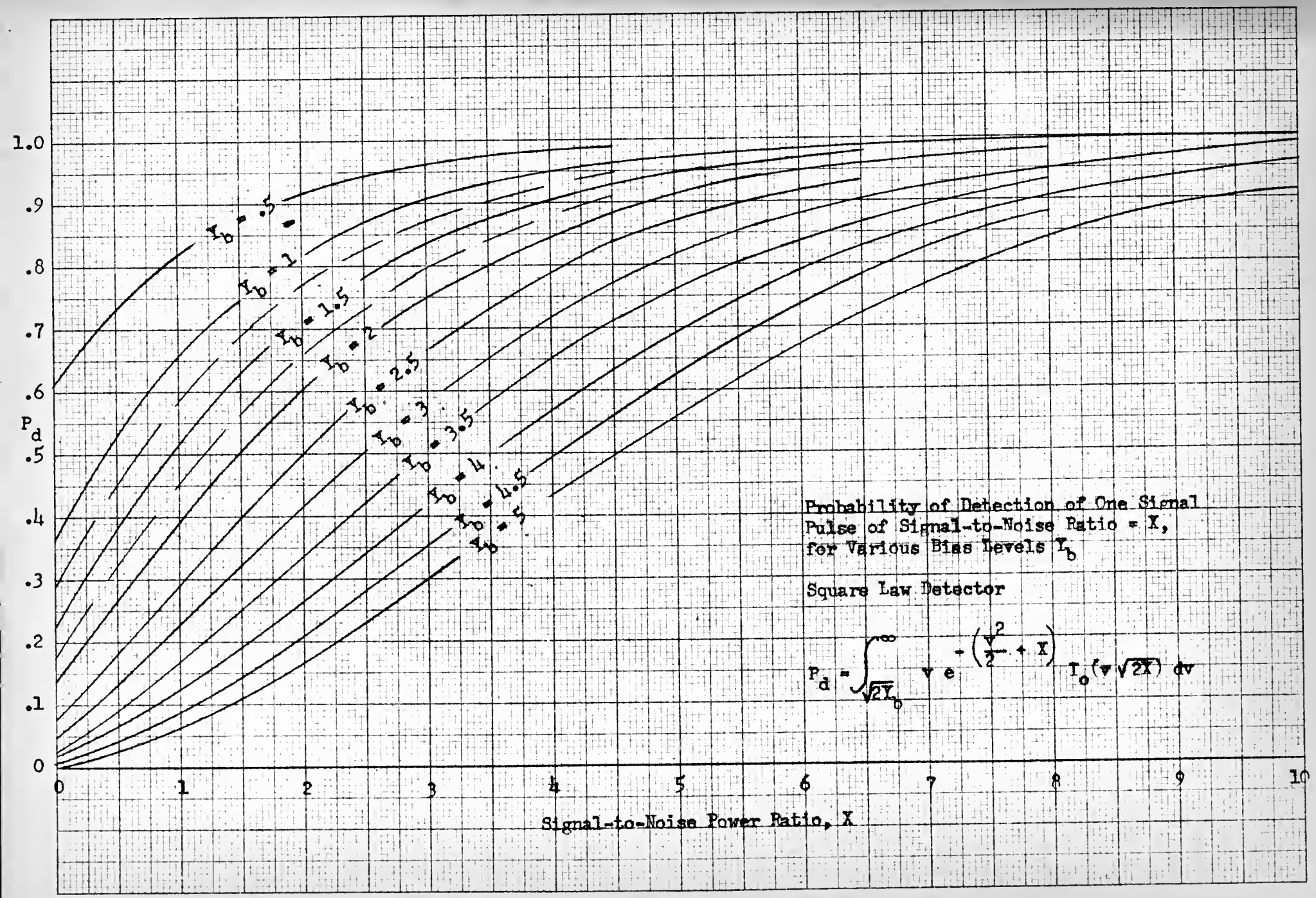
1.0
.9
.8
.7
.6
.5
.4
.3
.2
.1
0
P_d
$Y_b = .5$
$Y_b = 1$
$Y_b = 1.5$
$Y_b = 2$
$Y_b = 2.5$
$Y_b = 3$
$Y_b = 3.5$
$Y_b = 4$
$Y_b = 4.5$
$Y_b = 5$
0
1
2
3
4
5
6
7
8
9
10
Signal-to-Noise Power Ratio, X
Probability of Detection of One Signal Pulse of Signal-to-Noise Ratio = X, for Various Bias Levels Y_b
Square Law Detector
$P_d = \int_{\sqrt{2Y_b}}^{\infty} v\, e^{-\left(\frac{v^2}{2} + X\right)} I_o(v\sqrt{2X})\, dv$

FIGURE 54

L645 Linder
The "double threshold" radar receiver for reduction of false targets caused by interfering pulses.